Volume 44 | Number 17 | 7 September 2015 | Pages 5917–6388

Chem Soc Rev

Chemical Society Reviews

www.rsc.org/chemsocrev

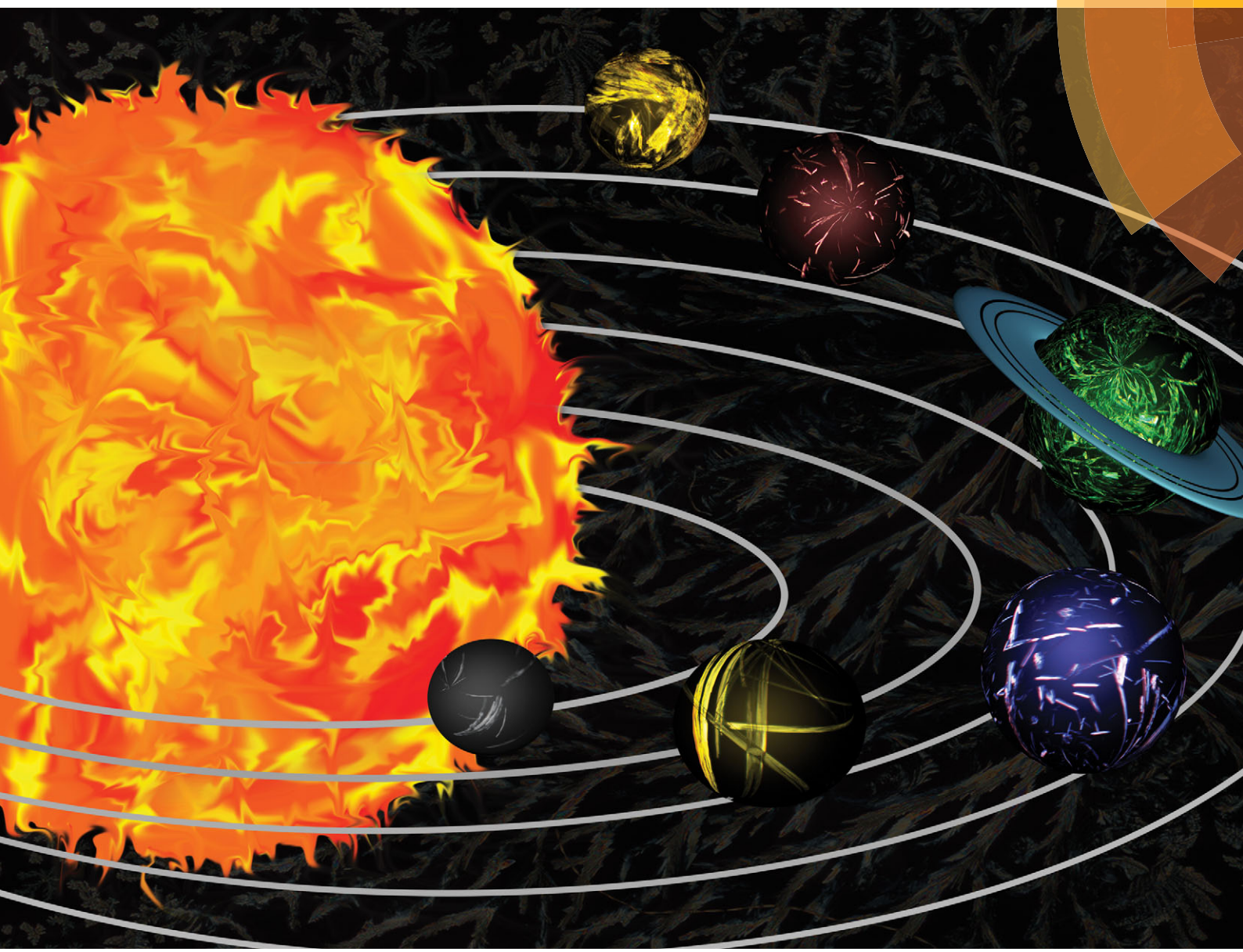

ISSN 0306-0012

ROYAL SOCIETY OF CHEMISTRY

REVIEW ARTICLE

M. A. Rogers *et al.*

To gel or not to gel: correlating molecular gelation with solvent parameters

Chem Soc Rev

REVIEW ARTICLE

Cite this: *Chem. Soc. Rev.*, 2015, **44**, 6035

To gel or not to gel: correlating molecular gelation with solvent parameters†

Y. Lan,[a] M. G. Corradini,[a] R. G. Weiss,[b] S. R. Raghavan[c] and M. A. Rogers*[d]

Received 12th February 2015

DOI: 10.1039/c5cs00136f

www.rsc.org/csr

Rational design of small molecular gelators is an elusive and herculean task, despite the rapidly growing body of literature devoted to such gels over the past decade. The process of self-assembly, in molecular gels, is intricate and must balance parameters influencing solubility and those contrasting forces that govern epitaxial growth into axially symmetric elongated aggregates. Although the gelator–gelator interactions are of paramount importance in understanding gelation, the solvent–gelator specific (*i.e.*, H-bonding) and nonspecific (dipole–dipole, dipole-induced and instantaneous dipole induced forces) intermolecular interactions are equally important. Solvent properties mediate the self-assembly of molecular gelators into their self-assembled fibrillar networks. Herein, solubility parameters of solvents, ranging from partition coefficients (log *P*), to Henry's law constants (HLC), to solvatochromic parameters ($E_T(30)$), and Kamlet–Taft parameters (β, α and π), and to Hansen solubility parameters (δ_p, δ_d, δ_h), are correlated with the gelation ability of numerous classes of molecular gelators. Advanced solvent clustering techniques have led to the development of *a priori* tools that can identify the solvents that will be gelled and not gelled by molecular gelators. These tools will greatly aid in the development of novel gelators without solely relying on serendipitous discoveries. These tools illustrate that the quest for the universal gelator should be left in the hands of Don Quixote and as researchers we must focus on identifying gelators capable of gelling classes of solvents as there is likely no one gelator capable of gelling all solvents.

What is a molecular gel?

Gels are comprised of chemically diverse systems that are frequently easier to recognize than to define.[1,2] Since the introduction of a gel theory by Thomas Graham in 1861, the definition of what is a gel has been evolving.[3] Among the numerous attempts made to define gels, Dr Dorothy Jordan Lloyd proposed that gels must be composed of two components with one being liquid at the temperature of consideration and the other one being solid (*i.e.*, the gelator). As well, the system must have mechanical properties of a solid.[2] This definition is useful in determining a gel but, imprecise because not all colloids are gels and not all gels are colloids.[4] Over several decades, the definition of a gel evolved to the point where Hermans depicted gels as "coherent colloid disperse systems of at least two components that exhibit mechanical properties characteristic of the solid state" and "both the dispersed component and dispersing medium extend themselves continuously throughout the whole system".[5] Due to the exclusivity of this definition, Ferry provided a less vigorous and more descriptive one: "A gel is a substantially diluted system which exhibits no steady state flow."[6] In order to link the microscopic and macroscopic properties, a substance can be classified as a gel if it: (1) has a continuous microscopic structure with macroscopic dimensions that is permanent on the time scale of an analytical experiment and (2) is solid-like in its rheological behavior despite being mostly liquid.[1] Depending on the continuous structures of gels discussed, Flory proposed a scheme and classified gels into four categories: (1) well-ordered lamellar structures, including gel mesophases; (2) covalent polymeric networks, completely disordered; (3) polymer networks formed through physical aggregation, predominantly disordered, but with regions of local order; (4) particulate, disordered structures.[7] Herein, molecular gels reside in category three and perhaps four.

Unlike polymeric gels, molecular gels are comprised of low molecular weight gelators (LMOGs) (arbitrarily limited to <3000 Da). The molecules self-assemble *via* highly specific, non-covalent interactions that lead usually to elongated fibrillar structures resulting in the formation of an entangled self-assembled network (a SAFIN).[8,9] The thermally-activated formation

[a] *School of Environmental and Biological Sciences, Rutgers University, New Brunswick, NJ, 08901, USA*
[b] *Department of Chemistry and Institute for Soft Matter Synthesis and Metrology, Georgetown University, Washington, DC, 20057, USA*
[c] *Department of Chemical & Biomolecular Engineering, University of Maryland, College Park, MD, 20742, USA*
[d] *Department of Food Science, University of Guelph, Guelph, Ontario, N3C3X9, Canada. E-mail: mroger09@uoguelph.ca; Tel: +1-519-824-4120 ext. 54327*

† Electronic supplementary information (ESI) available: Supplemental figures are included for data sets that do not illustrate obvious correlations between gel state and the solvent parameter. See DOI: 10.1039/c5cs00136f

of molecular gels follows a multi-step process. The initial step of gelation involves dissolution of LMOGs under specific conditions, such as elevated temperature, to obtain a solution or sol. Upon cooling, super-saturation drives the aggregation of LMOGs *via* stochastic nucleation.[1] Unlike common crystallization processes where macroscopic phase separation occurs and bulk solids and liquids are visible, the gelation here involves microscopic phase separation. The nucleation event requires highly specific interactions that promote preferential 1-dimensional (1D) growth. These interactions include hydrogen-bonding,[10,11] π–π stacking, electrostatic interactions, van der Waals interactions[12] and so on. The consequent fibers formed from 1D growth can be described in many cases as "crystal-like" and they play the same role as polymer chains in polymeric gels. The morphology of these fibers may be tubules, strands, tapes, chiral ribbons or any aggregate with a large aspect ratio.[1] The junction zones and branching between these SAFiN strands are responsible for the rigidity of the microstructure of the gel matrixes.[13] The junction zones serve as the "glue" that combines 1D fibers into 3-dimensional (3D) networks that pervade the whole system and entrap the liquid component macroscopically *via* capillary forces and surface tension.[1]

Practically, it is sometimes difficult to determine experimentally whether a material is a gel. For the purpose of this review, it is extremely important to be as inclusive as possible when defining gelation ability. The advantage of advanced rheological techniques in defining gels is that they are able to differentiate weak and strong gels. However, these determinations are very time consuming. Given the extremely large number of materials to be screened, the authors here have elected to use a simpler

Y. Lan

Yaqi Lan received her BA degree in food science and technology from Jiangnan University, China in 2011. She is currently a PhD candidate, under the mentorship of Dr Michael Rogers, and recipient of an Excellence Fellowship at Rutgers University, the State University of New Jersey.

M. G. Corradini

Maria G. Corradini received a MSc and PhD, under the mentorship of Dr Micha Peleg, from the Department of Food Science, University of Massachusetts – Amherst. From 2004 to 2007 she was a Postdoctoral Research Fellow working on microbial population dynamics at the same institution. Currently she holds a position as Assistant Research Professor at Rutgers, The State University of New Jersey, and since 2008 she has also been an Associate Professor at Universidad Argentina de la Empresa, Buenos Aires, Argentina. Her research interests mainly focus on the areas of modeling non-linear kinetics and photophysics.

R. G. Weiss

Richard G. Weiss received his PhD from the University of Connecticut with Eugene Snyder. He was an NIH Postdoctoral Fellow with George Hammond at CalTech and Visiting Assistant Professor at the Universidade de São Paulo in Brazil before joining Georgetown University. He is an IUPAC Fellow, member of the Brazilian Academy of Sciences, and received a doctorate honoris causa from Université de Bordeaux 1. He was a senior editor of Langmuir for 10 years and is on the editorial advisory board of Journal of the Brazilian Chemical Society. His research interests include investigations of reactions in anisotropic environments and the development and application of gels.

S. R. Raghavan

Srinivasa R. Raghavan holds a chaired professorship in the Dept. of Chemical and Biomolecular Engineering at the University of Maryland. He received his BTech. and PhD in Chemical Engineering from IIT-Madras and North Carolina State University, respectively. At UMCP, he heads the Complex Fluids and Nanomaterials Group (http://complexfluids.umd.edu), which seeks to engineer matter at the nano- and micro-scales using the strategies of self assembly and directed assembly. His work has resulted in more than 120 peer-reviewed publications and 18 patent applications. A class of biomaterials developed in his lab are being commercialized by Remedium Technologies, a company he co-founded.

rheological technique, the inverted tube method.[14] Specifically, a solid–liquid mixture in a glass vial was heated above the sol–gel transition temperature (*i.e.*, where all of the solid was dissolved) and allowed to cool to room temperature. After being stored at room temperature for 24 h, it was inverted for 1 h to observe flow. If no flow was detected, it was classified as a gel.

An arising question in the expanding field of molecular gels

Rational design of small molecular gelators has remained elusive, despite the vast and rapidly growing body of literature devoted to such gels over the past decade (Fig. 1).[15] Determining gelation by small molecules is still an empirical science, and the vast majority of new gelators are discovered serendipitously.[16] In polymer gels, the basic elements of the 3D network are 1D objects (*i.e.*, chains with covalent links between monomer units); conversely, the 3D network for molecular gels are composed of zero-dimensional (0D) objects (*i.e.*, molecules that must self-assemble through non-covalent interactions initially into 1D objects and then into 3D networks).[17,18] The fibrillar networks (SAFiNs) form spontaneously *via* aggregation-nucleation-growth pathways of the small molecule gelators.[19–31]

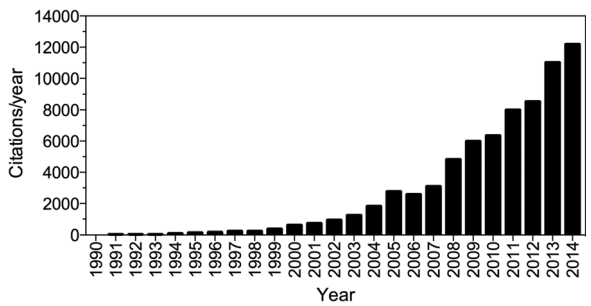

Fig. 1 Histogram of citations by year to 'organogel(s)' in the web of science.

M. A. Rogers

Michael Rogers received his PhD with Alejandro Marangoni and Amanda Wright from the University of Guelph. He was an Assistant Professor at the University of Saskatchewan and Rutgers University before joining the Department of Food Science at the University of Guelph. He has been awarded patents on molecular gels as edible fat replacers and as phase selective sorbent xerogels for reclamation of spilled oil. His research interests are on self-assembly of fibrillar aggregates in molecular gels, biomaterials and bio-mimics, and the biophysics of digestion. He won the 2015 Young Research Scientist Award from the American Oil Chemists Society.

At this time, the research community is faced with more questions than answers concerning molecular gels: (1) why do some molecules self-recognize and orient into supramolecular networks while others do not? (2) Why do these fibrillar aggregates grow without minimizing the surface area between the liquid and crystal interface, and hence have an excess of interfacial free energy? (3) Why do slight variations in molecular structure frequently have drastic consequences in the nanoscopic, microscopic and mesoscopic properties of the gels? (4) How does each molecule of these building blocks immobilize *macroscopically* up to one thousand (or more) liquid molecules? The intricate nature of SAFiNs lies in their hierarchical assembly process that must arise as a consequence of weak non-covalent interactions that include hydrogen-bonding, π–π stacking and van der Waals interactions.[32] However, the possibility of creating, *a priori*, or discovering serendipitously a 'universal' gelator for all solvents seems impossible given the importance of the solvent–gelator interplay in directing self-assembly.

The quest for rational design criteria in creating new gelators

Each class of molecular gelators can gel a limited set of solvents. No universal law may be applied to all gelator–solvent systems. As an example, originating with the simplest reported molecular gelators, *n*-alkanes, we have incrementally increased the complexity of the structures in an attempt to identify the features that lead to the most efficient gelators.[33–38] Alkanes are driven to assemble *via* van der Waals interactions. By inserting an oxygen at various positions along the carbon chain, other interactions such as dipole–dipole and hydrogen-bonding come into play, leading in some cases to SAFiNs and gels. Further addition of a terminal carboxylic acid to a C18 hydrocarbon chain leads to one of the most widely studied, highly efficient molecular gelators known to date, R-12-hydroxystearic acid (HSA).[21,22,33,34,36,37,39–55] The efficiency of gelation in silicone oil and aromatic solvents can be improved by modifying the carboxylic acid of HSA. Thus, the efficiency of gelation is in the order – primary amide > carboxylic acid > secondary amides ≫ amines – while impeding gelation of more polar solvents such as water (Fig. 2).[38] Therefore, the molecular features that make up an ideal gelator for silicone oil are clearly not the same as for water.

Without exception, every study has shown only select solvents are capable of being gelled by a given gelator! Thus, it is our opinion that the quest for the universal gelator should be left to Don Quixote. The diversity of attractive and repulsive forces that can operate between gelators and solvents is enormous. In that regard, a recent meta analysis of 50 individual gelators, with an extremely diverse set of molecular structures, has been conducted.[56] None was capable of gelling all of the solvents examined. However, analyses of solvent parameters and the gelator structures do provide an understanding of why certain gelators form gels in specific solvent types and others do not. For example, the molecules that act as gelators of benzene have

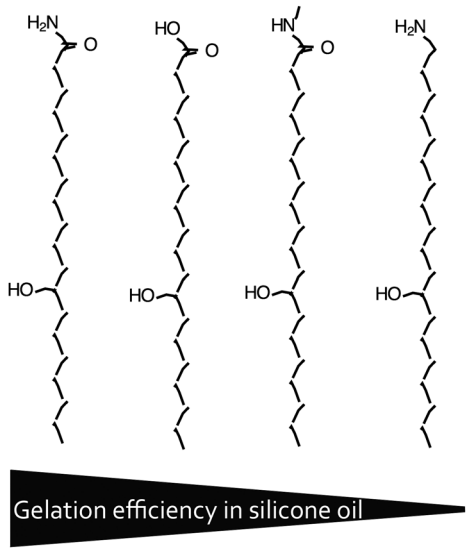

Fig. 2 Gelation efficiency of HSA deriveratives in silicone oil.

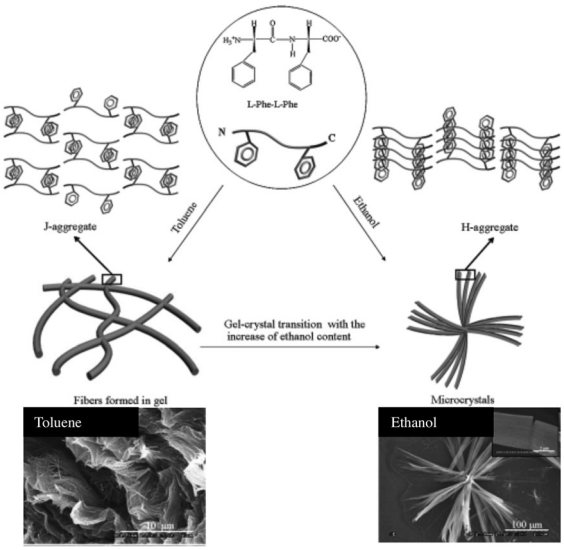

Fig. 3 Schematic illustration of the structural transition of diphenylalanine induced by varying the ethanol content in the mixed solvents, and the proposed molecular packing in the gel and in the microcrystal. SEM images are of samples formed in toluene and ethanol. Adapted from ref. 63.

strong hydrogen-bonding interactions, whereas molecules that form solutions/sols tend to interact mainly through dispersive forces. Therefore, the ''holy grail'' of this field of science may not be to develop a universal gelator; but, instead, to create reliable *a priori* methodologies to understand why molecular gels form in specific classes of solvents and not in others.

What role does solvent play in molecular gel formation?

The role of solvent chemistry on the capacity of small molecules to assemble into SAFiNs is as important as the gelator structure! The first pioneering work on the influence of both solvent and gelator structure on the formation of SAFiNs showed that the gelation number (*i.e.*, the maximum number of solvent molecules gelled per gelator molecule) correlated with Hildebrand solubility parameters when the primary functional group of the solvent remained constant.[57] In that study, various primary alcohols were gelled by trehalose-based gelators. The authors found that when the substituent R group was short (either a diacetate or dibutyrate) the capacity to gel solvents was inversely proportional to the Hildebrand solubility parameter of the solvent.[57] Since this finding, similar observations have been reported for HSA,[58] derivatives of HSA,[46,59] 1,3:2,4-dibenzylidene sorbitol (DBS),[60] two component dendritic gels,[61] L-lysine based gelators,[62] and di-peptides[63] (among others).

Changing the solvent can alter the morphology of the SAFiN. In a study with dipeptide (diphenylalanine) gelators, changing the solvent from toluene to ethanol led to a change in gel morphology from fibers to microcrystals (Fig. 3). Solvent-induced morphological changes have been observed with morphs of cholesteryl 4-(2-anthryloxy)butanoate (CAB) gelators[64] and HSA.[55,65,66] HSA gels in various alkanes and thiols have fibrous SAFiNs, with a hexagonal sub cell spacing and a multi-lamellar morphology in which the distance between lamellae is greater than the length of 2 molecules of HSA. HSA in solvents with nitriles, aldehydes and ketones as functional groups, assemble less effectively due to the formation of sphereulitic objects with a triclinic, parallel sub cell, and interdigitation in the lamellar arrangement.[55] It is clear that solvent properties are central in dictating non-covalent interactions driving self-assembly.[67–74]

Correlating molecular gelation to global solvent properties

Attempts have been made to correlate solvent parameters with gelation ability.[75–77] Important considerations include: (1) can the solvent be considered as a macroscopic continuum characterized only by bulk physical properties? (2) Can the outcome of all gelator–solvent systems, capable of forming a gel, be predicted by a universal set of solvent parameters? (3) What solvent parameters are most crucial in predicting the likelihood of gel formation?

In that regard, Parker established three primary classifications of solvents: protic, dipolar aprotic and apolar (low polarity) aprotic.[78] Although, solvent 'polarity' seems intuitively simple, Katrikzky *et al.* stated that ''. . .the simple concept of polarity as a universally determinable and applicable solvent characteristic is a gross oversimplification''.[79] Reichardt and Welton point out that solvent polarity may be interpreted as a permanent dipole moment of a solvent, its relative permittivity, or a sum of all of the molecular properties responsible for all interaction forces between a solvent and solute (*i.e.*, coulombic, directional, inductive, dispersion, and hydrogen-bonding forces).[80] To assess the correlation between gelation and solvent parameters, we have conducted studies and meta-analyses covering a total of 22 molecular gelators that were obtained from a combination of literature and from our laboratories. The gelators are sub-classified into azobenzene

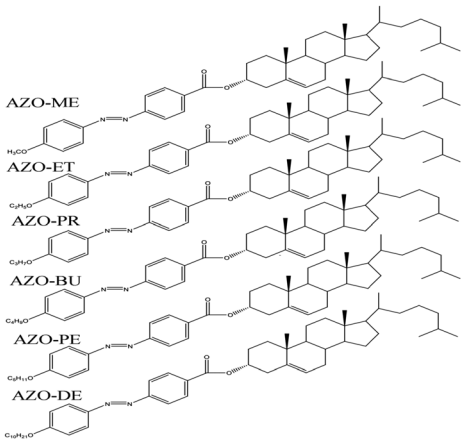

Scheme 1

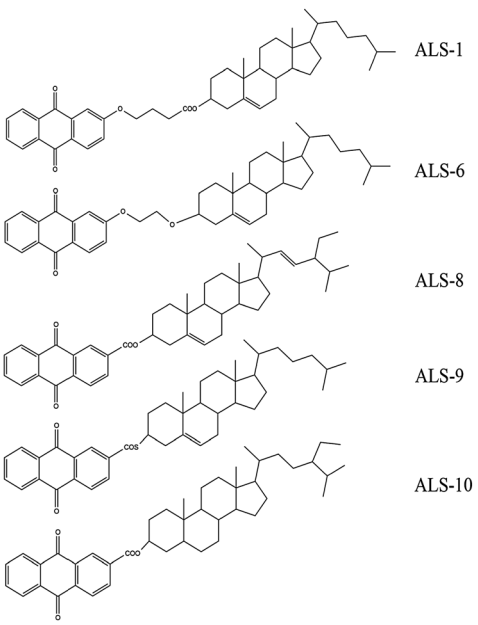

Scheme 2

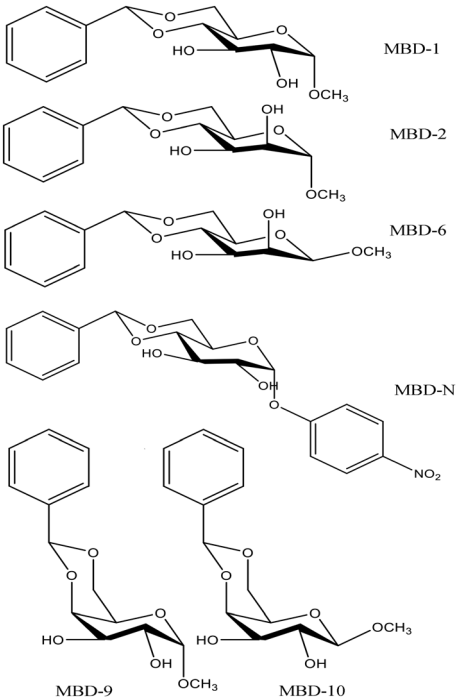

Scheme 3

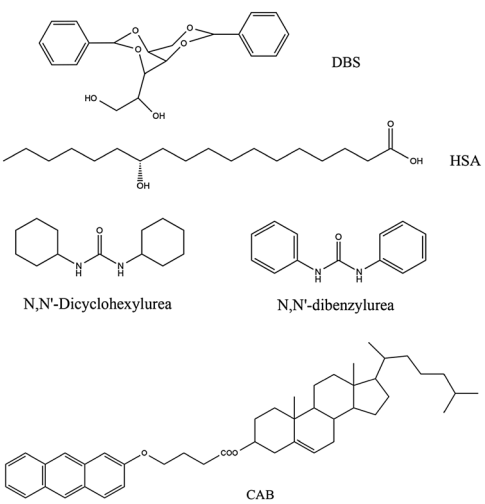

Scheme 4

gelators (Scheme 1),[18,81] ALS gelators (Scheme 2),[82] 1-*O*-methyl-4,6-*O*-benzylidene derivatives (MBD gelators) (Scheme 3),[83,84] and miscellaneous highly efficient gelators (Scheme 4).[16,58,60,85] The studies were conducted in 34 to 80 solvents, including protic, dipolar aprotic and apolar aprotic solvents! Data for all 80 solvents with every gelator were not obtained.

In this section, we discuss studies that have correlated molecular gelation with global solvent parameters, *i.e.*, where a single parameter is used to characterize the solvent as a macroscopic continuum. These are further subdivided into (1) physical properties, (2) solvatochromic properties, and (3) thermodynamic properties.

1.1 Global physical solvent properties

1.1.1 Dielectric constant. The dielectric constant ε_r (*i.e.*, static relative permittivity)[86] is routinely used to assess the 'polarity' of a solvent. Studies have attempted to correlate this parameter with molecular gelation, but the results have been mixed.[58,61] Only in limited cases have correlations between gel properties (*e.g.*, sol–gel transition temperature[61,87] or critical gelator concentration (CGC)[58]) and the dielectric constant been reported, and that too is only within a class of solvents with the same functional groups (*e.g.*, alcohols of differing alkyl chain length). Here, we take a closer look at the correlation between gelation and ε_r for the gelators shown in Schemes 1–4.

AZO gelators rely on π–π stacking and are unable to donate hydrogen bonds.[81] In the case of these gelators, there is no differentiation of solvents capable of being gelled and those that cannot, based simply on the ε_r (Fig. 4 and Fig. S1, ESI†). ALS gelators have similar cholesterol derivatives as the AZO gelators; however,

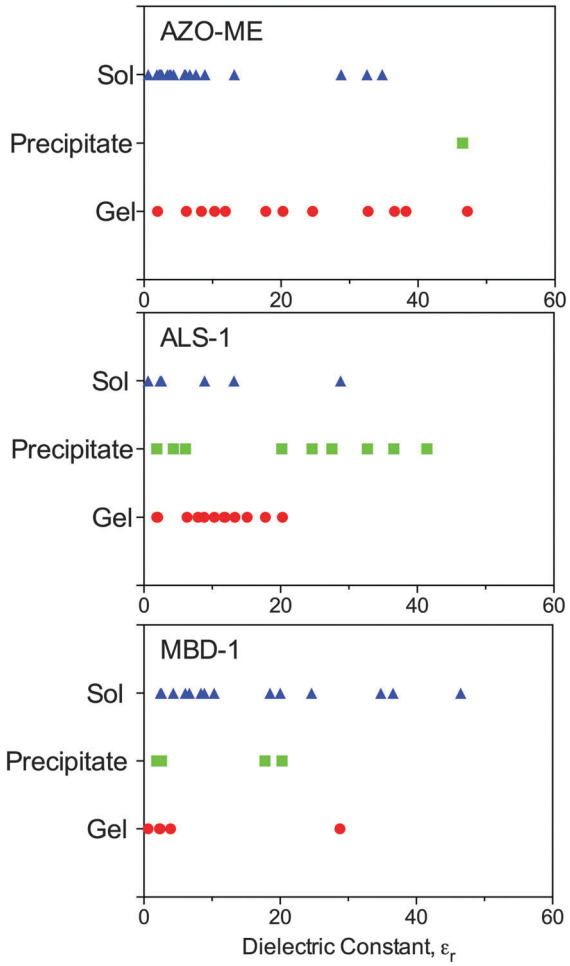

Fig. 4 AZO-ME (Scheme 1), ALS-1 (Scheme 2) and MBD-1 (Scheme 3) capacity to form gels, precipitates or solutions as a function of static relative permittivity.

the more polar azobenzene group is replaced with the less polar 2-anthraquinonyl group (Scheme 2).[64,88] ALS gelators are limited to gelling solvents with lower ε_r compared to AZO gelators (Fig. 4 and Fig. S2, ESI†). Again, dielectric constants are insufficient to differentiate the nature of the gelator–solvent phases.

Gelators based on 1-*O*-methyl-4,6-*O*-benzylidene derivatives (MBD-1 through MBD-10) (Scheme 3) are more polar compared to ALS and AZO, and hence form gels in lower polarity solvents (typically, $\varepsilon_r < 20$). When comparing the vastly different gelators in Scheme 4, some intuitive insights may be drawn from the dielectric constants (Fig. 4 and Fig. S3, ESI†). DBS, *N*,*N*′-DBU and *N*,*N*′-DCHU have both the ability to form hydrogen bonds as well as undergo π–π stacking and van der Waals interactions; thus, these gelators are able to gel a range of solvents with varying dielectric constants. HSA, on the other hand, relies mainly on hydrogen bonding and gels solvents with lower ε_r values. Conversely, CAB gelators rely on π–π stacking and tend to gel solvents with higher ε_r values. However, differentiation of outcomes based on ε_r is not possible for any of these gelators when the solvent structure varies greatly (Fig. S4, ESI†).

1.1.2 Refractive index. The refractive index n of a solvent increases with both the molecular mass and polarizability, where the larger the dipole moment the more efficiently the solvents respond to an applied electric field. n is related to its molar polarizability P_m by the Lorenz–Lorentz equation (eqn (1)):

$$P_m = \frac{(n^2 - 1)}{(n^2 + 1)} \quad (1)$$

It has been well established that the refractive index increases with the polarizability of the molecule, where the larger the dipole moment the more efficiently the molecule responds to an applied electric field.

Correlations between gelation and n or P_m for the gelators shown in Schemes 1–4 are now examined. For the AZO gelators, although n and P_m cannot differentiate gels from sols, important insights can once again be garnered (Fig. S5, ESI†). First, it is clear that an increase in the acyl chain length on the gelator increases the range of solvents (in terms of n and P_m) that are capable of being gelled. AZO-ME ($\sim CH_3$) gels solvents between $1.3 < n < 1.4$ while AZO-DE ($\sim C_{10}H_{21}$) gels solvents between $1.3 < n < 1.65$ (Fig. S5, ESI†). For ALS gelators, n and P_m are fairly useful in differentiating sample states (Fig. S6, ESI†). Empirically, it is shown that the linker (L) group in these gelators affects gelation.[82] For example, ALS-1 gels solvents with $1.38 < n < 1.45$; in this case, the linker group has both an ester and an ether. In comparison, ALS-8 has a shorter linker group with only an ester, and it gels solvents with $1.41 < n < 1.45$. These effects are amplified when comparing the polarizability P_m instead of n.

The relation of the MBD gelators with n and P_m is plotted in Fig. S7 (ESI†); here, we include the different isomers of the same sugar-based MBD gelators. For MBD-1, gels are found for $1.5 < n < 1.6$; while the other MBD gelators gel solvents over a much wider range of n, *i.e.*, $1.4 < n < 1.65$. Comparing MBD-1, -2, and -6, we see that even though the gelators are very similar structurally, a conformational modification of the sugar radically changes their ability to form gels. Numerous other studies have illustrated the importance of chirality and geometric isomerization on gelation ability, so albeit not a surprising finding, it points to the complexities in designing gelators.[33,36,37,52–54,89–95]

Finally, Fig. 5 depicts correlations with n and P_m for the gelators in Scheme 4. DBS is capable of gelling the broadest range of solvents with regard to n; however, differentiation of sample outcomes (gel *vs.* sol) based on n or P_m does not appear to be possible. *N*,*N*′-DCHU and *N*,*N*′-DBU are both derivatives of the smallest known organogelator, *N*,*N*′-dimethylurea, where the methyl groups are replaced with cyclohexyl or benzyl groups, respectively. Among the two, *N*,*N*′-DBU gels solvents that have relatively higher n, *i.e.*, are more polarizable. Also, in the case of *N*,*N*′-DCHU, the gel and precipitate states can be differentiated to some extent based on n and P_m. Overall, we conclude that n and P_m do not permit significant differentiation of sample outcomes across a range of solvents for any of the gelators in Schemes 1–4.

1.1.3 Octanol/water partition coefficients and Henry's law constants. The distribution of a pure substance between two partially miscible solvents, such as 1-octanol and water,

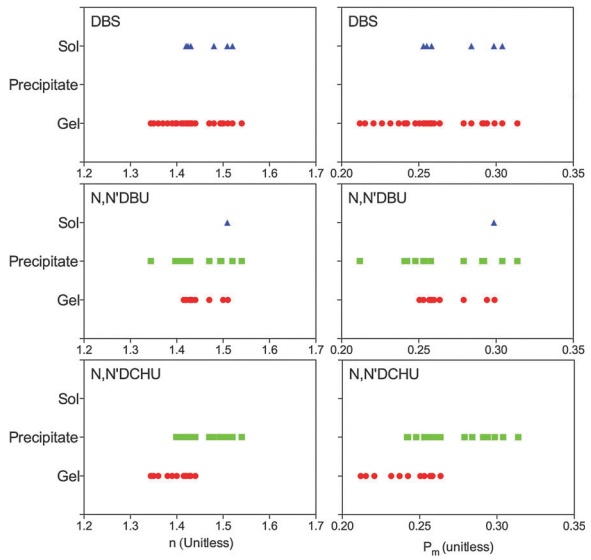

Fig. 5 The capacity of DBS, *N,N′*-DBU and *N,N′*-DCHU to form gels, precipitates or solutions as a function of the refractive index and polarizability.

which are in intimate contact is the basis of the partition coefficient parameter log *P* (eqn (2)).[96]

$$\log P = \log\left(\frac{\left[X^{\text{organic}}_{C_8H_{15}O}\right]}{\left[X^{\text{aqueous}}_{H_20}\right]}\right) \quad (2)$$

X is the mole fraction of the substance in each phase. Overall, the log *P* is related to the lipophilicity of the substance. Henry's law constants (HLCs) are influenced by the same factors associated with the log *P* constants.[96] Instead, HLCs measure the volatility of the substance or the water-to-air partition. This becomes a measure of the intermolecular interactions between molecules within the mixture.[97,98]

We have examined the correlation between gelation of the compounds in Schemes 1–4 with log *P* and HLC. Examples are shown in Fig. 6 for the AZO gelators, MBD (Fig. S8, ESI†), ALS (Fig. S9, ESI†), and other gelators (Fig. S10, ESI†). Neither of these parameters is useful in differentiating the sample states (*i.e.*, gel *vs.* sol *vs.* precipitate). The lack of differentiation is not surprising because log *P* and HLC are global parameters that cannot distinguish specific types of intermolecular interactions.

1.2 Global solvatochromic solvent properties

1.2.1 Reichardt's $E_T(30)$ solvent parameter. The notion that solvatochromic dyes are sensitive measures of solvent polarity was introduced nearly 70 years ago.[99] It was quickly realized that the solvent can alter absorption bands of a dye because of: (1) dipolar interactions between the solvent and dye; (2) changes in the dipole moment of a dye arising from an optical transition; and (3) the Franck–Condon principle.[100] Solvatochromic techniques rely on a pronounced change in the position of UV/VIS absorption bands of a solvatochromic dye caused by the solvent in which it is dissolved.[101] Reichardt's

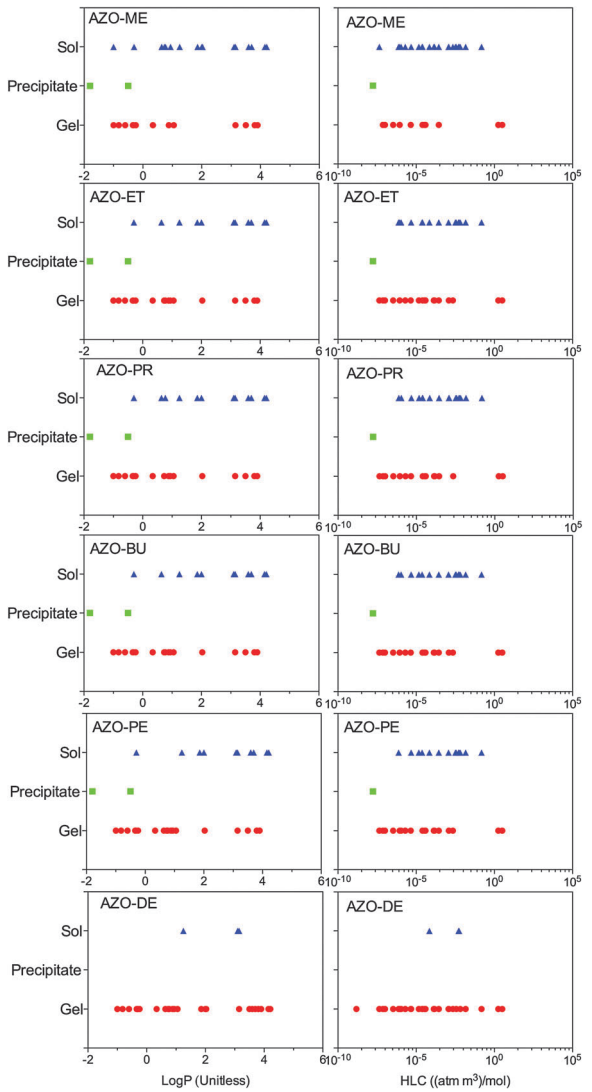

Fig. 6 The capacity of AZO derivatives to form gels, precipitates or solutions as a function of partition coefficients and Henry's law constants.

$E_T(30)$ parameter corresponds to the molar transition energy for the long wavelength electronic transition of diphenyl-4-(2,4,6-triphenylpyridinio)phenolate dye (Dimroth–Reichardt's betaine dye) in a solvent at 25 °C and at 0.1 MPa (Fig. 7). This parameter accounts for all possible (specific and nonspecific) intermolecular forces between solvent and solute molecules.[60,102] The $E_T(30)$ parameter is calculated (eqn (3)) using the shift in the longest wavelength (ν_{max}) absorption band of the dye.[103]

$$E_T(30) = hc\nu_{max}N_A \quad (3)$$

Here, *h* is Planck's constant, *c* is the speed of light and N_A is the Avogadro number.

The $E_T(30)$ parameter has been correlated with gel properties in very small sample sets and for some simple gelators.[57] However, our results for AZO (Fig. S11, ESI†) and ALS-based gelators (Fig. S12, ESI†) show that $E_T(30)$ has limited utility for explaining gel formation. AZO gelators gel solvents with $E_T(30)$ values from 30 to 55 kcal mol^{-1}. For the ALS gelators, the $E_T(30)$ values

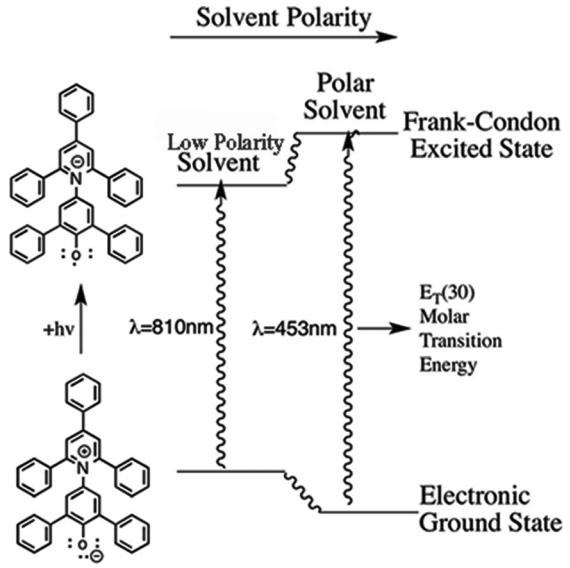

Fig. 7 Chemical structure and ground-state properties of 2,6-diphenyl-4-(2,4,6-triphenylpyridinium-1-yl)phenolate, and the influence of solvent polarity on its intramolecular charge-transfer transition with the electronic transition energies; adapted from Reichardt.[103] Reproduced by permission of The Royal Society of Chemistry.

tend to cluster for the higher polarity solvents and again with very low polarity solvents (*i.e.*, alkanes).

For the MBD-gelators (Fig. 8), some patterns emerge. In the case of MDB-1 and MBD-6, gels, precipitates and sols are differentiated based on $E_T(30)$. However, for MBD-9, the distinction between sols and precipitates is lost. Generally, a better correlation is seen when the gelator mainly exploits hydrogen-bonding for self-assembly. This can also be noted by comparing the results for *N*,*N*′-DCHU (with cyclohexyl groups) to those for *N*,*N*′-DBU (with benzyl groups). For *N*,*N*′-DCHU, which relies mainly on hydrogen bonding, the gel and sol states are well separated based on $E_T(30)$ (Fig. 8). However, for *N*,*N*′-DBU, which has the capacity for both hydrogen bonding and π–π stacking, the $E_T(30)$ parameter is insufficient to differentiate the different states of the samples.

1.2.2 Pyrene fluorescence solvent parameter. Two pyrene scales (I_1/I_3) are obtained as the ratio of I_1 and I_3 vibronic band intensities in absorbance or fluorescence spectra.[104–106]

The changes in the I_1 and I_3 band intensities are theoretically attributable to: (1) dipolar interactions between the transition moment of the pyrene and the permanent dipole moments of the solvent molecules in the immediate solvent sphere; (2) inductive interactions with the quadrupole moment of the solvent; (3) dispersive interactions; (4) hydrogen bonding interactions.[104] The I_1/I_3 scale is much less sensitive to hydrogen bonding effects than to dipolarity-polarizability of the solvent.[104] Also, the I_1/I_3 scale has been linearly correlated to the $E_T(30)$ parameter.[104] Correlations with the I_1/I_3 scale for the AZO (Fig. S11, ESI†) and ALS gelators (Fig. S12, ESI†), do not provide additional information than the $E_T(30)$ parameter. Similarly, for the MBD gelators, the same correlations are found with the I_1/I_3 scale (Fig. 9) and the $E_T(30)$ scale. In the case of HSA, both the $E_T(30)$ and I_1/I_3 scales show a region of sols with gel regions flanking it.

1.3 Global thermodynamic solvent properties

1.3.1 Hildebrand solubility parameter. For a solute–solvent pair, the molar Gibbs energy of mixing ΔG_m is related to the enthalpy of mixing ΔH_m and an entropy term $T\Delta S_m$. The Hildebrand solubility parameter, as proposed by Hildebrand and Scott[107] and Scatchard,[108] relies solely on the enthalpy ΔH_m (eqn (4)).

$$\Delta H_m = V\left(\left[\frac{\Delta E_1^v}{V_1}\right]^{1/2} - \left[\frac{\Delta E_2^v}{V_2}\right]^{1/2}\right)\phi_1\phi_2 \qquad (4)$$

Here V is the mixture volume, ΔE_i^v is the energy of vaporization, V_i is the molar volume, and ϕ_i is the volume fraction of component i.

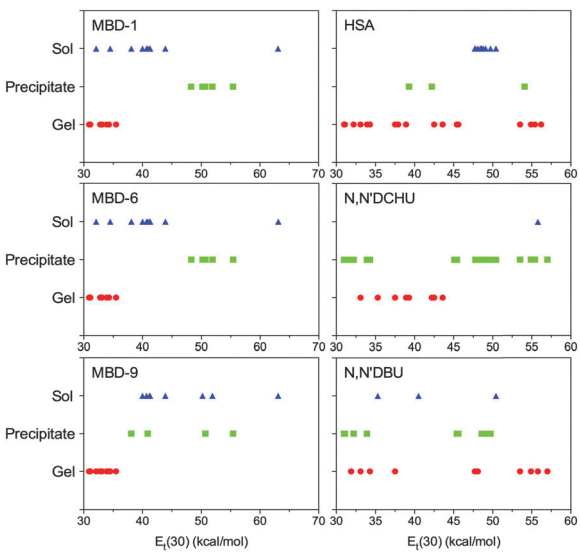

Fig. 8 The capacity of MDB, HSA and urea gelators to form gels, precipitates or solutions as a function of $E_T(30)$.

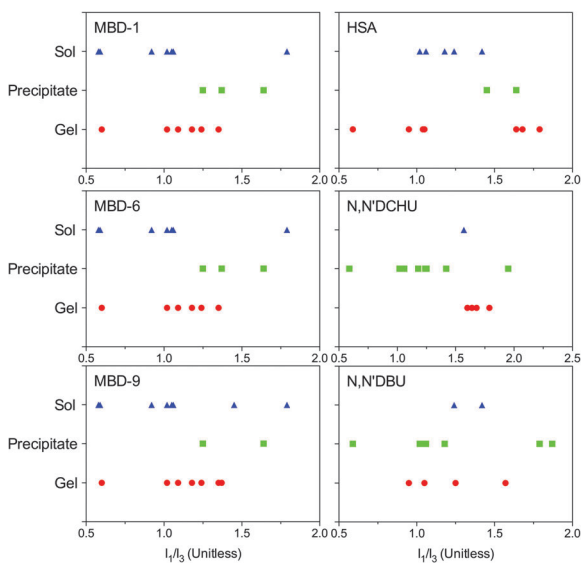

Fig. 9 The capacity of MDB, HSA and urea gelators to form gels, precipitates or solutions as a function of the Py scale.

Under conditions of isothermal vaporization of saturated liquid, the cohesive energy density (ΔE_i^v) is the negative of the energy of vaporization per cm^3 of sample, corresponding to the Hildebrand parameter, δ_I (eqn (5)).[109]

$$\delta_t = \left(\frac{\Delta E_i^v}{V_i}\right)^{1/2} \quad (5)$$

The cohesive energy combines the dispersion forces and polar interactions (including hydrogen bonding). The cohesive energy density has been shown to be important in determining whether a solvent will or will not promote self-assembly of amphiphiles.[110] It is related to the extent of intermolecular forces required to overcome solvent–solvent interactions.[111]

Previous studies have shown only weak correlations between gelation outcomes and δ_I; and only for small subsets of solvents.[57,61,112] For the gelators in Schemes 1–4, the same results hold. In the vast majority of gelators examined here (*i.e.*, HSA, DBS, *N*,*N*′-DBU, *N*,*N*′-DCHU (Fig. 10), and ALS (Fig. S13, ESI†), AZO (Fig. S14, ESI†), and MBD (Fig. S15, ESI†)), correlations between δ_i and gelation outcomes are very poor. The reason is that δ_i is only useful for low polarity solvents without hydrogen bonding.[113] CAB, a non-hydrogen-bond donating molecule, is the only gelator for which we see fairly good discrimination between sols, gels and precipitates (Fig. 10).

1.4 Conclusions derived for global solvent parameters

It is clear that global solvent parameters lack the specificity to predict gelation capabilities of a range of organogelators. While individual parameters may correlate well with individual gelators, global perspectives may not be derived from this class of solvent parameters. Considering a solvent as a macroscopic continuum characterized by a single physical constant (*e.g.*, dipole moment, dielectric constant, refractive index, *etc.*), solvatochormic shift, or Hildebrand solubility parameter is insufficient in predicting gelation behavior. Next, multi-term solvent parameters are considered, which can distinguish individual types of interactions and have been reported as better predictors of gelation.

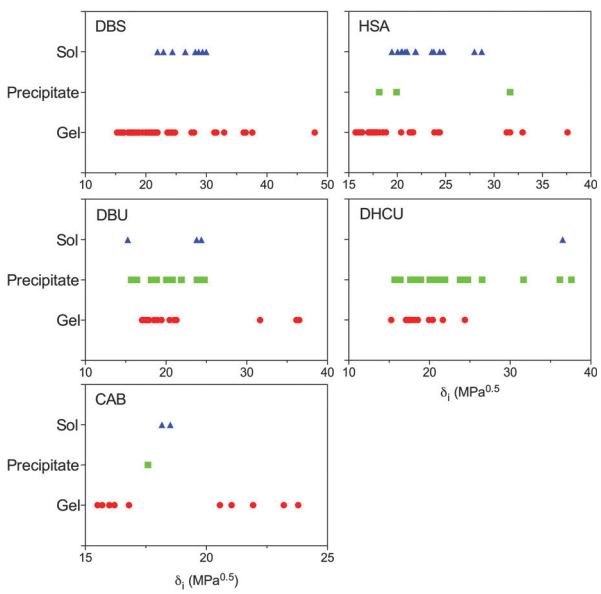

Fig. 10 The capacity of MDB, HSA and urea-based gelators to form gels, precipitates or solutions as a function of the Hildebrand solubility parameter.

Multi-term solvent parameters

Numerous multi-term parameters have been developed to define accurately solvent properties. These parameters attempt to separate the contributions of individual interactions such as ion–dipole, dipole–dipole, dipole induced-dipole, hydrogen bonding, electron pair donor–electron pair acceptor interactions (EPD/EPA), and solvophobic interactions. Examples include Kamlet–Taft,[114–119] Catalan[120–123] and Swain[116,124] solvatochromic parameters, as well as the Hansen,[58,75,125–129] Flory Huggins[130–133] and Modified Separation of Cohesive Energy Density Model (MOSCED)[134,135] thermodynamic models.

1.5 Multi-term solvatochromic solvent parameters

1.5.1 Kamlet–Taft solubility parameters. Kamlet–Taft parameters characterize a solvent with regards to its polarizability π, hydrogen-bond donating (the acidity parameter, α), and hydrogen-bond accepting (the basicity parameter, β) terms.[79,117,136,137] The polarizability parameter originates from electrostatic and dispersive interactions.[79,117,136,137] It is obtained using the spectra of either *p*-nitroanisole or *N*,*N*-dimethyl-*p*-nitroaniline (NNDN) (Fig. 11A) along with eqn (6).

$$\pi = \frac{\upsilon - 28.18}{-3.52} \quad (6)$$

The β parameter is specific to solute–solvent interactions where the solute plays the role of an electron-pair acceptor and the solvent is an electron-pair donor, while for the α parameter, the solute plays the role of an electron-pair donor and the solvent is an electron-pair acceptor.[79] The β parameter is determined using the difference in wavenumbers of the intensity maximum of the absorption bands between *p*-nitrophenol (ν_2) (Fig. 11B) and the non-hydrogen-bond accepting molecule, NNDN (ν_1) (eqn (7)).[136]

$$\beta = \frac{0.9841\nu_1 + 3.49 - \nu_2}{2.759} \quad (7)$$

The constants (in cm^{-1}) arise from a standardized value of 1 for hexamethylphosphoramide.[136] ν_1 is the frequency maximum of the NNDN UV-Vis absorption band (cm^{-1}), and the

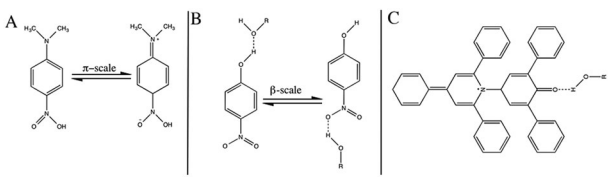

Fig. 11 Kamlet–Taft solvatochromic dyes in their solvent interacting forms, to determine the dipolarity/polarizability (π parameter) using *N*,*N*-dimethyl-*p*-nitroaniline (A), the hydrogen-bond accepting parameter using *p*-nitroaniline (β parameter) (B), and the hydrogen-bond donating parameter (α parameter) using the Dimroth–Reichardt betaine dye (C). Adapted from ref. 60.

constants (cm^{-1}) arise from normalization of the π parameter between 0.0 for cyclohexane and 1.0 for DMSO.[119] The α parameter is determined by the difference in the wavenumbers for the maximum intensities of the absorption bands for the Dimroth–Reichardt betaine dye (ν_3) (Fig. 11C), and for NNDN (ν_1) (eqn (8)).

$$\alpha = \frac{1.873\nu_1 - 74.58 + \nu_3}{5.47} \quad (8)$$

The constants are based upon a standardized value of 1 for methanol.[115]

Kamlet–Taft parameters have been applied to L-lysine bis-urea gelators to understand their capacity to form molecular gels.[137] The α parameter was correlated with gelling ability, while the β and π parameters had subsidiary roles: the magnitude of β affected the stability of the gel and π indicated the influence of fiber–fiber interactions.[137] More recently, Kamlet–Taft parameters have been used to show that 2,3-dihydroxycholestane-based steroids are incapable of gelling solvents with large α parameters while π is less important since solvents with both high and low polarizability could be gelled.[138]

In the present work, we have correlated the gelators from Schemes 1–4 with the Kamlet–Taft parameters. For DBS (Fig. 12), these parameters are quite effective at demarcating sol and gel regions. For example, sols fall in an intermediate range of polarizability π and electron-donating ability β. Also, when the α parameter of the solvents is close to 0, DBS forms a sol, whereas DBS gels the solvent when $\alpha > 0$. Similar to DBS, *N*,*N*′-DBU forms gels in solvents whose α parameters are sufficiently high (>0.7). Good demarcation is also seen for *N*,*N*′-DCHU: gels form in solvents with π parameters close to 0.75, intermediate β parameters (0.15 to 0.5) and α parameters close to 0. This is stark different from DBS and *N*,*N*′-DBU, where gels form in solvents when $\alpha > 0$. The difference is that DBS and *N*,*N*′-DBU are capable of π–π stacking interactions, whereas *N*,*N*′-DCHU is not. ALS gelators also show strong correlations with Kamlet–Taft parameters (Fig. 13). Much like DBS, gels are found in solvents of either low π (<0.5) or high π (>0.8). For $0.5 < \pi < 0.8$. For MBD gelators (Fig. S16, ESI†) and AZO gelators (Fig. S17, ESI†), outcomes were not well distinguished based on Kamlet–Taft parameters.

1.5.2 Catalan's solubility parameters. Catalan's multi-term solvatochromic parameters are similar to Kamlet–Taft's α, β, and π parameters, differing only in the use of an alternate series of probes/homomorphs.[120–122] Here, the three solvent parameters characterize solvent polarizability (SPP), solvent acidity (SA) and solvent basicity (SB). SPP is determined using the long wavelength absorption of 2-(dimethylamino)-7-nitrofluorene (DMANF) and its homomorph, 2-fluoro-7-nitrofluorene (FNF).[120] DMANF is sensitive to the polarizability while the homomorph FNF has a similar structure with much lower dipole moment because of the strong electron withdrawing fluorine atom. The difference between the maxima of the lowest energy absorption bands for DMANF and FNF ($\Delta\nu$) is determined for the solvent and with DMSO and cyclohexane as references SPP is then calculated using eqn (9).

$$\mathrm{SPP} = \frac{\Delta\nu_{(\mathrm{solvent})} - \Delta\nu_{(\mathrm{cyclohexane})}}{\Delta\nu_{(\mathrm{DMSO})} - \Delta\nu_{(\mathrm{cyclohexane})}} \quad (9)$$

The SB parameter is determined using the acidic molecule, 5-nitroindoline (NI), and its 'non-acidic' analogue, 1-methyl-5-nitroindoline (MNI), which lacks the amino group.[121] The SB parameter for a solvent is determined by eqn (10).

$$\mathrm{SB} = \frac{\Delta\nu_{(\mathrm{solvent})} - \Delta\nu_{(\mathrm{gas})}}{\Delta\nu_{(\mathrm{TMG})} - \Delta\nu_{(\mathrm{gas})}} \quad (10)$$

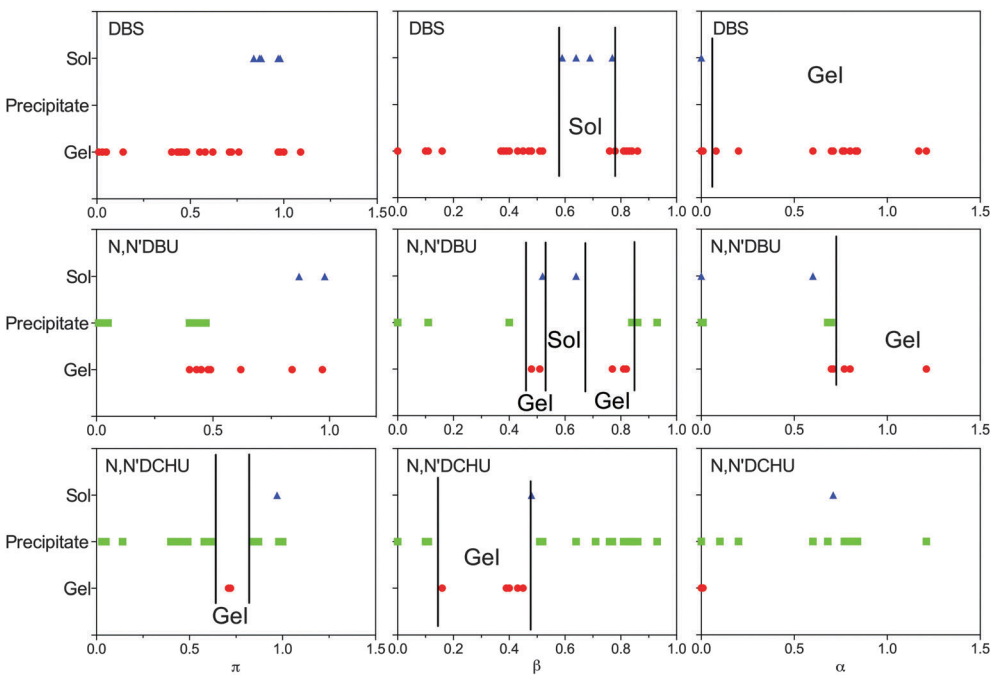

Fig. 12 The capacity of DBS and urea gelators to form gels, precipitates or solutions as a function of Kamlet–Taft parameters.

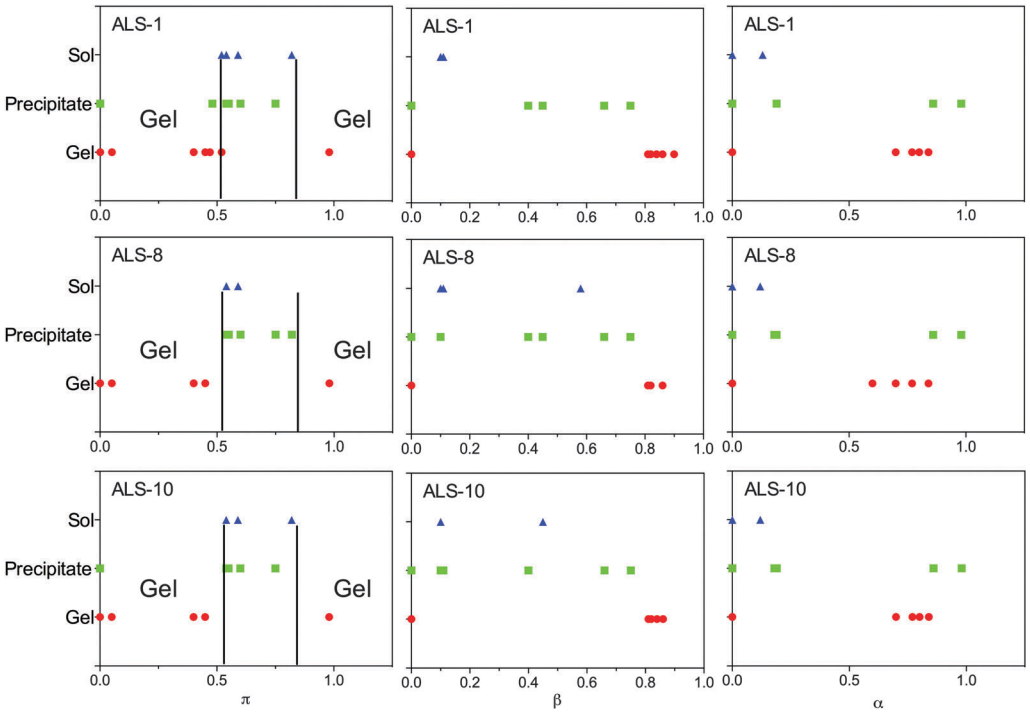

Fig. 13 The ability of ALS gelators to form gels, precipitates or solutions as a function of Kamlet–Taft parameters.

Here, $\Delta\nu_{(solvent)}$ is the difference between the maxima of the lowest energy absorption bands between 350 and 400 nm for NI and MNI, $\Delta\nu_{(TMG)}$ is the difference between the lowest energy absorption bands for NI and MNI in tetramethylguanidine (TMG), and $\Delta\nu_{(gas)}$ is the lowest energy absorption band in a series of *n*-alkanes and extrapolating the Lorenz–Lorentz function $f(n^2) = (n^2 - 1)/(n^2 + 1)$ $n = 0$.[120,123] Finally, the SA parameter is measured using a basic probe (*o*-*tert*-butylstilbazolium betaine, TBSB) and its 'non-basic' analogue (*o*,*o*-di-*tert*-butylstilbazolium betaine, DTBSB). The SA scale is set at 0.2 for ethanol (eqn (11)).

$$SA = \frac{\Delta\nu_{(solvent)} \times 0.4}{1299.9} \quad (11)$$

Catalan's parameters show some trends similar to those of the Kamlet–Taft parameters for the gelators in Schemes 1–4, although the demarcation into distinct sol, gel, and precipitate regions is not as good. Among the gelators in Fig. 14 (DBS, *N*,*N*′-DBU and *N*,*N*′-DCHU), the best demaracation is for *N*,*N*′-DCHU when examined with the SB parameter. That is, *N*,*N*′-DCHU gels are confined to solvents with an SB between 0.2 and 0.4; for both lower and higher SB, precipitates (or sols) form. MBD gelators do not show as convincing trends (Fig. S18, ESI†), and neither do the AZO (Fig. S19, ESI†) and ALS gelators (Fig. S20, ESI†).

1.6 Multi-term thermodynamic solvent parameters

1.6.1 Hansen solubility parameters. Hansen solubility parameters (HSPs) were devised to overcome the limitations of the Hildebrand solubility parameter that do not include the effects of specific intermolecular interactions such as polar and hydrogen-bonding.[126] To derive the HSPs, it is assumed that the energy of vaporization of a species, which is a measure of its total cohesive energy *E*, is the sum of three individual energetic components, *i.e.*, due to dispersion interactions (E_d), dipole–dipole interactions (E_p) and hydrogen-bonding interactions (E_h) (eqn (12)).

$$E = E_d + E_p + E_h \quad (12)$$

The dispersive component E_d dominates for simple, low polarity solvents such as saturated hydrocarbons. The second component E_p accounts for interactions due to polar groups on the solvent. Nitroparaffins, propylene carbonate, and tri-*n*-butyl phosphate are examples of solvents that are polar, but immiscible with water.[126] The third component E_h arises from hydrogen bonding interactions. Dividing eqn (12) by the molar volume (*V*) gives the square of the total HSP (which is identical to the Hildebrand solubility parameter) as the sum of squares of the individual HSP components (eqn (13) and (14)).

$$\frac{E}{V} = \frac{E_d}{V} + \frac{E_p}{V} + \frac{E_h}{V} \quad (13)$$

$$\delta_t^2 = \delta_d^2 + \delta_p^2 + \delta_h^2 \quad (14)$$

HSPs have been commonly used to select solvents for dissolving polymers.[139–141] However, their importance in new fields is rapidly emerging and they were first introduced to the field of molecular gels by Raynal and Bouteiller[75] in 2011. When considering a gelator in a given solvent, the HSPs of the solvent are typically known (*e.g.*, from Hansen's book);[125,126] however, the HSPs of the gelator are typically not known. The HSPs of the gelator may be estimated, *e.g.*, using the group contribution method, where it is assumed that the different functional groups that affect the energy of vaporization are additive. However,

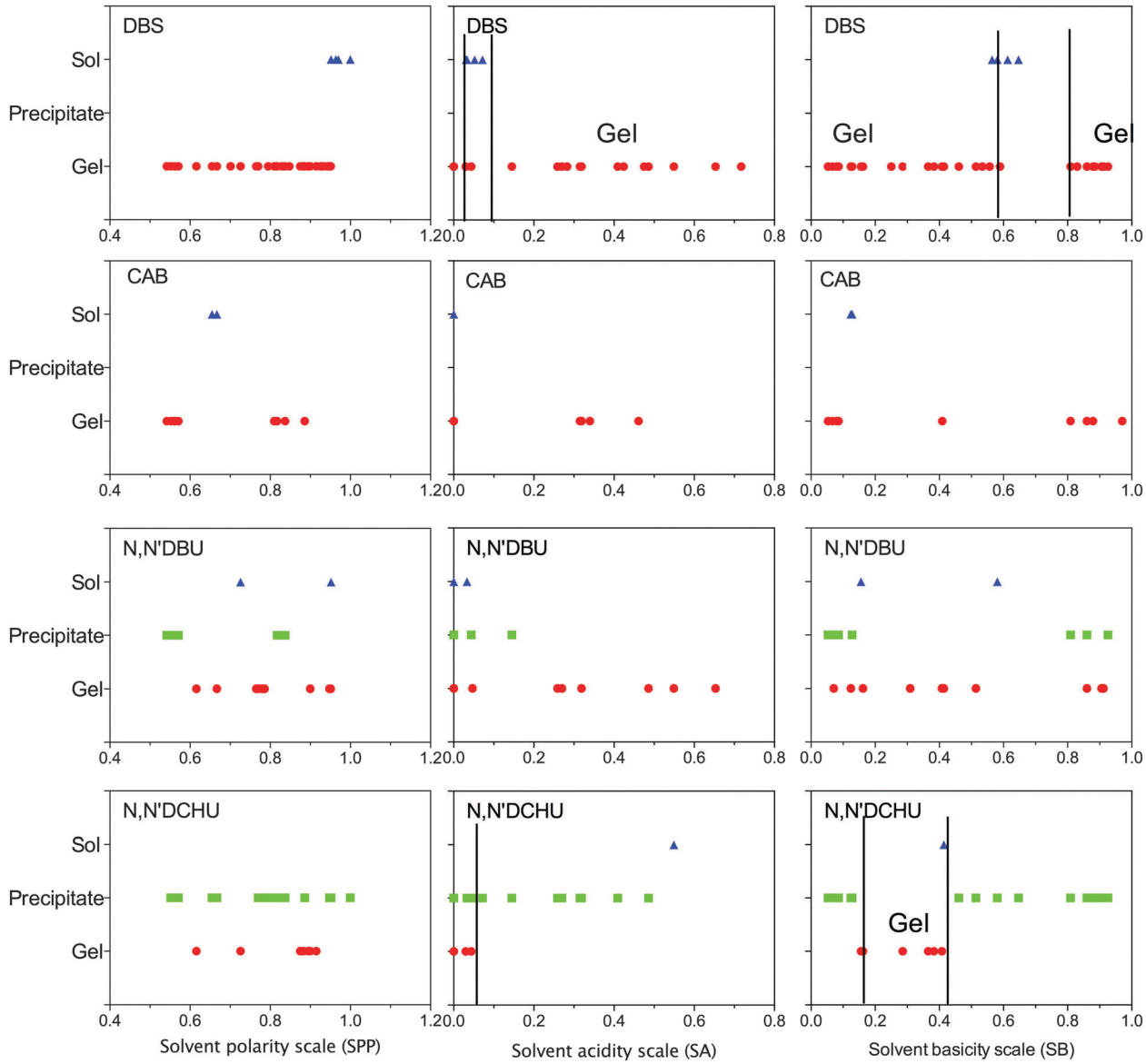

Fig. 14 The capacity of DBS, CAB, *N,N′*-DBU, *N,N′*-DCHU gelators to form gels, precipitates or solutions as a function of Catalan's SPP, SA, and SB parameters.

this method is seldom applicable for complex types of molecules such as most of the gelators shown in Schemes 1–4 because it does not differentiate among positional of stereo isomers.[109] We now discuss the correlation between sample outcomes (sol, gel, or precipitate) for gelator–solvent pairs *versus* each of the HSPs. This was done for the gelators in Schemes 1–4 and the results are shown in Fig. 15 and Fig. S21–S23 (ESI†). The dispersive HSP δ_d did not correlate with sample behavior for any gelator investigated. The correlation was better in the case of the polar HSP δ_p and the hydrogen-bonding HSP δ_h, *i.e.*, sample outcomes clustered over different regions of these parameters. For example, consider MBD-6 and MBD-9 (Fig. 15). These molecules form gels in solvents with low δ_p and precipitates in solvents with higher δ_p. Similar trends were observed in δ_h, also, with minor exceptions. Also, AZO-ME and AZO-BU form sols or gels in solvents with low δ_h and precipitates at high δ_h (the two points in the precipitate side refer to water and glycerol) (Fig. S21 and S22, ESI†). Note, however, that none of the HSPs is able to distinguish sols from gels.

1.6.2 Determining Hansen space. Although the correlation with individual HSPs is marginal, their key utility is manifested when they are examined in their entirety. Note that the three HSPs can each be treated as the three axes on a 3D plot, which is referred to as Hansen space. Each solvent is represented as a point in this space. In the context of polymer–solvent miscibility, the closer a polymer and a solvent are in Hansen space, the higher the probability that they are miscible.[126] To extend this approach to gelators, it is necessary to examine gelator–solvent outcomes in Hansen space. The idea was first proposed by Raynal and Bouteiller.[75] They noted that when data for a given gelator

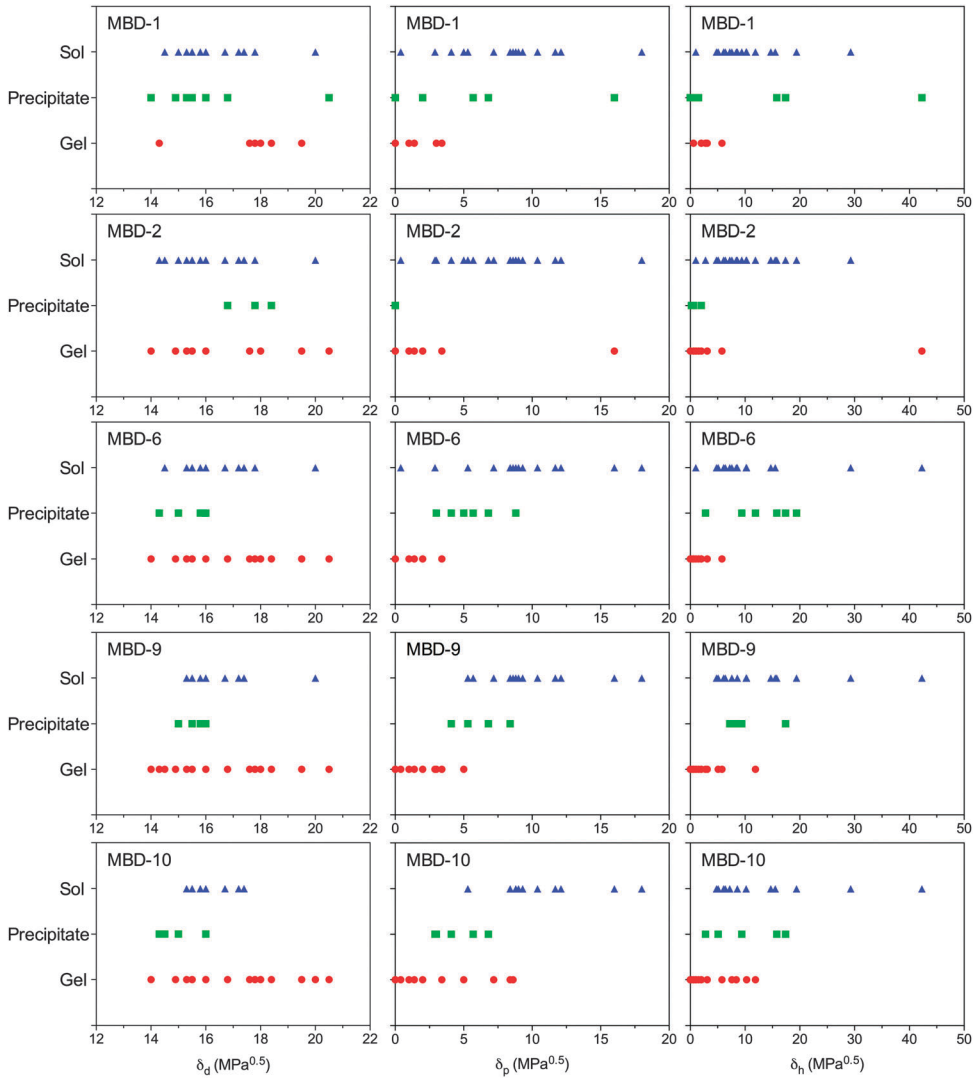

Fig. 15 The capacity of MBD derivatives to form gels, precipitates or solutions as a function of the dispersive Hansen solubility parameter (δ_d), polar Hansen solubility parameter (δ_p) and hydrogen-bonding Hansen solubility parameter (δ_h).

are plotted in Hansen space, one can discern clusters corresponding to solvents in which sols, gels, and precipitates are formed. The vast majority of the LMOG data sets analyzed so far have shown compact and globular domains.[129] Therefore, the observed clusters of points can be enclosed in spheres, following the methodology proposed by Hansen. For example, the sol sphere (S) encloses all (or most of) the solvents in which the gelator forms a sol, while excluding the solvents in which the gelator gives rise to a different outcome.

The parameters of the estimated spheres, *i.e.*, center location and radius, have been extensively used to improve the analysis and predictive ability of LMOG datasets, *e.g.*, calculation of the distance between the center of the sphere and particular solvents to optimize solvent selection.[56,60,75,129,142] Different approaches have been employed to obtain meaningful spheres that adequately characterize each domain. In this section the main features of the available methodologies will be discussed.

The HSPiP software, developed by Hansen, Abbott and Yamamoto, allows for the numerical determination of solution (or, alternatively, gel and precipitate) spheres and also provides 2D and 3D visualizations of the enclosed region.[143] This software was originally envisioned to find adequate, *i.e.*, effective and safe, solvents or solvent mixtures that solubilize specific polymers. It calculates the sphere that includes all the "good" solvents (defined in HSPiP as "inside" the sphere) and excludes all the "bad" solvents by implementing a minimization algorithm coupled with a desirability function that, in principle, reduces the likelihood of misclassifications. This specialized software does not allow the simultaneous estimation of several spheres. Therefore, estimations for different gelation outcomes have to be independently performed. For the estimation to run, the data set should include at least one outside ("bad") solvent. It should be noted that the selection of outside ("bad") solvent(s) from different domains during the single estimation of the sphere domain might yield different results depending on whether the

outside solvent is selected from an overlapping or distant location. The HSPiP software allows easy identification of wrongly classified data points (a feature provided only in this software). Thus, sequential running of this software aids in the identification of "outside" data sets and in obtaining reliable results. A reference value, *e.g.*, HSP parameters of the gelator, can be included during the estimations so that concentric spheres can be determined.

Bonnet *et al.*[129] have implemented a similar approach to the one provided by Hansen's HSPiP software using the Nelder–Mead optimization algorithm[144] and a default minimization routine, the Solver function, in Microsoft Excel (Microsoft Corporation, Seattle, WA). Although the parameters of the gelation sphere can be estimated using this simple method, only a 2D rendition of the distance to the center of the sphere is automatically plotted in this application. Additionally, and as the authors have pointed out, the robustness of the estimates highly depends on the completeness of the data set.[129]

Following the principles described by Hansen[126] and Bonnet *et al.*,[129] Lan *et al.*[60] have applied a global constrained optimization procedure programmed in Mathematica 9 (Wolfram Research, Champaign, IL) to calculate minimal enclosing spheres that contained all the points pertaining to each outcome, *i.e.*, solution, gel, and precipitate. This program uses the "NMinimize" built-in function in Mathematica to obtain the location of the center of each sphere while solving for the smallest possible radius. The NMinimize function was combined with a direct search method, namely differential evolution, to reach a numerical global optimum solution. The selection of this direct search method was based on its robustness despite being computationally more expensive. Any proficient user of this software can easily implement this program in Mathematica. It allows the simultaneous estimation of independent and concentric spheres and 2D and 3D plots can be included. Similar procedures can be programmed and implemented in alternative mathematical softwares.

The UMD Complex Fluids and Nanomaterials Laboratory's Hansen Solubility Parameter Data Fitting Software, developed by Diehn *et al.*,[128] is comprised of a user-friendly, self-explanatory, graphical interface that facilitates LMOG data analysis and visualization. Although this program has been coded using MATLAB (MathWorks, Natick, MA), no programing knowledge is needed and its use requires only the installation of the MATLAB Compiler Runtime (MCR – Version 8.1). The LMOG solubility data, displayed following a pre-set format, can be directly input from Excel spreadsheets, which facilitates its use. The UMD Complex Fluids HSP Program offers three fitting methods.

The "concentric sphere shell fit" method fits all categories radiating out from a center sphere (the solution sphere). This method first optimizes the fit of the solution sphere. The center of the solution sphere is then fixed as the optimal center and is used to estimate the radii of the subsequent classifications (gels, precipitates, *etc.*). The "non-concentric sphere shell fit" recalculates an optimal center for every data class. Finally, the "independent sphere fit" treats each sub-classification independently, optimizing the radius and center for each sphere. As in the case of the Hansen parameters, the UMD Complex Fluids HSP Program implements a desirability function that allows for the optimization of the radii of the spheres so that most of the data of a single category are included within the enclosed region at the same time that most of the data points corresponding to other categories are excluded.

Hansen's HSPiP software, Lan *et al.*'s approach and the UMD Complex Fluids HSP Program, have been used to obtain the individual spheres of 4 LMOG types—DBS, AZO-ET, ALS-10, and MBD-10. It should be pointed out that the same premises were employed when performing the estimations to facilitate the comparison of the outcomes. Although similar 3D plots for all tested LMOGs were obtained using the described methods (Fig. 16), the radii estimated using the UMD program are, in most cases, smaller than the ones reported using the two other approaches (Table 1). The implementation of the desirability function narrows the scope of the sphere, providing tighter regions where prediction reliability will be high. This feature will be extremely useful to predict the behavior of constrained data sets such as solvent mixtures. However, certain regions of the HSP 3D space might be mischaracterized if the data set is not sufficiently comprehensive. In the particular case of DBS,

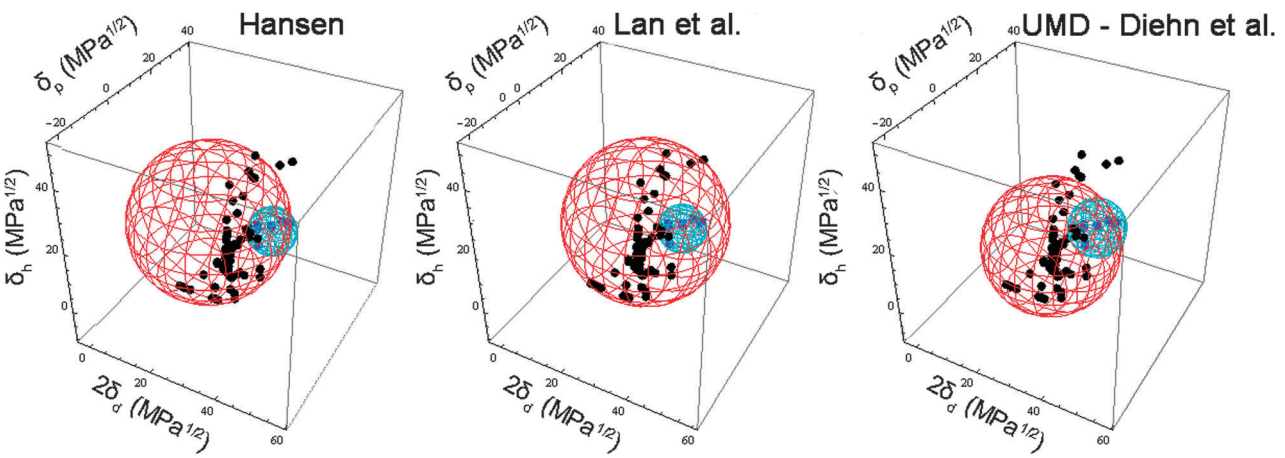

Fig. 16 Spherical regions corresponding to solution (blue), and gel (red) domains for DBS calculated using 3 different applications.

Table 1 Hansen coordinates for the center of the solution, gel and precipitate spheres and the radii of the spheres for the independent Hansen space plots estimated using the three described approaches

			Parameters			
Gelator	Sphere	Method	δ_D (MPa$^{1/2}$)	δ_P (MPa$^{1/2}$)	δ_H (MPa$^{1/2}$)	Radius (MPa$^{1/2}$)
DBS	SOLUTION	Hansen	18.3	17.5	7.8	5.5
		Diehn *et al.*	18.3	16.9	8.8	6.5
		Lan *et al.*	18.1	17.5	7.9	5.4
	GEL	Hansen	14.1	4.8	15.5	17.0
		Diehn *et al.*	15.5	6.3	9.0	14.8
		Lan *et al.*	15.4	10.9	12.0	17.8
AZO-ET	SOLUTION	Hansen	18.5	8.6	4.1	10.1
		Diehn *et al.*	17.5	3.9	1.0	9.1
		Lan *et al.*	18.5	7.9	5.1	9.9
	GEL	Hansen	15.3	7.0	10.7	12.8
		Diehn *et al.*	14.3	5.1	8.5	9.4
		Lan *et al.*	15.2	6.3	11.1	12.7
	PRECIPITATE	Hansen	16.5	14.0	35.8	7.1
		Diehn et al	17.9	13.0	30.5	7.4
		Lan *et al.*	16.5	14.1	35.8	7.1
ALS-10	SOLUTION	Hansen	17.1	2.5	4.8	4.6
		Diehn *et al.*	17.1	1.1	6.4	4.7
		Lan *et al.*	17.1	2.7	4.6	4.5
	GEL	Hansen	14.9	3.3	6.5	8.1
		Diehn *et al.*	16.0	3.7	7.5	6.4
		Lan *et al.*	16.1	3.0	7.0	7.6
	PRECIPITATE	Hansen	15.0	6.6	10.9	12.8
		Diehn *et al.*	15.9	7.5	13.8	6.2*
		Lan *et al.*	15.0	6.3	11.1	12.7
MBD-10	SOLUTION	Hansen	14.6	20.1	23.0	19.6
		Diehn *et al.*	16.4	16.5	21.3	15.8
		Lan *et al.*	16.5	12.7	23.6	19.1
	GEL	Hansen	17.6	4.1	5.1	8.5
		Diehn *et al.*	18.0	0.2	5.3	8.1
		Lan *et al.*	17.6	4.2	5.0	8.4
	PRECIPITATE	Hansen	15.1	4.8	10.2	7.8
		Diehn *et al.*	15.3	4.9	11.8	8.1
		Lan *et al.*	15.2	4.9	10.1	7.7

the approach taken by Lan *et al.* provides a gel sphere almost 20% larger than the one estimated by the UMD Program. The points corresponding to DBS in polyols are not included in the gel sphere estimated by the UMD program, which might be a result of the scarcity of data points in that region or a hint of a gel sub-class that should be further differentiated or a subset that should be excluded from the analysis. Different approaches to analyze the data will provide important and equally valuable information, such as the identification of broad regions for each domain to further scout solvent–gelator combinations *versus* identification of regions with extremely high predictability. Therefore, the data analysis tool should be selected based on the user's needs.

From the presented data, it can be inferred that not only magnitude but also directionality can play a role in predicting the behavior of an LMOG. It is reasonable to expect a progression from solutions to gels to precipitates which will be well-characterized by a concentric shell approach. However, relying *a priori* or solely on this assumption might result in loss of relevant information. Regardless of the approach selected, continuous efforts to increase the comprehensiveness of the data sets will result in more robust and reliable predictions. Until then, a careful and critical examination of the data sets to be fit should be conducted to obtain meaningful results.

1.6.3 Vector distance in Hansen distance. In turn, we can calculate R_{ij}, the vector distance in Hansen space from a solvent (j) to the center of the sol sphere (i). We refer to this as the Hansen distance, and it is calculated by eqn (15).

$$R_{ij} = \sqrt{4\left(\delta_{di} - \delta_{dj}\right)^2 + \left(\delta_{pi} - \delta_{pj}\right)^2 + \left(\delta_{hi} - \delta_{hj}\right)^2} \qquad (15)$$

Note that the factor of 4 for δ_d comes into play because typically the axis with the dispersive HSP is plotted as $2\delta_d$ for reasons of convenience described by Hansen.[125,126]

The relevance of R_{ij} is as follows: the greater the similarity in HSPs between a solvent (j) and a gelator (i), the shorter the Hansen distance R_{ij}. This implies a greater likelihood that a gelator will form a sol in a solvent with a short R_{ij}. Conversely, if the HSPs of the gelator and solvent are very different, it implies a long R_{ij}, and a precipitate is likely to be obtained. By extension then, a gel is formed when the gelator and solvent are moderately incompatible, *i.e.*, for moderate values of R_{ij}. Thus, R_{ij} allows us to

quantify the intermolecular interactions between a solvent and a gelator. We should point out that the gelator–solvent scenario is more complicated than that for polymers and solvents. This is because there are at least three possible outcomes in the gelator–solvent case: sol, gel, and precipitate. For the polymer–solvent case, the only outcomes considered are soluble *vs.* insoluble. The related complication for the gelator–solvent case arises when drawing the best-fit spheres in Hansen space for the various outcomes. The spheres corresponding to sol (S), gel (G), and precipitate (P) are typically not concentric. For the polymer–solvent case, only one sphere needs to be drawn, encompassing the soluble points, and so this complication is absent.

We now examine the sample outcomes (sol, gel, precipitate) for the gelators in Schemes 1–4. They are shown in Hansen space, *i.e.*, as 3-D plots, and the outcomes are also plotted on 2-D plots against R_{ij}. They were created using the software application developed by the Rogers group; the other software packages give similar results for the most part.

An excellent confinement of solutions was found within solubility sphere for DBS, HSA and CAB (Fig. 17). For DBS, none of the gel points was found in the solubility sphere. This can also be graphically represented using R_{ij}. Similar phenomena were observed for HSA where only 2 gel points were found within the solubility sphere. The gelation spheres appear to be less effective in determining the ability to cluster points in Hansen space. Only in the gelation sphere of CAB were all the solution points excluded. The other two gel spheres fail to exclude solution points and precipitate points. We offer three possible explanations: (1) few solvents formed solutions, resulting in poorly defined solution spheres; (2) the gelation ability is not equally sensitive to the three individual HSP components; (3) the presence of outliers or data pertaining to additional subsets not excluded during estimations might have caused overlapping. Similar observations have been found in a previous study where the magnitude of R_{ij} of two urea gelators is about the same, while yielding completely different material states in the same solvent:[56] 1,3-dibutylurea (R_{ij} = 11.5 MPa$^{0.5}$; δ_d = 17.1 MPa$^{0.5}$, δ_p = 9.5 MPa$^{0.5}$, δ_h = 7.9 MPa$^{0.5}$) formed a solution in benzene while *N*,*N*′-dibenzylurea (R_{ij} = 11.3 MPa$^{0.5}$; δ_d = 19.2 MPa$^{0.5}$, δ_p = 9.2 MPa$^{0.5}$, δ_h = 8.3 MPa$^{0.5}$) formed a gel.

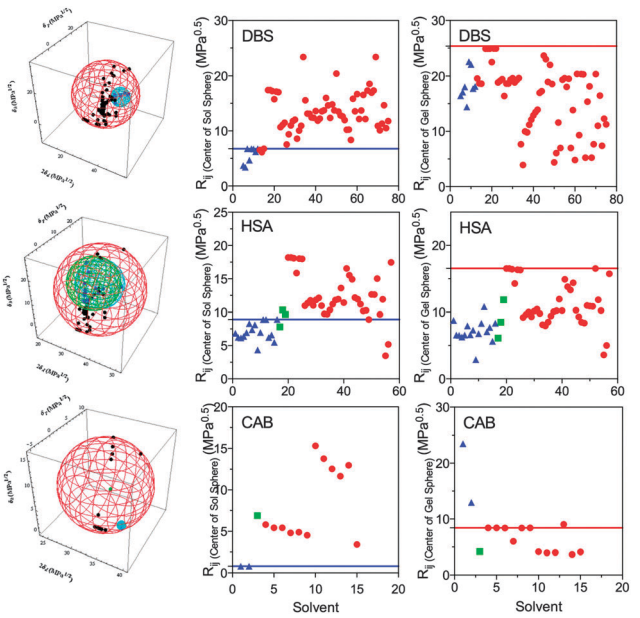

Fig. 17 3D Hansen space (left) and distances to the center of sol spheres (middle) and gelation spheres (right) for miscellaneous gelators. The blue horizontal lines represent the radii of solubility spheres, and red lines represent the radii of gel spheres.

Good confinement for the solubility spheres of the ALS gelators was also observed (Fig. S24, ESI†). For ALS-8, the solubility sphere limits the inclusion of all gels and precipitates and for ALS-10, a few exceptions of gel and precipitate were found inside the solubility sphere. It was observed that ALS-1 was able to dissolve in a broader range of solvents and the size of its solubility sphere is three times bigger than those of ALS-8 and ALS-10. This comportment may be a result of the different linker groups; for example, ALS-1 has an ether and an ester groups and ALS-8 has an ester group only.[82] By removing the ether group, the radius of the solubility sphere is decreased from 12.9 MPa$^{0.5}$ (ALS-1) to 4.5 MPa$^{0.5}$ (ALS-8). Additionally, ALS-1 could be dissolved in aromatic solvents such as benzene, toluene and styrene (which also dissolved ALS-8 and ALS-9), as well as in more polar solvents including 2-ethanolamine and hexanoic acid.[82] For MBD gelators, no good confinement within the solubility or gelation spheres was observed; however, comparisons can still be made between different MBD isomers (Fig. S25, ESI†). Unlike AZO gelators, where solubility spheres, gelation spheres and precipitation spheres were similar in size and position between different derivatives (Table 2), those of MBD gelators varied significantly, revealing the importance and challenges that chirality and geometric isomerization pose to gelation ability.

From the data presented, it can be inferred that not only magnitude but also the directionality of R_{ij} can play a role in predicting the behavior of an LMOG. This is clear for DBS and MBD-10 (Fig. 18) where both gelators have excellent confinement in Hansen Space using the UMD software; however, for MDB-10 this does not translate to a clear correlation with R_{ij}. It is reasonable to expect a progression from solutions to gels to precipitates, which will be well characterized by a concentric shell approach. However, and as it was mentioned before, relying *a priori*, or solely, on this assumption might result in loss of relevant information. Regardless of the approach selected, continuous efforts to increase the comprehensiveness of the data sets will result in more robust and reliable predictions.

1.6.4 Modified Separation of Cohesive Energy Density Model (MOSCED) model. MOSCED (MOdified Separation of Cohesive Energy Density) is a thermodynamic model that was first proposed to predict limiting activity coefficients (γ^{∞}'s) using only pure component parameters.[145] Several versions of MOSCED models have been reported.[134,146,147] The most updated revision and extension of the parameters was done in 2005 to include binary systems of low polarity, polar and hydrogen-bonding compounds.[134] MOSCED utilizes 5 adjustable parameters

Table 2 Hansen coordinates ($MPa^{0.5}$) for the center of the solution, gel and precipitate spheres as well as the radii of the spheres for AZO and ALS gelators

	Solution				Gel				Precipitate			
Gelator	$2\delta_d$	δ_p	δ_h	R_{sphere}	$2\delta_d$	δ_p	δ_h	R_{sphere}	$2\delta_d$	δ_p	δ_h	R_{sphere}
AZO Me	36.9	7.7	5.4	10.0	30.4	6.3	11.1	12.7	32.9	14.1	35.8	7.1
AZO Et	36.9	7.9	5.1	9.9	30.4	6.3	11.1	12.7	32.9	14.1	35.8	7.1
AZO Pr	36.9	7.9	5.1	9.9	30.4	6.3	11.1	12.7	32.9	14.1	35.8	7.1
AZO Bu	37.0	7.9	5.1	9.9	31.7	6.2	11.1	12.9	32.9	14.1	35.8	7.1
AZO Pe	37.0	7.9	5.1	9.9	31.7	6.2	11.1	12.9	32.9	14.0	35.8	7.1
ALS 1	34.8	7.8	10.9	12.9	31.3	3.4	8.7	9.4	31.9	5.6	13.0	14.3
ALS 6	35.2	4.4	4.6	6.0	32.3	3.4	8.7	9.4	31.9	5.6	13.0	14.3
ALS 8	35.6	2.7	4.2	3.6	34.3	3.2	6.9	7.9	30.0	6.3	11.1	12.7
ALS 9	34.2	2.7	4.6	4.5	32.2	3.0	7.0	7.6	30.0	6.3	11.1	12.7
ALS 10	34.2	2.7	4.6	4.5	32.2	3.0	7.0	7.6	30.0	6.3	11.1	12.7

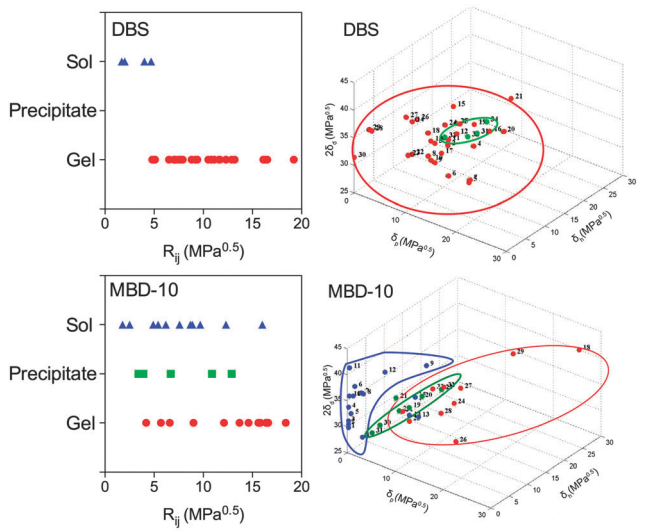

Fig. 18 R_{ij} and UMD software groupings in Hansen space for DBS and MBD-10.

(λ, τ, q, α and β) to characterize the energy of interaction of a solute in solution. These 5 parameters are partly derived from experimental values and partly fitted to experimental data. The original formulations of MOSCED are shown below (eqn (16)–(22)). MOSCED parameters can be considered as modifications of Hansen solubility parameters, which divides the regular solubility parameters into three components—dispersion, polarity and hydrogen bonding. Analyses of sample outcomes by MOSCED improved the poor performance of the Hansen model for associated and solvating systems.[134]

$$\ln\gamma_2^{\infty} = \frac{v_2}{RT}\left((\lambda_1-\lambda_2)^2 + \frac{{q_1}^2{q_2}^2\left(\tau_1^{T}-\tau_2^{T}\right)^2}{\phi_1} + \frac{\left(\alpha_1^{T}-\alpha_2^{T}\right)\left(\beta_1^{T}-\beta_2^{T}\right)}{\xi_1}\right] + d_{12} \quad (16)$$

$$d_{12} = \ln\left(\frac{v_2}{v_1}\right)^{aa} + 1 - \left(\frac{v_2}{v_1}\right)^{aa} \quad (17)$$

$$aa = 0.953 - 0.002314\left((\tau_2^{T})^2 + \alpha_2^{T}\beta_2^{T}\right) \quad (18)$$

$$\alpha^{T} = \left(\frac{293\ K}{T}\right)^{0.8},\ \beta^{T} = \left(\frac{293\ K}{T}\right)^{0.8},\ \tau^{T} = \left(\frac{193\ K}{T}\right)^{0.4} \quad (19)$$

$$\varphi_1 = POL + 0.0002629\left(\alpha_1^{T}\beta_1^{T}\right) \quad (20)$$

$$\xi_1 = 0.68(POL-1) + \left[3.24 - 2.4\exp\left(-0.002687\left(\alpha_1\beta_1\right)^{1.5}\right)\right]^{(293\ K/T)^2} \quad (21)$$

$$POL = {q_1}^4\left[1.15 - 1.15\exp\left(-0.002337\left(\tau_1^{T}\right)^3\right)\right] + 1 \quad (22)$$

The adjustable parameters for each molecule are the dispersion parameter λ, the polarity parameter τ, the induction parameter q, the hydrogen-bond acidity α and the hydrogen-bond basicity parameter β. Eqn (17) is the combinatorial Flory–Huggins expression with the empirically derived exponent aa calculated from eqn (18). Eqn (19) describes the temperature dependence of α, β and τ. The φ_1 and ξ_1 are empirical asymmetry terms calculated from eqn (20)–(22).[134]

The dispersion parameter λ describes the polarizability of a molecule. The polarity parameter τ measures the fixed dipole of a compound in a solution. The induction parameter q measures the dipole-induced dipole and induced dipole-induced dipole interactions that can be found in molecules with large dispersion (polarizability) parameters, such as halogenated compounds and aromatic compounds. The strong interaction of dispersion forces tends to lessen the dipolar interaction, leading to decreased values of q (*i.e.*, <1). For aromatic compounds, q is arbitrarily set to 0.9; for halogenated compounds, q is varied for best fit. The acidity and basicity parameters α and β account for specific interactions from hydrogen bond formation through both association and solvation.[134]

The MOSCED parameters are effective at discerning solvents that resulted in different material states (Fig. 19). For DBS, albeit the differentiation of dispersion parameter λ is not perfect, useful trends can still be observed: solvents with relatively higher λ values or higher polarizability are more likely to form sols. Similar conclusions were drawn from the Kamlet–Taft π parameter and Catalan's SPP parameter as noted previously. It appears that both the acidity and basicity are important in determining the final states formed upon cooling for DBS. Gels tended to form

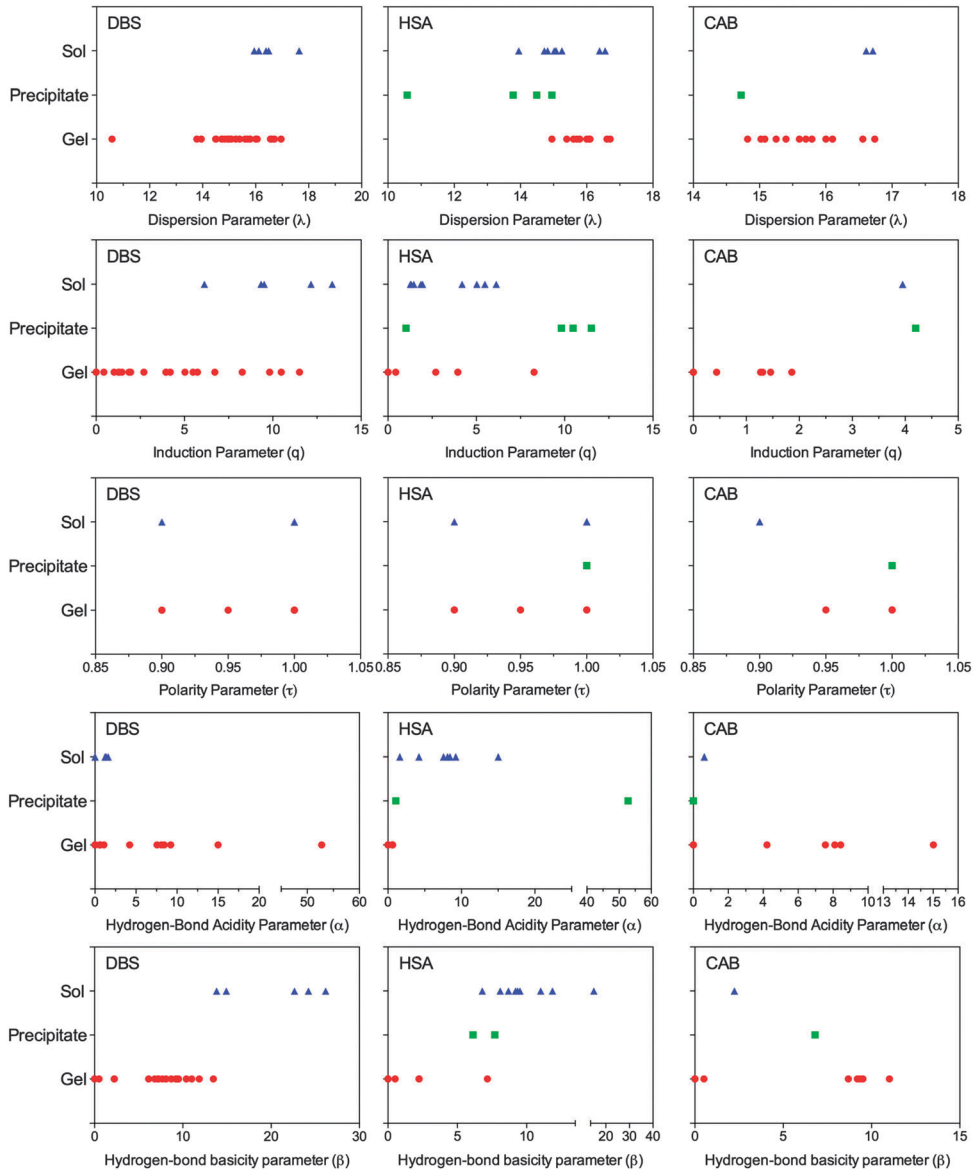

Fig. 19 Ability of DBS, HSA and CAB to form gels, precipitates or solutions as a function of the MOSCED parameters.

in more acidic solvents, while solvents that formed sols resided at very low α values ($\alpha < 2$). There is a stark difference between the basicity parameter of solvents that formed gels *vs.* sols. Gels clustered at low and β values ($\beta < 13$), while solvents that formed solutions resided at relatively higher region when $\beta > 13$. MOSCED parameters also predict the gelation behavior of HSA very well. The dispersion parameter λ differentiated gels from precipitates but not from sols, and α seems to be an important parameter. All gel points clustered at $\alpha < 1$, where solvents have very low acidities. This behavior is interesting when compared with DBS, whose gels formed in both very low and high acidity ranges. The enhanced gelation capability of DBS is a result of its ability to form a wider variety of non-covalent interactions than can HSA (whose primary driving force for aggregation is hydrogen bonding and van der Waals interactions). In solvents with high acidity, aromatic groups promote insolubility and π–π interactions aid formation of SAFIN structures. Although some correlations were also found with CAB, convincing conclusions could not be drawn due to the small number of data points. Similar trends involving acidity and basicity parameters α and β were observed for the two urea gelators (Fig. S26, ESI†). For both, gels were observed in weakly acidic solvents; precipitates formed in more acidic solvents. The basicity parameter β seems to be more promising at differentiating material states for *N*,*N*′-DBU. At low ($\beta < 2.23$) and intermediate ($7.8 < \beta < 12$) regions of the β scale, precipitates formed. All gels clustered between $2.23 < \beta < 7.8$ and solutions formed in very basic solvents (*i.e.*, $\beta > 14$). The same trend for the basicity parameters was obtained with *N*,*N*′-DCHU except that no solution data was available.

For the AZO gelators, the hydrogen-bond acidity and basicity parameters α and β are most important (Fig. S27, ESI†). Solvents that resulted in solutions clustered at low α and β values.

Good separation between gels and solutions was observed for AZO-ME and AZO-BU based on the β scale where the cut off points are 7 and 5, respectively. When comparisons were made within AZO groups, it was found that when the length of the aliphatic side chain was increased, the homologue was able to gel a broader range of solvents based on the α and β scales. This behavior is ascribed to the decreased solubility in high acidity and basicity solvents in the presence of longer aliphatic side chains that promote epitaxial growth of fibers.

Compared to AZO gelators, the replacement of more polar azobenzene group to less polar anthraquinonyl group (ALS derivatives) limits the gelation ability of ALS derivatives, and more precipitates were also observed (Fig. S28, ESI†). MOSCED parameters showed some evidence in predicting gelation behaviors of ALS derivatives. Solvents with lower polarizability tended to form precipitates and either gels or sols formed in highly polarizable solvents. Good separation of points for precipitates from the other two material states was observed with λ, but not between gels and sols. Gels also tended to cluster with low values of q when dipolar interactions in solvents are weaker. The hydrogen-bond acidity parameter α seemed able to separate gels from other material states only for ALS-10. Although the differences among the behaviors of the ALS derivatives may involve the natures of the C-17 alkyl side chains,[82] the reason is not yet clear.

For MBD-based gelators, only the hydrogen-bond acidity and basicity parameters α and β have good correlations with gelation behaviors (Fig. S29, ESI†). Solvents with low acidity ($\alpha < 4.2$) tended form gels for all MBD derivatives, and solvents with high acidity ($\alpha > 4.2$) were more likely to form precipitates. Solvents that resulted in gels tended to cluster at low β values for *gluco* (MBD-1) and *manno* (MBD-6) isomers. The *galacto* isomer (MBD-10) was able to gel solvents with both low ($\beta < 3.3$) and intermediate ($7 < \beta < 9.5$) β values. The enhanced gelation ability is attributed to the geometric isomerization; however, details of the reason are unclear. From these observations, it is clear that MOSCED parameters can be useful tools to predict the gelation behaviors of different gelators, and that hydrogen-bond acidity and basicity of solvents are especially important in determining whether SAFiN structures will be formed in a particular solvent.

1.7 Conclusions derived from multi-term solvent parameters

The ability to differentiate solvents capable of being gelled by a particular gelator, remaining as solutions or forming precipitates is better when using multi-term solvent parameters than when using global solvent parameters. Although the most significant insights gleened involve the ability to accept or donate a hydrogen bond, other important conclusions and insights are available from analyses of other parameters.

General classification of solvents using a multivariate statistical treatment of quantitative solvent parameter

Organic solvents have been classified by a Fage nonhierarchical, multivariate, statistical method using eight solvent variables that include the Kirkwood function, molecular refraction, dipole moment, the Hildebrand parameter, index of refraction, boiling point, and HOMO and LUMO energies.[148] Using this approach, 83 solvents were categorized into 9 classes: aprotic dipolar, aprotic highly dipolar, aprotic highly dipolar and highly polarizable, aromatic low-polarity, aromatic relatively polar, electron pair donating, hydrogen bonding, strongly-associated hydrogen bonding, and others that do not fit into one of the categories mentioned.[148] Because the solvents are classified using their physical properties rather than their chemical structure, some oddities are observed, such as CCl_4 being classified as an 'aromatic polar solvent'. This statistical approach is not intended to develop an all-encompassing and rigid classification, but, instead, a quantitative, logical approach to solvent classification.[148] Using it, we have identified solvents that were included in their analysis and with the data sets which have been the focus of this review. Thus, parameters that are insensitive to predicting self-assembly of molecular gels, when combined, become useful in grouping material states. For example, DBS is incapable of crystallizing only in aprotic highly dipolar solvents and in all other solvent categories DBS will form gels (Table 3).

In the case of HSA, similar groupings are observed: it remains in the solution state in aprotic highly dipolar, hydrogen bonding and hydrogen bonding self-associating solvents (Table 4). In comparison, it is likely that DBS relies on π–π stacking in the hydrogen bonding and hydrogen bonding self-associating solvents. HSA is capable of gelling the aromatic apolar, aromatic polar, electron pair donor and most of the aprotic dipolar solvents. In a similar manner to DBS, the only category to have overlapping results is the aprotic dipolar solvents, where both precipitates and gels are observed.

For the MBD gelators, the ability to differentiate gel states is less apparent (Table 5). It is clear that MBD-1 forms solutions in both aprotic dipolar and aprotic highly dipolar solvents and gels in aromatic apolar and aromatic polar solvents. However, in the electron pair donor, hydrogen boding and hydrogen bonding self-associating solvents, either sols or precipitates are observed. With more advanced clustering tools or more refined solvent categories, predictability may be enhanced, allowing for

Table 3 DBS solution (blue), precipitate (green) and gel (red) states clustered using a Fage nonhierarchical multivariate statistical method using eight solvent variables[148]

Aprotic	Aprotic highly	Aprotic highly	Aromatic	Aromatic
Acetonitrile	DMSO	N/A	Benzene	Benzyl
Butyronitril	DMF		Toluene	1-Octanol
Propionitrile	NMP		Xylene	
Acetone	Pyridine			
3-Pentanone				
Ethyl				

Electron	Hydrogen	Hydrogen	Misc.
Dioxane	Ethanol	Formamide	CCl_4
	Butanol	Glycol	
	Isopropanol	Diethylene	
	1-Propanol		
	Isobutanol		
	1-Pentanol		

Table 4 HSA solution (blue), precipitate (green) and gel (red) states clustered using a Fage nonhierarchical multivariate statistical method using eight solvent variables[148]

Aprotic	Aprotic highly	Aprotic highly	Aromatic	Aromatic
Acetonitrile	Pyridine	N/A	Benzene	CCl_4
Butyronitrile			Toluene	
Propionitrile			Xylene	
Acetone				
3-Pentanone				

Electron pair	Hydrogen	Hydrogen	Misc.
Hexane	Ethanol	NMF	N/A
Cyclohexane	Butanol	Diethylene	
Triethylamine	Isopropanol		
Dioxane	Isobutanol		
	2-Pentanol		
	1-Pentanol		

Table 5 MBD-1 solution (blue), precipitate (green) and gel (red) states clustered using a Fage nonhierarchical multivariate statistical method using eight solvent variables[148]

Aprotic	Aprotic	Aprotic highly	Aromatic	Aromatic
Acetonitrile	Nitrobenzene	N/A	Benzene	Diphenyl
Acetone			Toluene	CCl_4
Butanone			Xylene	
Acetic				
Methyl acetate				
Ethyl acetate				
CH_2Cl_2				

Electron pair	Hydrogen	Hydrogen	Misc.
Hexane	Ethanol	Glycol	Carbon
Cyclohexane	Butanol		$CHCl_3$
Triethylamine	1-Propanol		
Diethyl ether			

very useful *a priori* tools which provide deeper insights into the structure-function mechanisms that govern the formation of fibrillar aggregates in different organic solvents.

Cluster analysis of dual solvent parameter data to assess their combined predictive ability

The use of cluster analysis of dual solvent parameter data sets has been proposed as a means to pinpoint synergistic parameter combinations with enhanced predictive ability. This approach provides, in principle, a way to assess the relevance of pair (or higher order) parameter combinations in the design of novel molecular gels.

As has been presented in previous sections, individual solvent parameters, including physical solvent properties and thermodynamic solvent parameters can predict gelation outcomes only to a limited extent. The availability of larger data sets on organogelators will allow additional data analyses to extract important information that is difficult to attain using limited databases. Cluster analysis is an unsupervised learning technique that allows the organization of a collection of data points, in our case solvent parameter combinations, into clusters based on a distance or dissimilarity function. The capability of the combinations to predict gelator behavior can be evaluated based on their probability to group data points pertaining to a single type of outcome (solution, gel or precipitate) into distinctive clusters. This technique requires some minimal data pre-processing. For example, to avoid larger-scale parameters to dominate others, each parameter is commonly normalized by mean removal and

Table 6 Classification of DBS–solvent mixtures based on cluster analyses using two solvent parameters and the degree of their predictability as %

	sa	sb	spp	Et30	Py	FH	Rij	dtotal	d	h	p	HD/A	A	HD	alpha	beta	pi	Henry	RI	DI	Dipole	logP
sa		40	38	42	50	59	43	41	60	38	65	45	42	42	48	48	55	50	48	71	50	46
sb			38	37	42	46	41	44	39	39	36	57	37	40	43	41	45	47	45	46	42	44
spp				47	42	53	37	46	46	37	46	69	38	38	42	50	61	60	45	39	57	45
Et30					56	72	46	42	48	44	42	41	47	40	54	46	44	51	50	45	57	37
Py						56	44	48	56	48	52	63	46	50	50	44	62	41	58	48	48	57
FH							66	46	47	53	60	59	47	55	52	58	60	49	50	53	61	41
Rij								65	45	49	74	61	50	60	50	40	66	75	64	71	48	52
dtotal									61	60	50	43	50	42	50	43	49	50	56	67	53	57
d										58	66	46	42	53	50	40	52	53	58	56	50	62
h											76	41	48	42	43	40	45	46	56	67	50	51
p												55	61	71	53	60	69	55	64	47	36	49
HD/A													40	47	52	48	46	53	54	41	61	44
A														43	48	48	54	48	52	66	51	43
HD															48	48	46	42	43	39	51	42
alpha																59	48	48	52	50	47	52
beta																	40	42	48	43	47	44
pi																		61	58	70	56	50
Henry																			51	62	55	44
RI																				59	50	53
DI																					55	39
Dipole																						50
logP																						

SA, SB and SPP are Catalan parameters; $E_T(30)$ is Reichardt's parameter; Py corresponds to the shift in pyrene absorbance; FH is the Flory Huggins Parameter; R_{ij} is the distance in Hansen space; D_{total} is the total Hansen solubility parameter; d, h and p are the individual HSPs; HD/A is the hydrogen bond donor/acceptor ratio; alpha, beta and pi are Kamlet–Taft parameters; Henry is Henry's law constant; DI is the dielectric constant; Dipole is the dipole moment of the solvent; log *P* is the octanol/water partitioning coefficient.

variance scaling prior to the classification stage. Cluster analysis then can be performed using, for example, a k-medoids algorithm (related to k-means algorithm). This clustering technique can be programmed in most mathematical software, such as Mathematica, which through an iterative approach finds a local optimum clustering. Several distance functions can be used to reflect dissimilarity between two data points. Although the Euclidean distance (*i.e.*, square root of the sums of the squares of the differences between the coordinates of the points in each dimension) is often used, other distance functions such as Canberra or Chebyshev's functions are commonly implemented. It should be noted that utilization of centroid based algorithms, such as the k-medoids, for classification requires specification in advance of the number of output clusters. In our case, the number of output clusters was set to 3, which accounts for all possible outcomes—solution, gel or precipitate for our samples.

The predictive ability of the solvent parameter pair combinations for DBS, evaluated based on the percentage of correct grouping, is presented in Table 6. As can be observed, several of the solvent parameter pairings did not cluster the solvents effectively into their appropriate group, producing values slightly above those that can attributed to random grouping. That is the case for all the combinations of the Kamlet–Taft β parameter with any of the Hansen solubility parameters; values are 40–43%. This analysis also corroborates findings reported in previous sections, in which the performance of R_{ij} as a classification criterion was enhanced by its pairing with additional parameters such as Flory–Huggins, HLC and dielectric constant. These pairings consistently placed $>60\%$ of the solvents into their appropriate cluster. The results also point out that parameters that do not allow an appropriate classification alone, such as most of the physical properties parameters, might produce better outcome estimations when combined with other parameters. The combinations may reflect polarity and/or the gelation mechanism more completely than individual solvent properties.

The effectiveness of this kind of statistical data analysis relies on the availability of comprehensive, well-curated data sets. However, the preliminary results presented here suggest that the applicability of particular combinations might not be universal since parameters that are better related to the mechanism of gelation will also have a better performance on the classification.

Conclusions

It is apparent that without consideration of the solvent properties, the ability to develop *a priori* tools for designing new and unique molecular gels, as well to gain truly fundamental understanding of the driving forces for epitaxial growth, will continue to be unsuccessful. Clearly, global solvent parameters lack the specificity to predict gelation capacity for organogelators with diverse structures. Although individual parameters may correlate well with individual gelators, global perspectives may not be derived from this approach. Considering a solvent as a macroscopic continuum, characterized by a single physical constant (*e.g.*, dipole moment, dielectric constant, refractive index, *etc.*), solvachormic shift, or Hildebrand solubility parameter is insufficient in predicting gelation behavior. Although multi-term solvent parameters drastically improve the predictive abilities of solvent gelator states, they are far from perfect; however, they greatly aid in understanding the mechanism of assembly. True insights into developing *a priori* tools will only be garnered when developing complex relationships between numerous solvent parameters. However, the benefits of greater accuracy afforded by this kind of analysis must be considered in terms of the additional analytical procedures that must be applied and the balance will have to be determined by the information sought.

Acknowledgements

MAR would like to acknowledge support from NSERC (371824-2009) entitled mechanisms of self-assembly in nanostructure edible oils. RGW would like to acknowledge the National Science Foundation (Grant CHE-1147353) for its financial support of the research performed at Georgetown.

Notes and references

1 R. G. Weiss and P. Térech, in *Molecular Gels: Materials with Self-Assembled Fibrillar Networks*, ed. R. G. Weiss and P. Térech, Springer, Dordrecht, The Netherlands, 2006, pp. 1–12.
2 D. Jordan Lloyd, *Colloid Chemistry*, The Chemical Catalog Company Inc., New York, 1926.
3 T. Graham, *Philos. Trans. R. Soc. London*, 1861, **151**, 183–224.
4 R. B. Dean, *Modern Colloids*, D. Van Nostrand Co., New York, 1948.
5 P. H. Hermans, in *Colloid Science*, ed. H. R. Kruyt, Elsevier, Amsterdam, 1949, ch. XII, vol II, p. 484.
6 J. D. Ferry, *Viscoelastic Properties of Polymers*, Wiley, New York, 1961.
7 P. J. Flory, *Faraday Discuss.*, 1974, **57**, 7–18.
8 Y. Wu, S. Wu, G. Zou and Q. Zhang, *Soft Matter*, 2011, **7**, 9177–9183.
9 A. Bui and N. Virgilio, *Ind. Eng. Chem. Res.*, 2013, **52**, 14185–14191.
10 R. Y. Wang, P. Wang, J. L. Li, B. Yuan, Y. Liu, L. Li and X. Y. Liu, *Phys. Chem. Chem. Phys.*, 2013, **15**, 3313–3319.
11 F. P. Duval, J. P. M. van Duynhoven and A. Bot, *J. Am. Oil Chem. Soc.*, 2006, **83**, 905–912.
12 D. Farbi, J. Guan and A. Cesaro, *Thermochim. Acta*, 1998, **321**, 3–16.
13 P. Terech, I. Furman and R. G. Weiss, *J. Phys. Chem.*, 1995, **99**, 9558–9566.
14 S. R. Raghavan and B. H. Cipriano, in *Molecular Gel. Materials with Self-Assembled Fibrillar Networks*, ed. R. G. Weiss and P. Terech, Springer, Netherlands, 2006, pp. 214–252.
15 R. G. Weiss, *J. Am. Chem. Soc.*, 2014, **136**, 7519–7530.

16 Y.-C. Lin, B. Kachar and R. G. Weiss, *J. Am. Chem. Soc.*, 1989, **111**, 5542–5551.
17 D. J. Abdallah, S. A. Sirchio and R. G. Weiss, *Langmuir*, 2000, **16**, 7558–7561.
18 P. Terech and R. G. Weiss, *Chem. Rev.*, 1997, **97**, 3133–3159.
19 M. A. Rogers, A. J. Wright and A. G. Marangoni, *Curr. Opin. Colloid Interface Sci.*, 2009, **14**, 33–42.
20 M. A. Rogers, A. J. Wright and A. G. Marangoni, *Soft Matter*, 2008, **4**, 1483–1490.
21 M. A. Rogers and A. G. Marangoni, *Cryst. Growth Des.*, 2008, **8**, 4596–4601.
22 R. Lam, L. Quaroni, T. Pederson and M. A. Rogers, *Soft Matter*, 2010, **6**, 404–408.
23 X.-Y. Lui, P. D. Sawant, W. B. Tan, I. B. M. Noor, C. Pramesti and B. H. Chem, *J. Am. Chem. Soc.*, 2002, **124**, 15055–15063.
24 J. L. Li and X. Y. Lui, *Adv. Funct. Mater.*, 2010, **20**, 3196–3216.
25 P. Jonkheijm, P. van der Schoot, A. P. H. J. Schenning and E. W. Meijer, *Science*, 2006, **313**, 80–83.
26 X. Y. Liu and P. D. Sawant, *ChemPhysChem*, 2002, **4**, 374–377.
27 X. Y. Liu and P. D. Sawant, *Adv. Mater.*, 2002, **14**, 421–426.
28 B. Yuan, J.-L. Li, X. Y. Liu, Y.-Q. Ma and Y. J. Wang, *Soft Matter*, 2012, **8**, 5187–5193.
29 M. M. J. Smulders, A. P. H. J. Schenning and E. W. Meijer, *J. Am. Chem. Soc.*, 2008, **130**, 606–611.
30 Z. Chen, A. Lohr, C. R. Saha-Möllera and F. Würthner, *Chem. Soc. Rev.*, 2009, **38**, 564–584.
31 C. Kulkarni, S. Balasubramanian and S. J. George, *ChemPhysChem*, 2013, **114**, 661–673.
32 A. Dawn, T. Shiraki, S. Haraguchi, S.-i. Tamaru and S. Shinkai, *Chem. – Asian J.*, 2011, **6**, 266–282.
33 M. A. Rogers, S. Abraham, F. Bodondics and R. G. Weiss, *Cryst. Growth Des.*, 2012, **12**, 5497–5504.
34 A. Pal, S. Abraham, M. A. Rogers, J. Dey and R. G. Weiss, *Langmuir*, 2013, **29**, 6467–6475.
35 V. A. Mallia and R. G. Weiss, *J. Phys. Org. Chem.*, 2014, **27**, 310–315.
36 S. Abraham, Y. Lan, R. S. H. Lam, D. A. S. Grahame, J. J. H. Kim, R. G. Weiss and M. A. Rogers, *Langmuir*, 2012, **28**, 4955–4964.
37 D. A. S. Grahame, C. Olauson, R. S. H. Lam, T. Pedersen, F. Borondics, S. Abraham, R. G. Weiss and M. A. Rogers, *Soft Matter*, 2011, **7**, 7359–7365.
38 M. A. Rogers and R. G. Weiss, *New J. Chem.*, 2015, **39**, 785–799.
39 H. Takeno, T. Mochizuki, K. Yoshiba, S. Kondo and T. Dobashi, in *Gels: Structures, Properties, and Functions – Fundamentals and Applications*, ed. M. Tokita and K. Nishinari, 2009, vol. 136, pp. 47–53.
40 C. A. Elliger, D. G. Guadagni and C. E. Dunlap, *J. Am. Oil Chem. Soc.*, 1972, **49**, 536–537.
41 X. Huang and R. G. Weiss, *Tetrahedron*, 2007, **63**, 7375–7385.
42 M. Kamijo, H. Nagase, T. Endo, H. Ueda and M. Nakagaki, *Anal. Sci.*, 1999, **15**, 1291–1292.
43 T. Kuwahara, H. Nagase, T. Endo, H. Ueda and M. Nakagaki, *Chem. Lett.*, 1996, 435–436.
44 R. S. H. Lam and M. A. Rogers, *Cryst. Growth Des.*, 2011, **11**, 3593–3599.
45 M. Lescanne, P. Grondin, A. d'Aleo, F. Fages, J.-L. Pozzo, O. M. Monval, P. Reinheimer and A. Colin, *Langmuir*, 2003, **20**, 3032–3041.
46 V. A. Mallia, M. George, D. L. Blair and R. G. Weiss, *Langmuir*, 2009, **25**, 8615–8625.
47 V. A. Mallia, H.-I. Seo and R. G. Weiss, *Langmuir*, 2013, **29**, 6476–6484.
48 M. A. Rogers, S. Abraham, F. Bodondics and R. G. Weiss, *Cryst. Growth Des.*, 2012, **12**, 5497–5504.
49 M. A. Rogers and A. G. Marangoni, *Langmuir*, 2009, **25**, 8556–8566.
50 M. A. Rogers, T. Pedersen and L. Quaroni, *Cryst. Growth Des.*, 2009, **9**, 3621–3625.
51 T. Tachibana and H. Kambara, *J. Colloid Interface Sci.*, 1968, **28**, 173–178.
52 T. Tachibana, T. Mori and K. Hori, *Bull. Chem. Soc. Jpn.*, 1980, **53**, 1714–1719.
53 P. Terech, *J. Phys. II*, 1992, **2**, 2181–2195.
54 P. Terech, V. Rodriguez, J. D. Barnes and G. B. McKenna, *Langmuir*, 1994, **10**, 3406–3418.
55 S. Wu, J. Gao, T. Emge and M. A. Rogers, *Cryst. Growth Des.*, 2013, **13**, 1360–1366.
56 Y. Lan, M. G. Corradini and M. A. Rogers, *Cryst. Growth Des.*, 2014, **14**, 4811–4818.
57 G. Zhu and J. S. Dordick, *Chem. Mater.*, 2006, **18**, 5988–5995.
58 J. Gao, S. Wu and M. A. Rogers, *J. Mater. Chem.*, 2012, **22**, 12651–12658.
59 M. George and R. G. Weiss, *Langmuir*, 2003, **19**, 1017–1025.
60 Y. Lan, M. G. Corradini, X. Liu, T. E. May, F. Borondics, R. G. Weiss and M. A. Rogers, *Langmuir*, 2014, **30**, 14128–14142.
61 A. R. Hirst and D. K. Smith, *Langmuir*, 2004, **20**, 10851–10857.
62 M. Suzuki, Y. Nakajima, M. Yumoto, M. Kimura, H. Shirai and K. Hanabusa, *Langmuir*, 2003, **19**, 8622–8624.
63 P. Zhu, X. Yan, Y. Su, Y. Yang and J. Li, *Chem. – Eur. J.*, 2010, **16**, 3176–3183.
64 I. Furman and R. G. Weiss, *Langmuir*, 1993, **9**, 2084–2088.
65 J. Gao, S. Wu, T. Emge and M. A. Rogers, *CrystEngComm*, 2013, **15**, 4507–4515.
66 S. Wu, J. Gao, T. Emge and M. A. Rogers, *Soft Matter*, 2013, **9**, 5942–5950.
67 R. Wang, C. Geiger, L. Chen, B. Swanson and D. G. Whitten, *J. Am. Chem. Soc.*, 2000, **122**, 2399–2400.
68 Y. Jeong, K. Hanabusa, H. Masunaga, I. Akiba, K. Miyoshi, S. Sakurai and K. Sakurai, *Langmuir*, 2005, **21**, 586–594.
69 G. Qing, X. Shan, W. Chen, Z. Lv, P. Xiong and T. Sun, *Angew. Chem.*, 2014, **126**, 2156–2161.
70 X. Wang and M. Liu, *Chem. – Eur. J.*, 2014, **20**, 10110–10116.

71 M.-M. Su, H.-K. Yan, L.-J. Ren, P. Zheng and W. Wang, *Soft Matter*, 2014, **11**, 741–748.
72 X. Chen, P. Fei, K. A. Cavicchi, W. Yan and N. Ayres, *Colloid Polym. Sci.*, 2014, **292**, 477–484.
73 D. Dasgupta, S. Srinivasan, C. Rochas, A. Ajayaghosh and J.-M. Guenet, *Soft Matter*, 2011, **7**, 9311–9315.
74 M. Bielejewski, J. Kowalczuk, J. Kaszyńska, A. Łapiński, R. Luboradzki, O. Demchuk and J. Tritt-Goc, *Soft Matter*, 2013, **9**, 7501–7514.
75 M. Raynal and L. Bouteiller, *Chem. Commun.*, 2011, **47**, 8271–8273.
76 K. Fan, L. Niu, J. Li, R. Feng, R. Qu, T. Liu and J. Song, *Soft Matter*, 2013, **9**, 3057–3062.
77 L. Niu, J. Song, J. Li, N. Tao, M. Lu and K. Fan, *Soft Matter*, 2013, **9**, 7780–7786.
78 A. J. Parker, *Chem. Rev.*, 1969, **69**, 1–32.
79 A. R. Katritzky, D. C. Fara, H. Yang, K. Tämm, T. Tamm and M. Karelson, *Chem. Rev.*, 2004, **104**, 175–198.
80 C. Reichardt and T. Welton, *Solvents and Solvent Effects in Organic Chemistry*, Wiley-VCH, Weinheim, Germany, 4th edn, 2011.
81 K. Murata, M. Aoki, T. Suzuki, T. Harada, H. Kawabata, T. Komori, F. Ohseto, K. Ueda and S. Shinkai, *J. Am. Chem. Soc.*, 1994, **116**, 6664–6676.
82 R. Mukkamala and R. G. Weiss, *Langmuir*, 1996, **12**, 1474–1482.
83 K. Yoza, N. Amanokura, Y. Ono, T. Akao, H. Shimnmori, M. Takeuchi, S. Shinkai and D. N. Reinhoudt, *Chem. – Eur. J.*, 1999, **5**, 2722–2729.
84 N. Amanokura, K. Yoza, H. Shinmori, S. Shinkai and D. N. Reinhoudt, *J. Chem. Soc., Perkin Trans. 2*, 1998, 2585–2592.
85 M. George, G. Tan, V. T. John and R. G. Weiss, *Chem. – Eur. J.*, 2005, **11**, 3243–3254.
86 D. R. Lide, *CRC Handbook of Chemistry and Physics*, CRC Press, Boca Raton, FL, 2005.
87 J. Makarevic, M. Jokic, B. Peric, V. Tomisic, B. Kojic-Prodic and M. Zinic, *Chem. – Eur. J.*, 2001, **7**, 3328–3341.
88 Y.-C. Lin and R. G. Weiss, *Macromolecules*, 1987, **20**, 414–417.
89 G. John, G. Zhu, J. Li and J. S. Dordick, *Angew. Chem., Int. Ed.*, 2006, **45**, 4772–4775.
90 A. Brizard, R. Oda and I. Huc, *Top. Curr. Chem.*, 2005, **256**, 167–215.
91 A. Brizard, D. Berthier, C. Aime, T. Buffeteau, D. Cavagnat, L. Ducasse, I. Huc and R. Oda, *Chirality*, 2009, **21**, E153–E162.
92 T. Sakurai, Y. Masuda, H. Sato, A. Yamagishi, H. Kawaji, T. Atake and K. Hori, *Bull. Chem. Soc. Jpn.*, 2010, **83**, 145–149.
93 P. V. Vassil, R. W. Malcolm and W. Chi-Huey, *Chem. Commun.*, 1998, 1865–1866.
94 A. Bot, R. den Adel, E. Roijers and C. Regkos, *Food Biophys.*, 2009, **4**, 266–272.
95 M. Pal and J. Dey, *RSC Adv.*, 2014, **4**, 17521–17525.
96 J. Sangster, *J. Phys. Chem. Ref. Data*, 1989, **18**, 1111–1227.
97 J. Staudinger and P. V. Robers, *Chemosphere*, 2001, **44**, 561–576.
98 PubChem Compound Summaries. National Center for Biotechnology Information, U.S. National Library of Medicine, http://www.ncbi.nlm.nih.gov/guide, Bethesda, MD, 2009.
99 L. G. S. Brooker, G. H. Keyes and D. W. Heseltine, *J. Am. Chem. Soc.*, 1951, **73**, 5350–5356.
100 N. S. Bayliss and E. G. McRae, *J. Phys. Chem. B*, 1954, **58**, 1002–1006.
101 C. Reichardt, *Solvents and Solvent Effects in Organic Chemistry*, VCH, Weinheim, Germany, 2nd edn, 1988.
102 J. Kaszynska, A. Lapinski, M. Bielejewski, R. Luboradzki and J. Tritt-Goc, *Tetrahedron*, 2012, **68**, 3803–3810.
103 C. Reichardt, *Green Chem.*, 2005, **7**, 339–351.
104 D. C. Dong and M. A. Winnik, *Can. J. Chem.*, 1984, **62**, 2560–2565.
105 D. C. Dong and M. A. Winnik, *Photochem. Photobiol.*, 1982, **35**, 17–21.
106 K. W. Street Jr. and W. E. Acree Jr., *J. Liq. Chromatogr.*, 1986, **9**, 2799–2808.
107 J. H. Hildebrand and R. L. Scott, *The Solubility of Non-electrolytes*, Dover Publications, Reinhold, NY, 3rd edn, 1959.
108 G. Scatchard, *Chem. Rev.*, 1949, **44**, 7–35.
109 *Solubility Parameter Values*, ed. E. A. Grulke, John Wiley & Sons, NewYork, 4th edn, 2005.
110 A. F. M. Barton, *Chem. Rev.*, 1975, **75**, 731–753.
111 Y. L. Greaves and C. J. Drummond, *Chem. Soc. Rev.*, 2013, **42**, 1096–1120.
112 H. Xu, J. Song, T. Tian and R. Feng, *Soft Matter*, 2010, **8**, 3478–3486.
113 S. Liu, W. Yu and C. Zhou, *Soft Matter*, 2013, **9**, 864–874.
114 T. Yokoyama, R. W. Taft and M. J. Kamlet, *J. Am. Chem. Soc.*, 1976, **98**, 3233–3237.
115 R. W. Taft and M. J. Kamlet, *J. Am. Chem. Soc.*, 1976, **98**, 2886–2894.
116 R. W. Taft, J.-L. M. Abboud and M. J. Kamlet, *J. Org. Chem.*, 1984, **49**, 2001–2005.
117 A. E. Lagalante, C. Wood, A. M. Clarke and T. J. Bruno, *J. Solution Chem.*, 1998, **27**, 887–900.
118 M. J. Kamlet and R. W. Taft, *J. Am. Chem. Soc.*, 1976, **98**, 377–383.
119 M. J. Kamlet, J. L. Abboud and R. W. Taft, *J. Am. Chem. Soc.*, 1977, **99**, 6027–6038.
120 J. Catalan, V. Lopez, P. Perez, R. Martin-Willamil and J.-G. Rodriguez, *Liebigs Ann. Chem.*, 1995, **1995**, 241–252.
121 J. Catalan, C. Diaz, C. Lopez, P. Perez, J.-L. G. de Paz and J.-G. Rodriguez, *Liebigs Ann. Chem.*, 1996, **1996**, 1785–1794.
122 J. Catalan and C. Diaz, *Liebigs Ann. Chem.*, 1997, **1997**, 1941–1949.
123 J. Catalan, *Chem. Phys. Lett.*, 1994, **223**, 159–161.
124 C. G. Swain, M. S. Swain, A. L. Powell and S. Alunni, *J. Am. Chem. Soc.*, 1983, **105**, 502–513.
125 C. M. Hansen, 2013, http://www.Hansen-Solubility.com.
126 C. M. Hansen, *Hansen Solubility Parameters*, CRC Press, Boca Raton, FL, 2nd edn, 2007.

127 C. M. Hansen, *Prog. Org. Coat.*, 2004, **51**, 77–84.
128 K. K. Diehn, H. Oh, R. Hashemipour, R. G. Weiss and S. R. Raghavan, *Soft Matter*, 2014, **10**, 2632–2640.
129 J. Bonnet, G. Suissa, M. Raynal and L. Bouteiller, *Soft Matter*, 2014, **10**, 3154–3160.
130 T. Lindvig, M. L. Michelsen and G. M. Kontogeorgis, *Fluid Phase Equilib.*, 2002, **203**, 247–260.
131 P. J. Flory, *Principles of Polymer Chemistry*, Cornell University Press, Ithaca, NY, 1953.
132 P. J. Flory, *J. Chem. Phys.*, 1949, **17**, 223–240.
133 P. J. Flory, *J. Chem. Phys.*, 1941, **9**, 660–661.
134 M. J. Lazzaroni, D. Bush, C. A. Eckert, T. C. Frank, S. Gupta and J. D. Olson, *Ind. Eng. Chem. Res.*, 2005, **44**, 4075–4083.
135 E. R. Thomas and C. A. Eckert, *Ind. Eng. Chem. Process Des. Dev.*, 1984, **23**, 194–209.
136 V. T. Wyatt, B. Bush, J. Lu, J. P. Hallett, C. L. Liotta and C. A. Eckert, *J. Supercrit. Fluids*, 2005, **36**, 16–22.
137 W. Edwards, C. A. Lagadec and D. K. Smith, *Soft Matter*, 2011, **7**, 110–117.
138 V. C. Edelsztein, A. S. Mac Cormack, M. Ciarlantini and P. H. Di Chenna, *Beilstein J. Org. Chem.*, 2013, **9**, 1826–1836.
139 C. Hansen and A. L. Smith, *Carbon*, 2004, **42**, 1591–1597.
140 C. M. Hansen, *Prog. Org. Coat.*, 1995, **26**, 113–120.
141 T. A. Misev, *J. Coat. Technol.*, 1975, **63**, 23–28.
142 N. Yan, Z. Xu, K. K. Diehn, S. R. Raghavan, J. Fang and R. G. Weiss, *J. Am. Chem. Soc.*, 2013, **135**, 8989–8999.
143 S. Abbott and C. Hansen, *Hansen Solubility Parameters (HSP) Application Notes: Hansen Solubility parameters in Practice*, Hansen-Solubility.com, 2013.
144 F. Gharagheizi, *J. Appl. Polym. Sci.*, 2007, **103**, 31–36.
145 E. R. Thomas and C. A. Ecker, *Ind. Eng. Chem. Process Des. Dev.*, 1984, **23**, 194–209.
146 M. J. Hait, C. L. Liotta and C. A. Eckert, *Ind. Eng. Chem. Res.*, 1993, **32**, 2905–2914.
147 W. J. Howell, A. M. Karachewski, K. M. Stephenson and C. A. Eckert, *Fluid Phase Equilib.*, 1989, **52**, 151–160.
148 M. Chastrette, M. Rajzmann, M. Chanon and K. F. Purcell, *J. Am. Chem. Soc.*, 1985, **107**, 1–11.

Supplemental Information

To Gel or Not to Gel: Correlating Molecular Gelation with Solvent Parameters

*Yaqi Lan,[1] Maria G. Corradini,[1] Richard G. Weiss,[2] Srinivasa R. Raghavan,[3] Michael A. Rogers[4]**

1) School of Environmental and Biological Sciences, Rutgers University, New Brunswick, NJ, 08901, USA.

2) Department of Chemistry and Institute for Soft Matter Synthesis and Metrology, Georgetown University, Washington, DC, 20057, USA.

3) Department of Chemical & Biomolecular Engineering, University of Maryland, College Park, MD, 20742, USA.

4) Department of Food Science, University of Guelph, Guelph, Ontario, N3C3X9, Canada.

* Corresponding Author: Prof. Michael A Rogers; Department of Food Science; University of Guelph; email: mroger09@uoguelph.ca; ph: 519-824-4120 ext. 54327

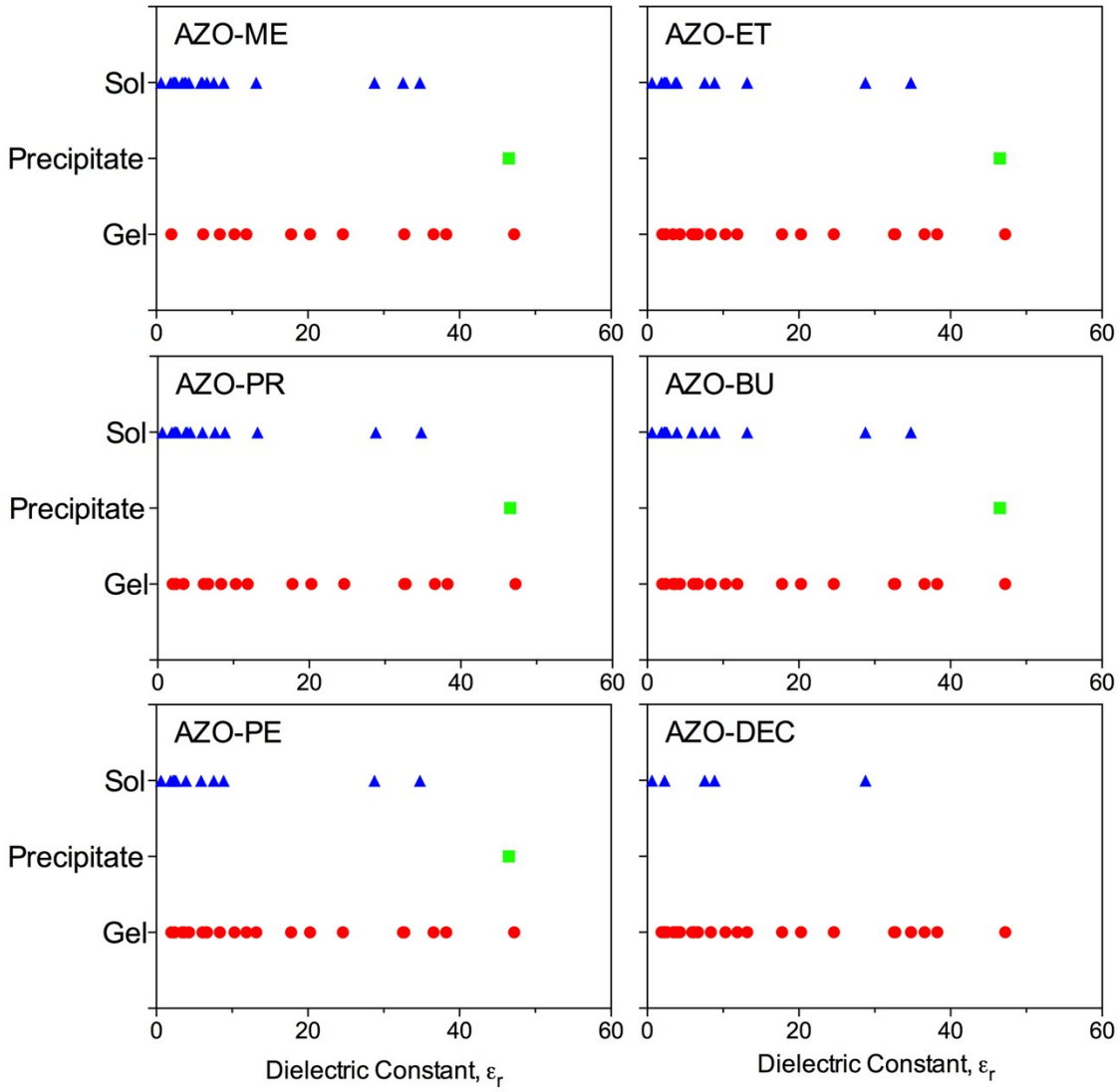

Figure S1: The capacity of the AZO derivatives (scheme 1) to form gels, precipitates or solutions as a function of the static relative permittivity of the solvents.

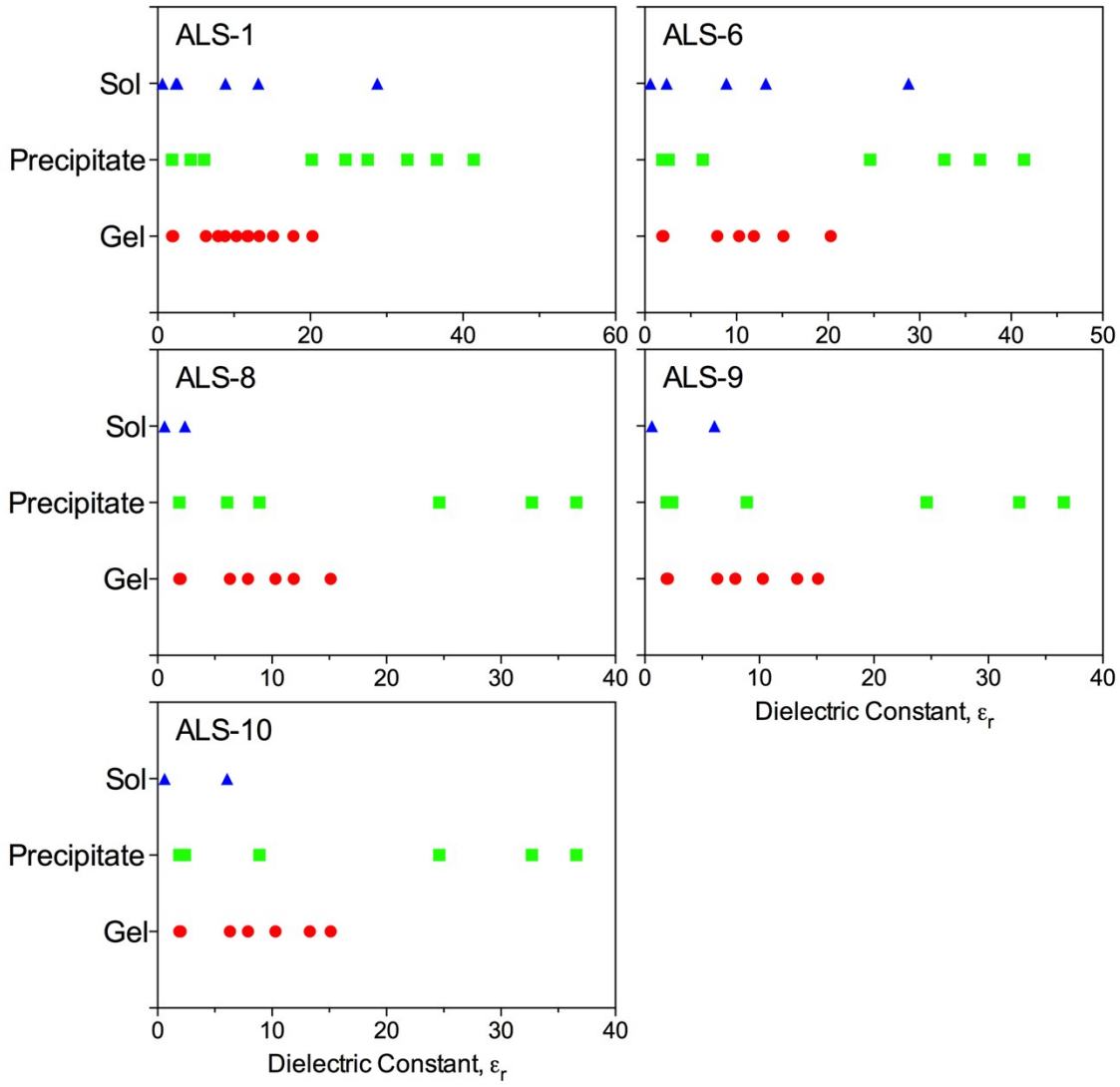

Figure S2: The capacity of the ALS gelators (Scheme 2) to form gels, precipitates or remain as solutions as a function of the static relative permittivity of the solvents.

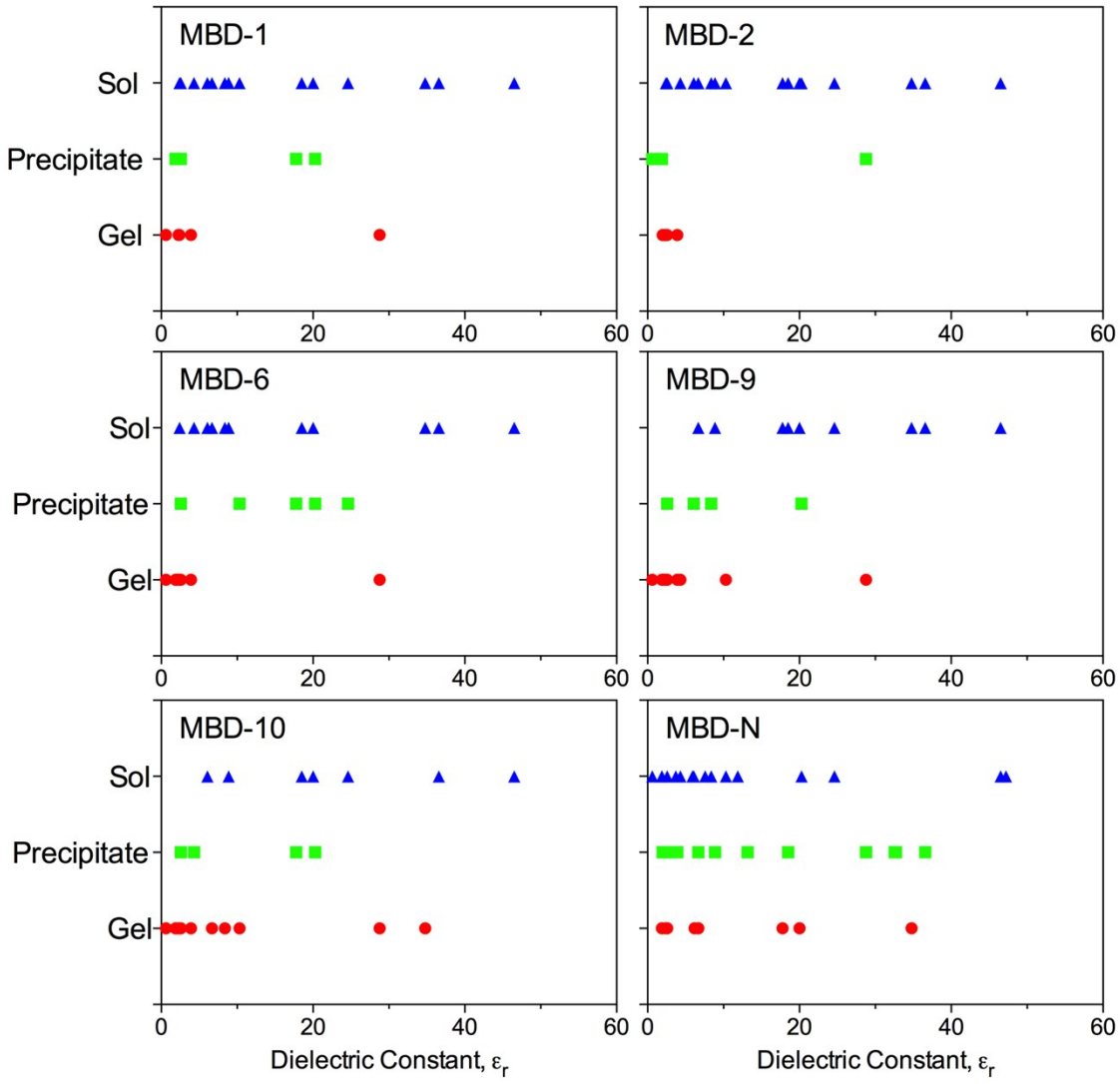

Figure S3: The capacity of the MBD gelators (Scheme 3) to form gels, precipitates or remain as solutions as a function of the static relative permittivity of the solvents.

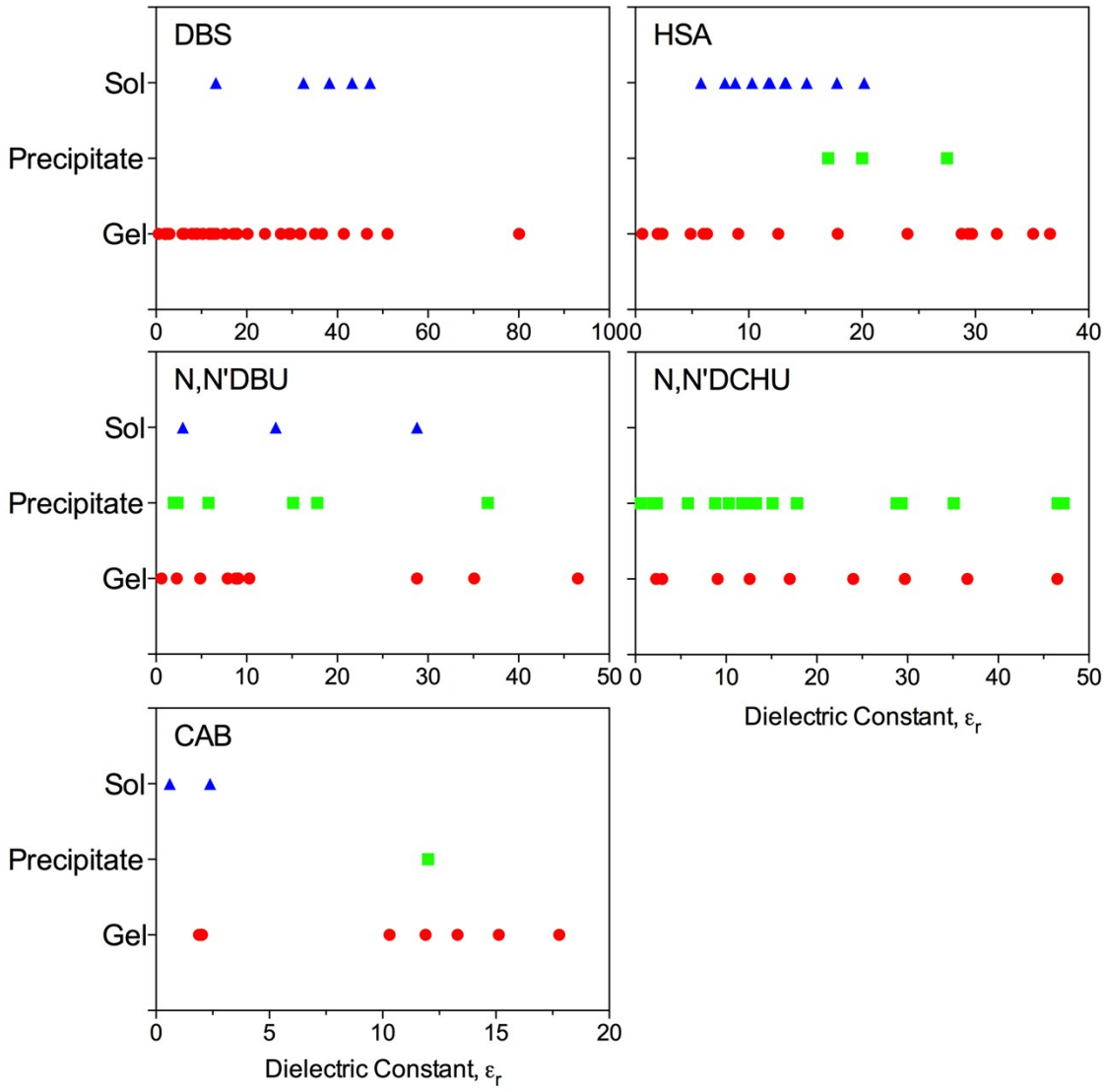

Figure S4: The capacity of the miscellaneous highly efficient gelators (Scheme 4) to form gels, precipitates or remain as solutions as a function of the static relative permittivity of the solvents.

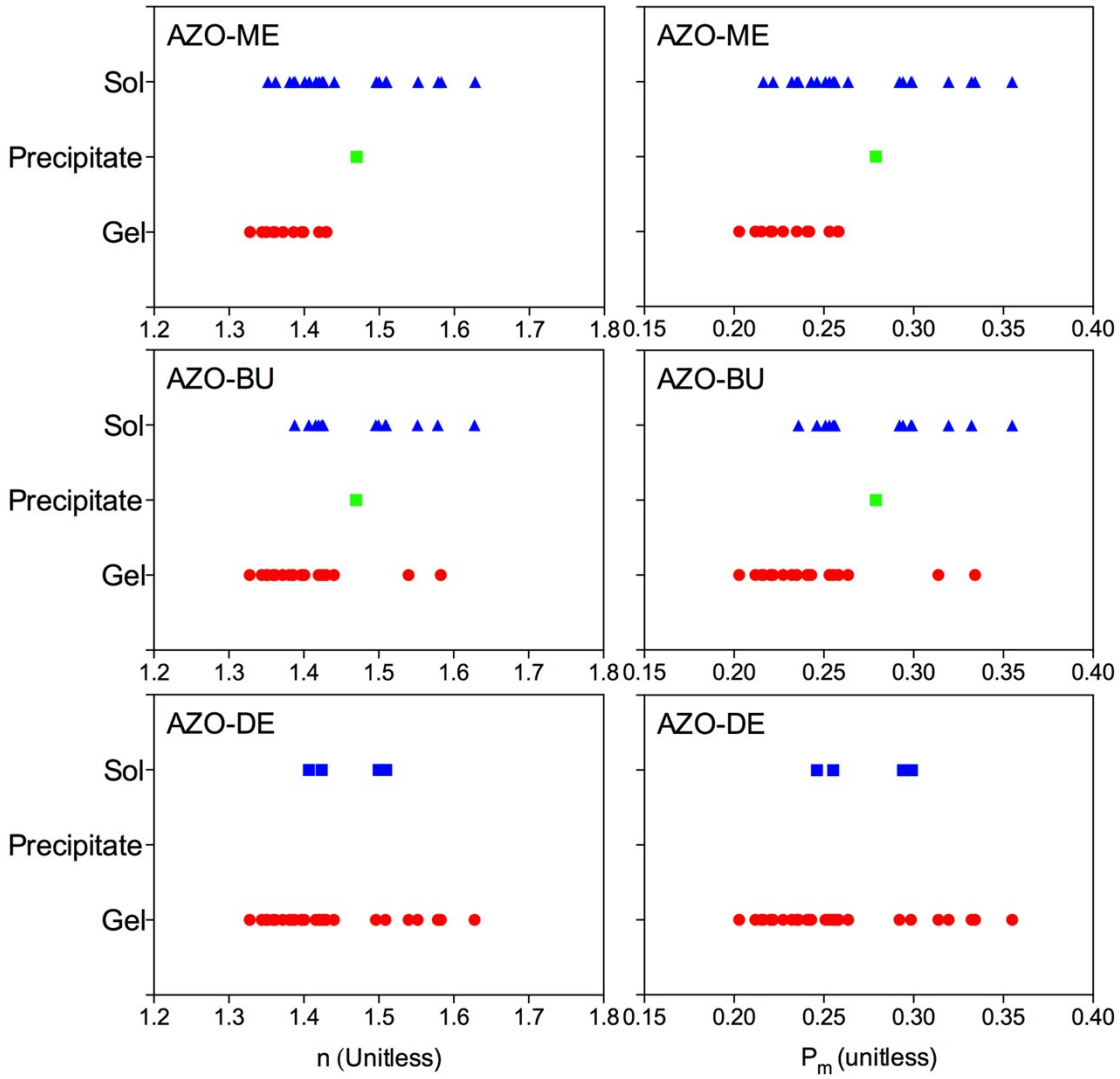

Figure S5: The capacity of the AZO derivatives to form gels, precipitates or solutions as a function of the refractive index and polarizability of the solvents.

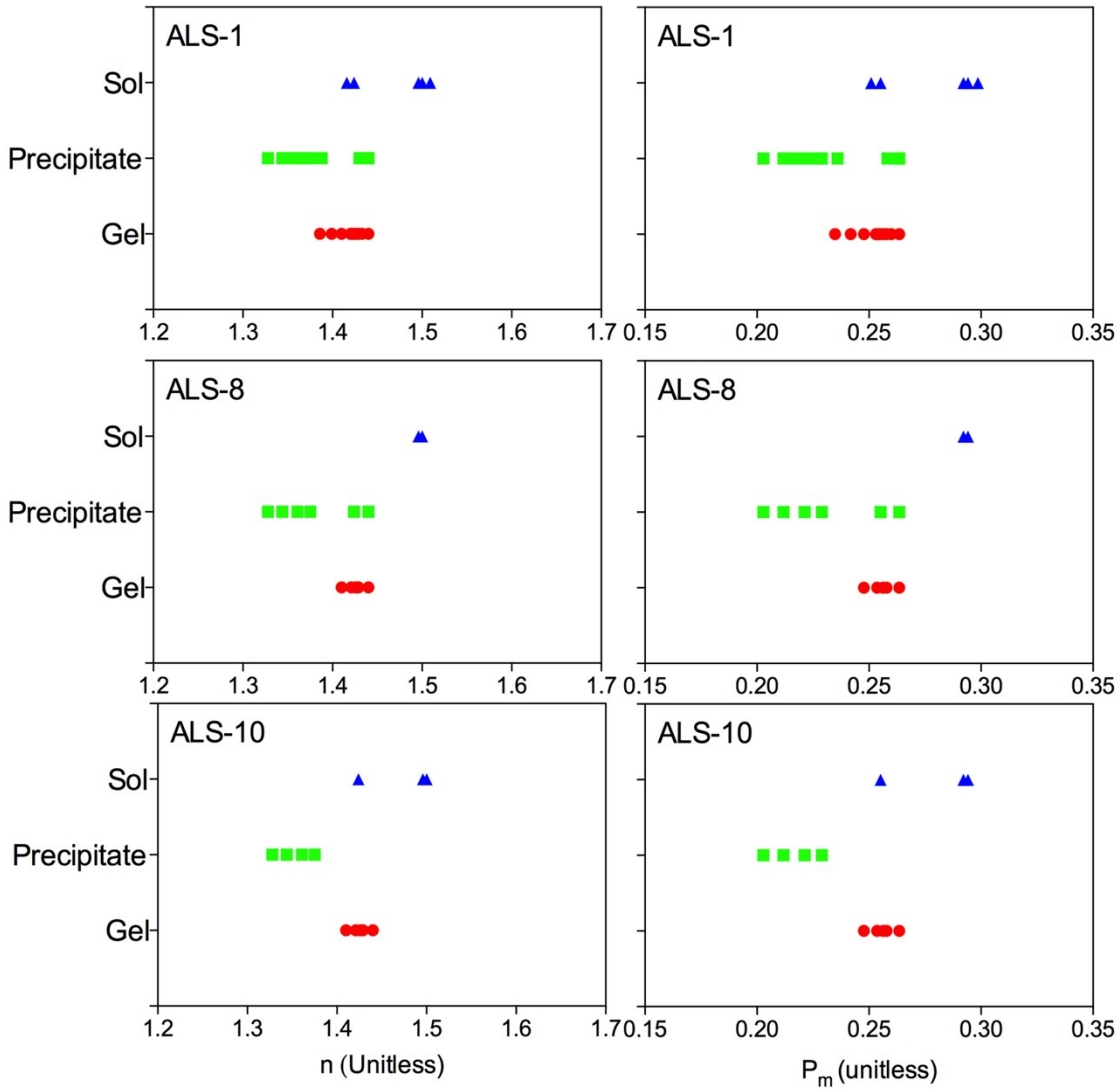

Figure S6: The capacity of the ALS gelators to form gels, precipitates or solutions as a function of the refractive index and polarizability of the solvents.

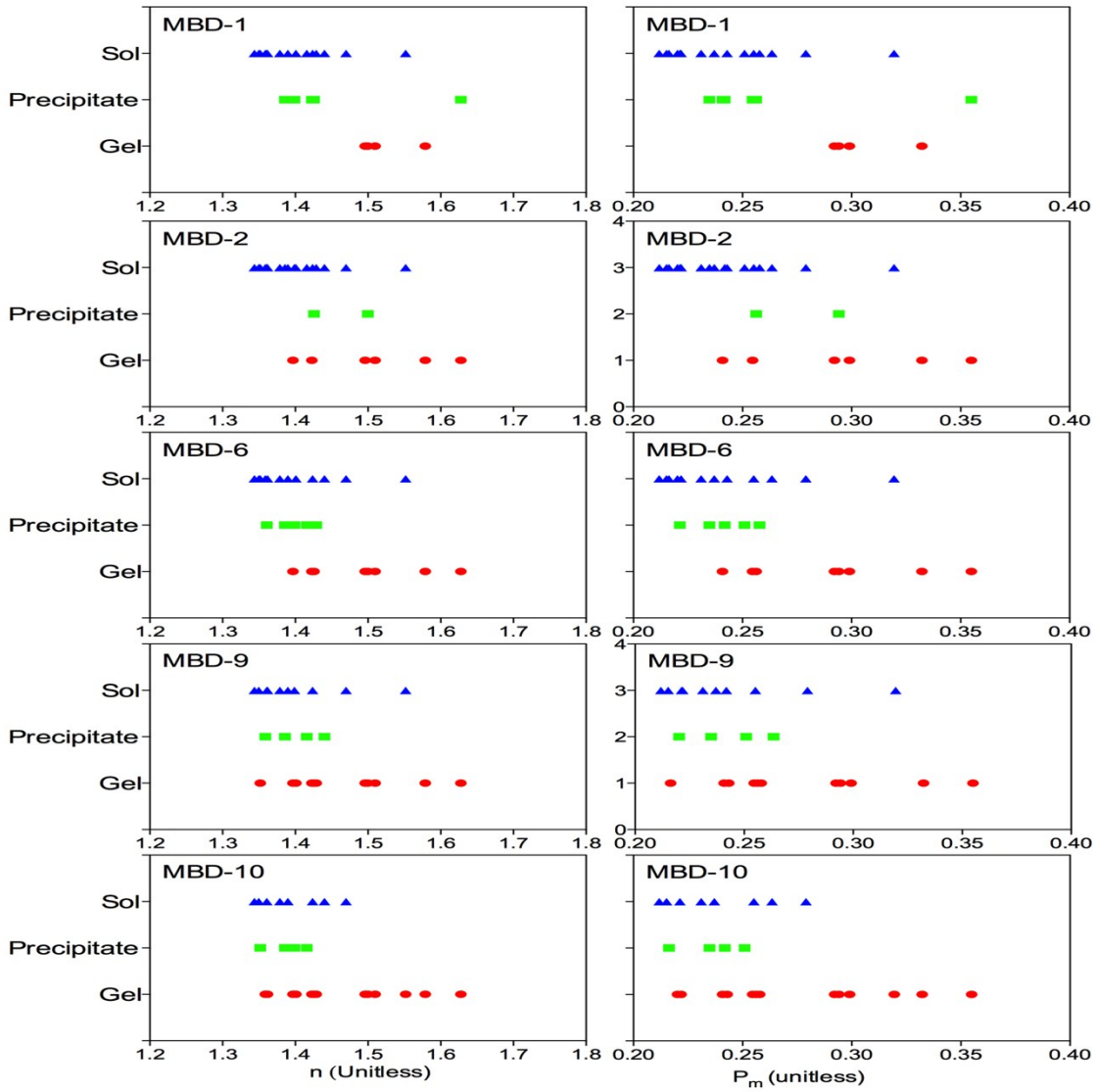

Figure S7: The capacity of the MBD derivatives to form gels, precipitates or solutions as a function of the refractive index and polarizability of the solvents.

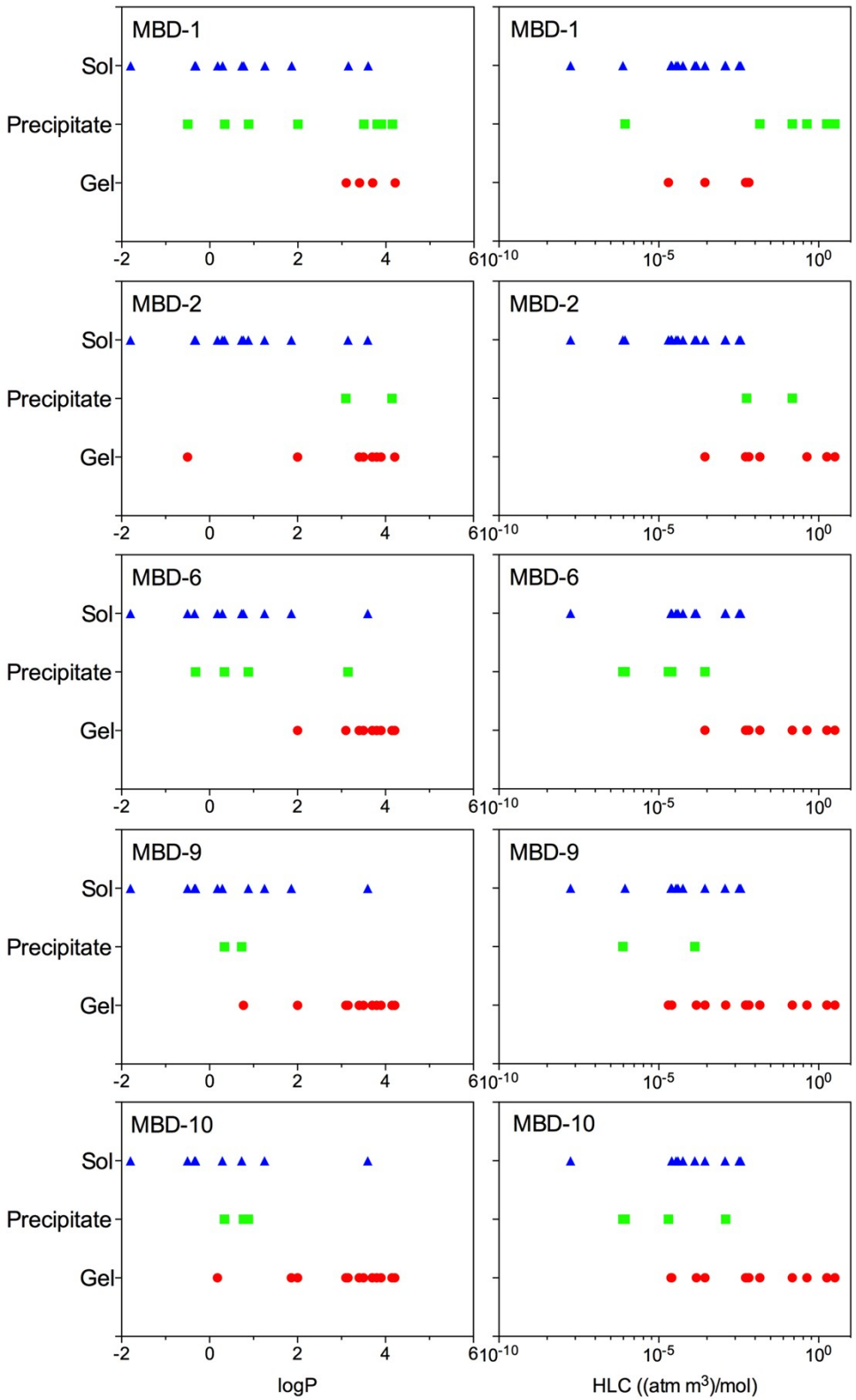

Figure S8: The capacity of the MBD derivatives to form gels, precipitates or solutions as a function of partition coefficients and Henry's law constants of the solvents.

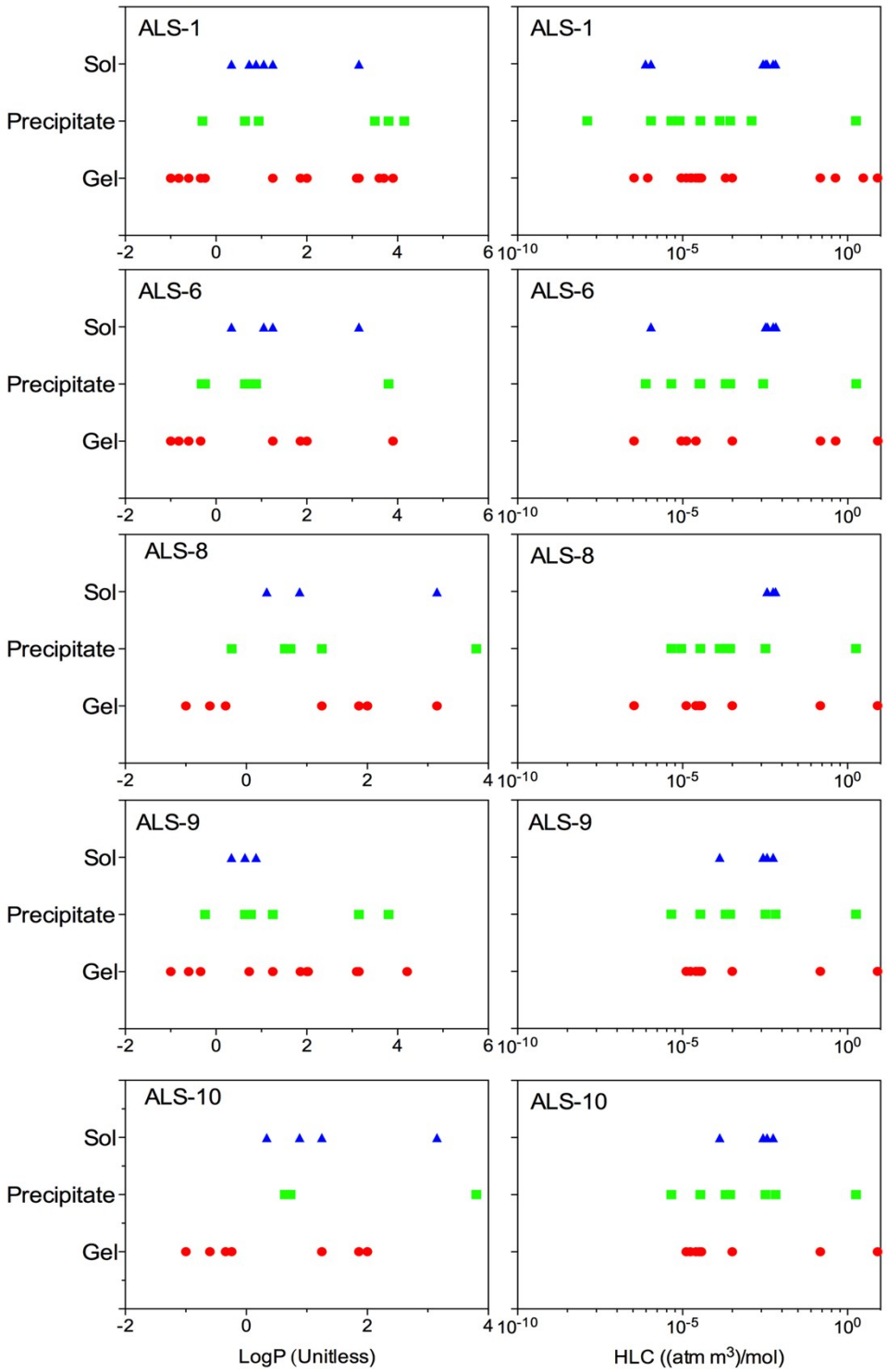

Figure S9: 15: The capacity of the ALS derivatives to form gels, precipitates or solutions as a function of partition coefficients and Henry's law constants of the solvents.

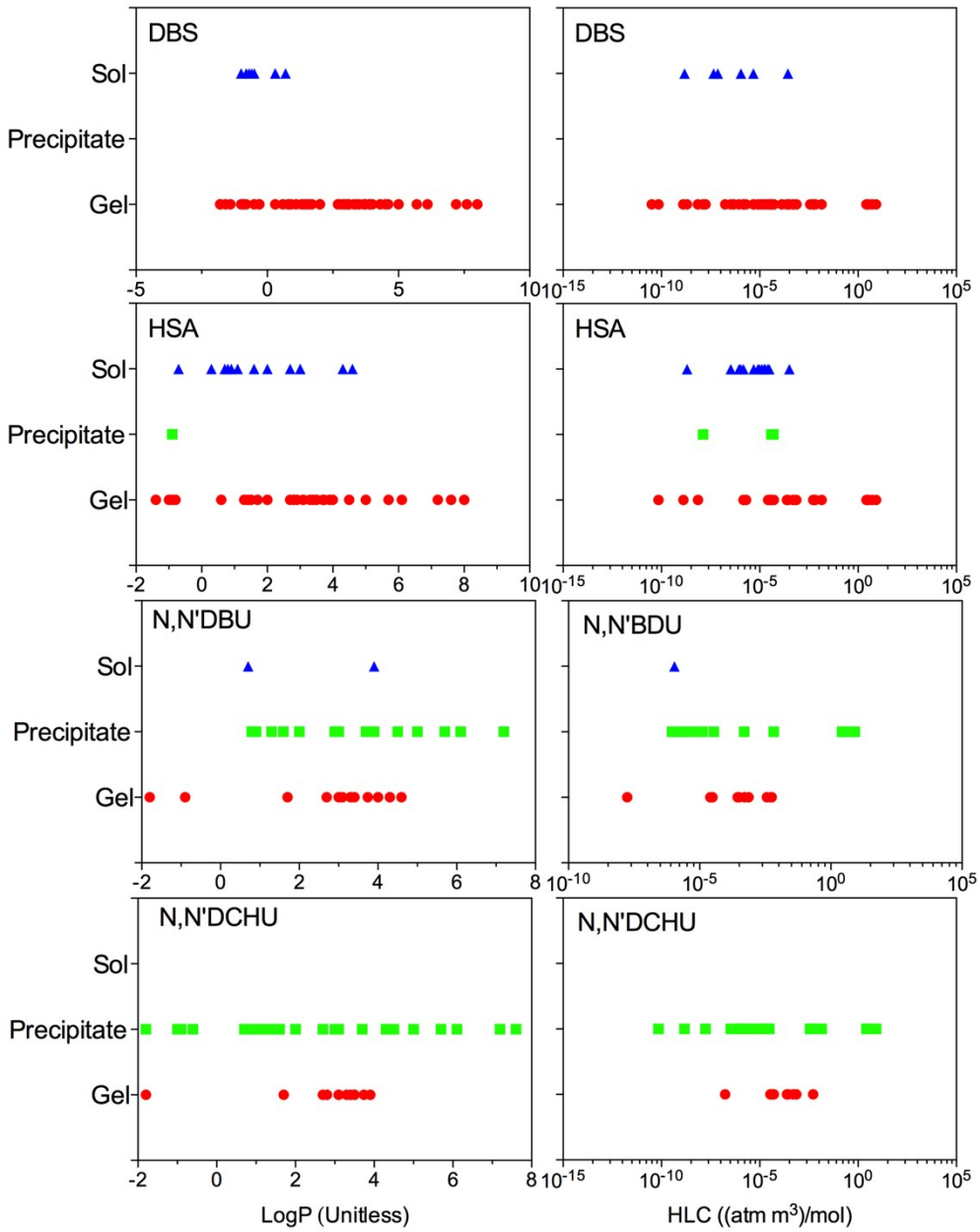

Figure S10: The capacity of DBS, HSA, N,N'-DBU and N,N'-DCHU to form gels, precipitates or solutions as a function of partition coefficients and Henry's law constants of the solvents.

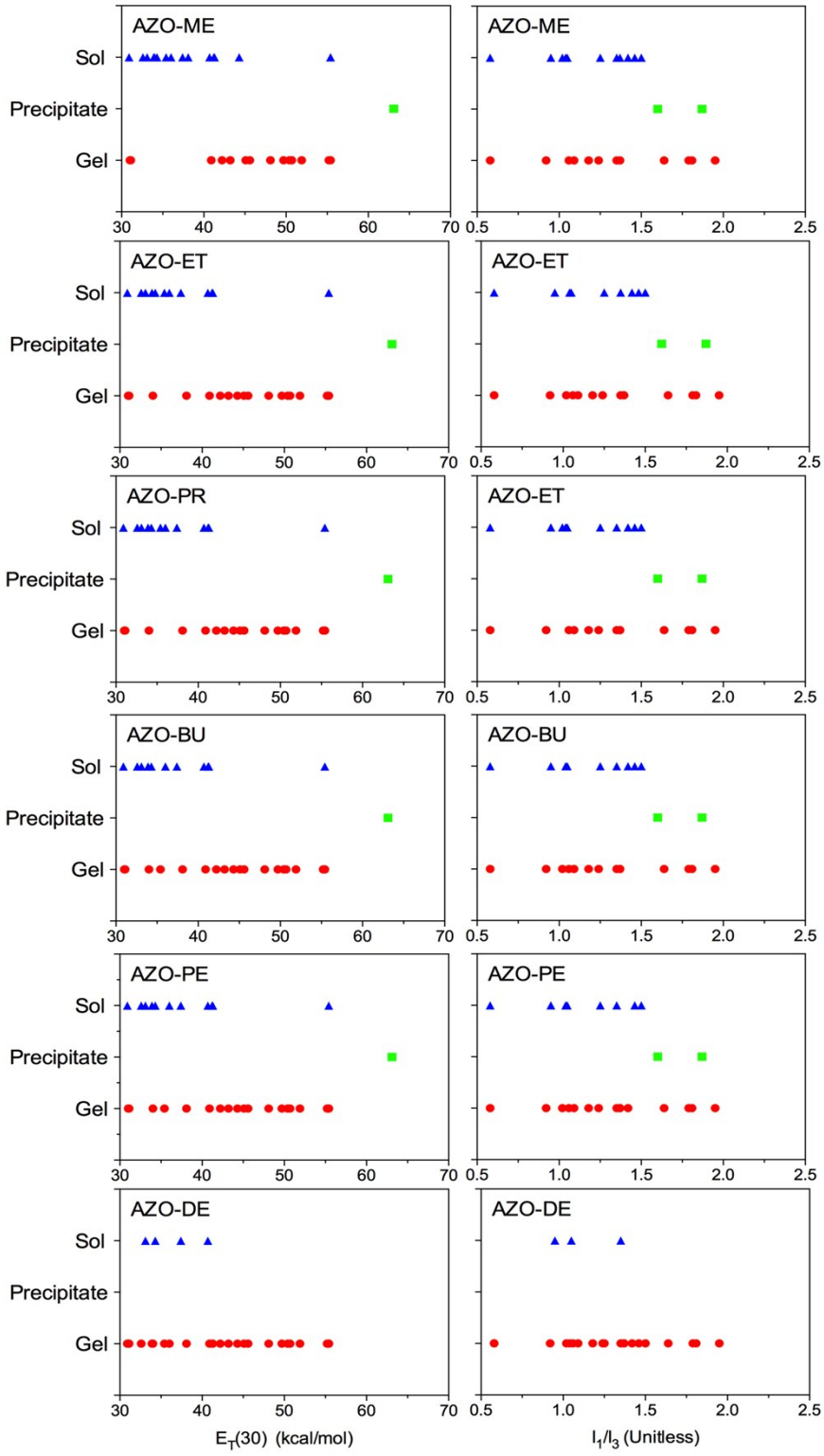

Figure S11: The capacity of the AZO derivatives to form gels, precipitates or solutions as a function of $E_T(30)$ and the Py scale of the solvents.

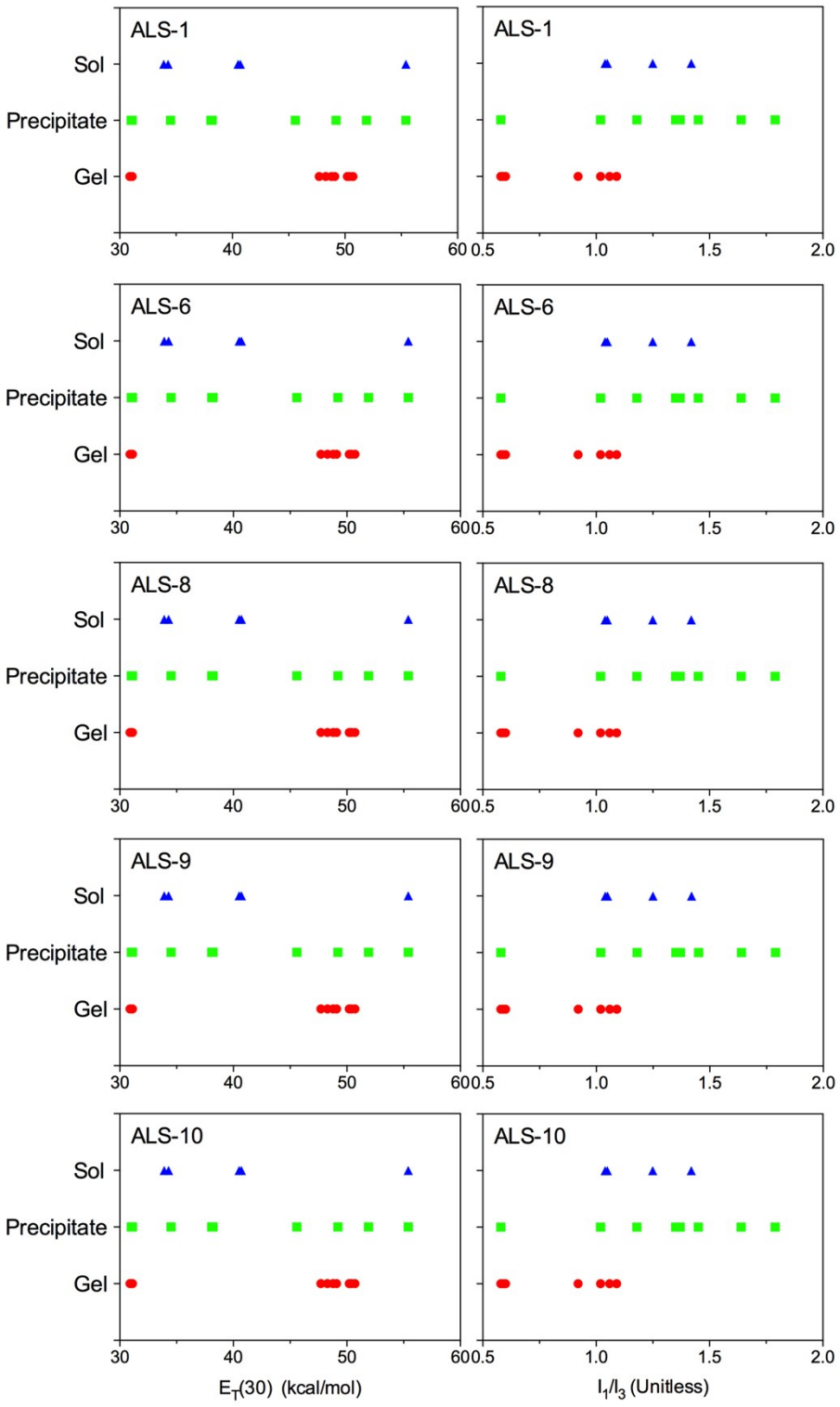

Figure S12: The capacity of the ALS derivatives to form gels, precipitates or solutions as a function of $E_T(30)$ and the Py scale of the solvents.

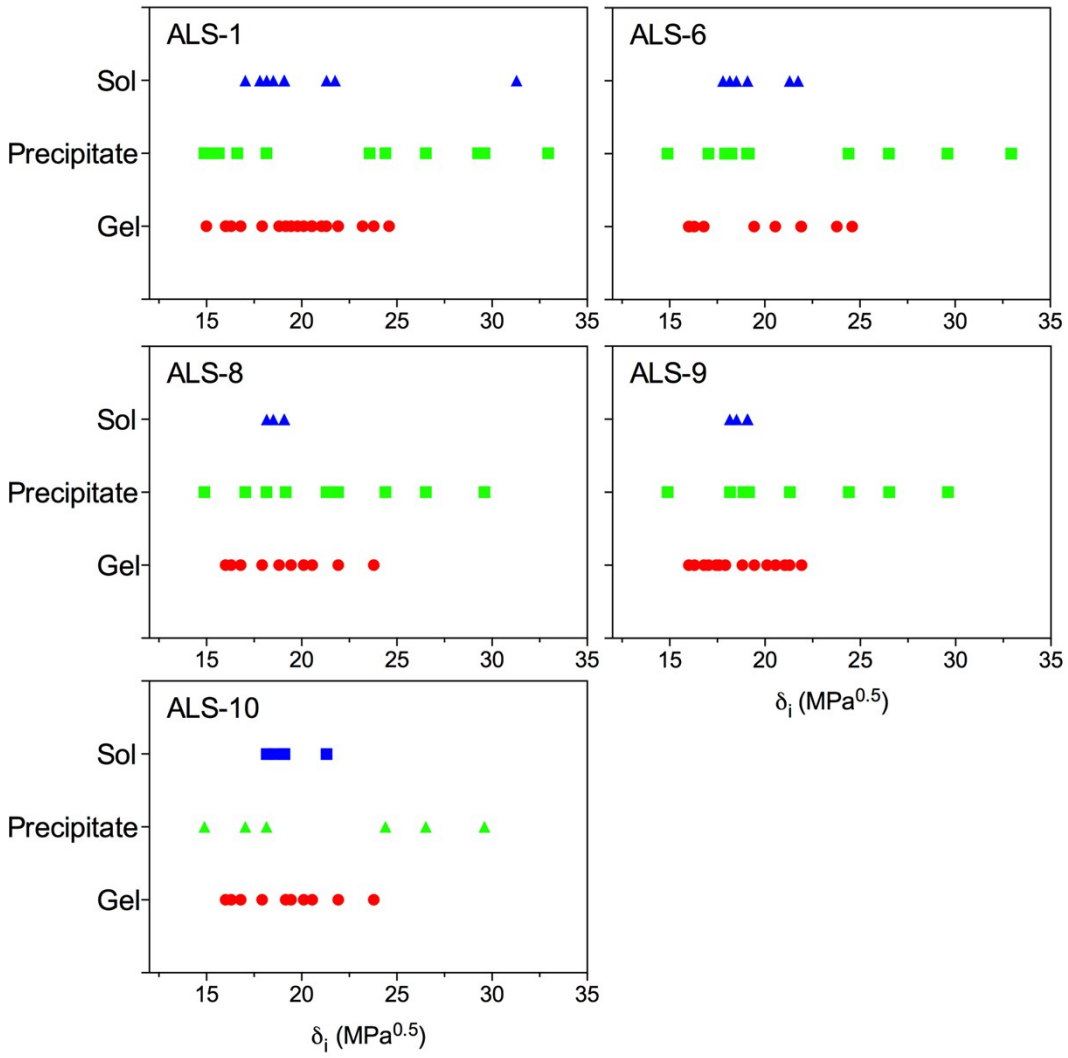

Figure S13: The capacity of the ALS derivatives to form gels, precipitates or solutions as a function of the Hildebrand solubility parameter of the solvents.

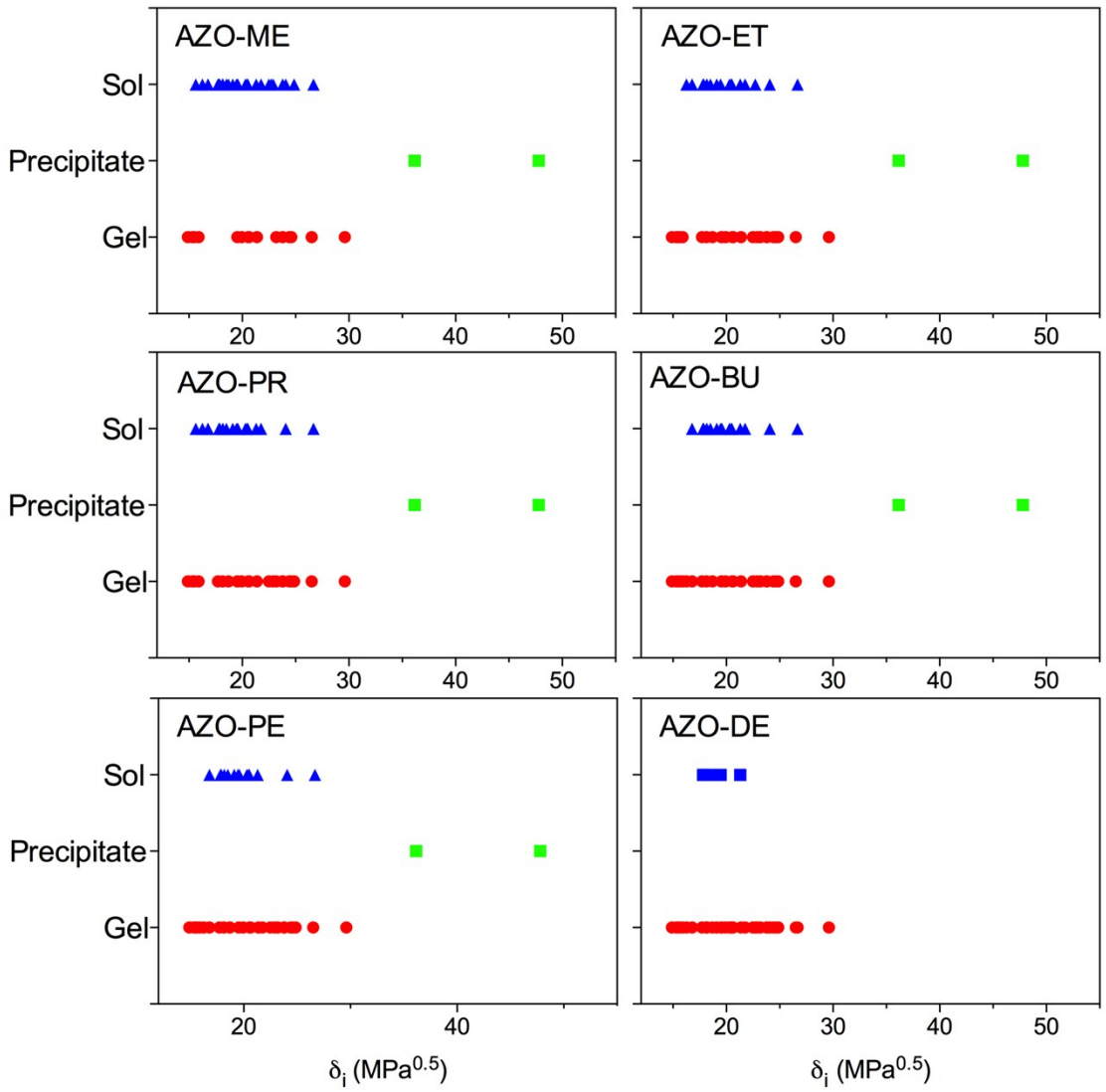

Figure S14: The capacity of the AZO derivatives to form gels, precipitates or solutions as a function of the Hildebrand solubility parameter of the solvents.

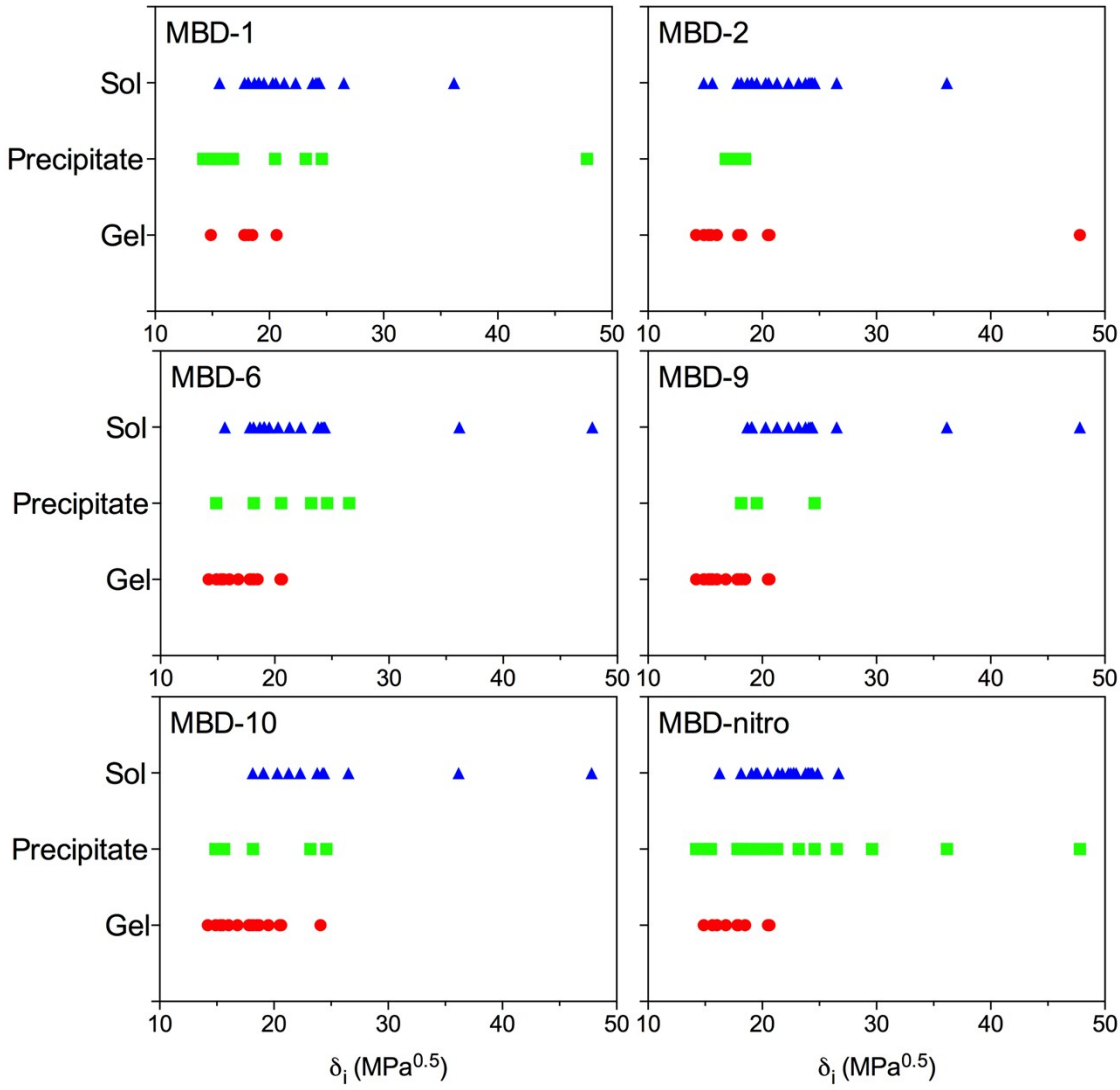

Figure S15: The capacity of the MBD derivatives to form gels, precipitates or solutions as a function of the Hildebrand solubility parameter of the solvents.

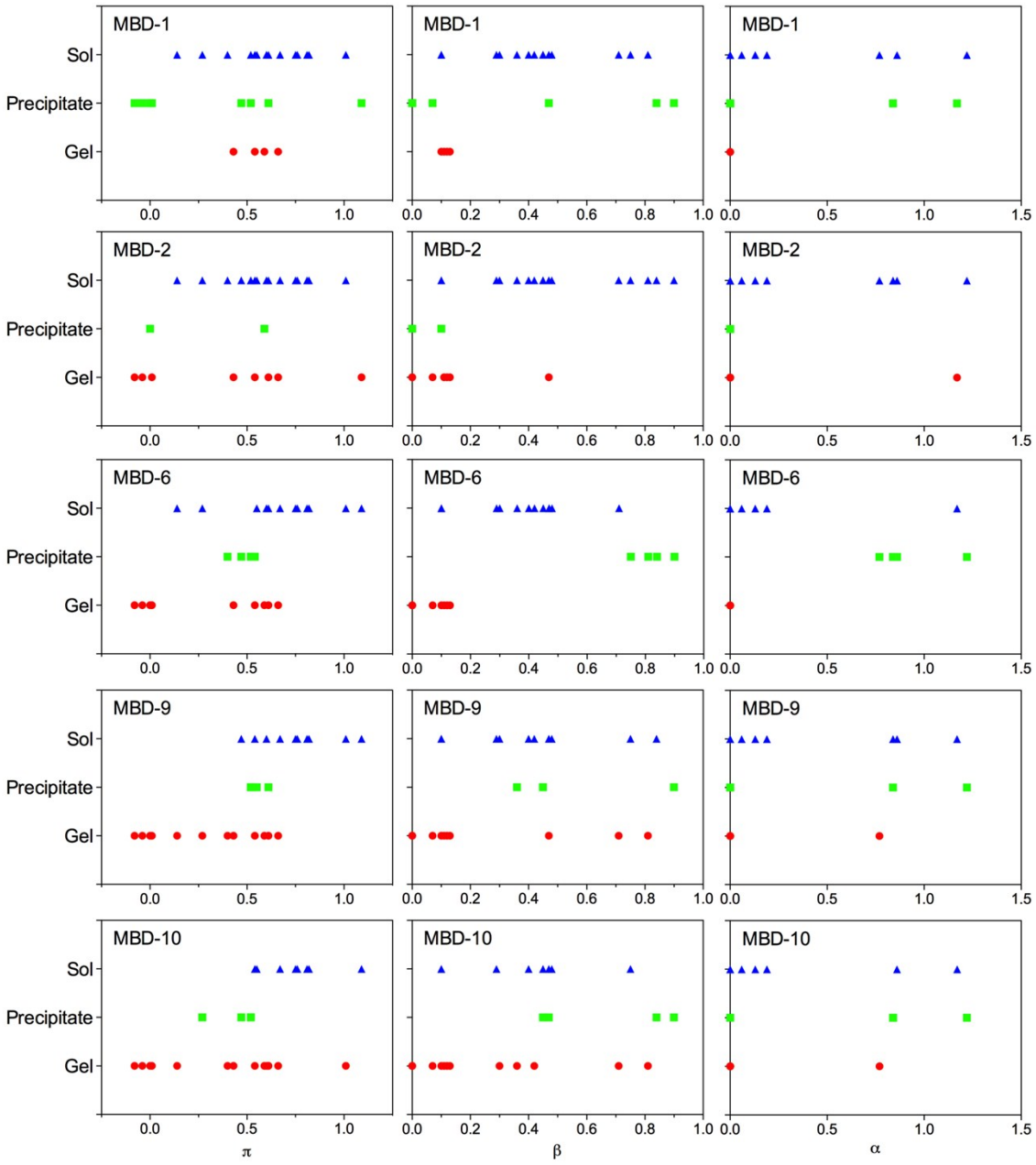

Figure S16: The capacity of the MBD gelators to form gels, precipitates or solutions as a function of Kamlet Taft Parameters, π, β, and α, of the solvents.

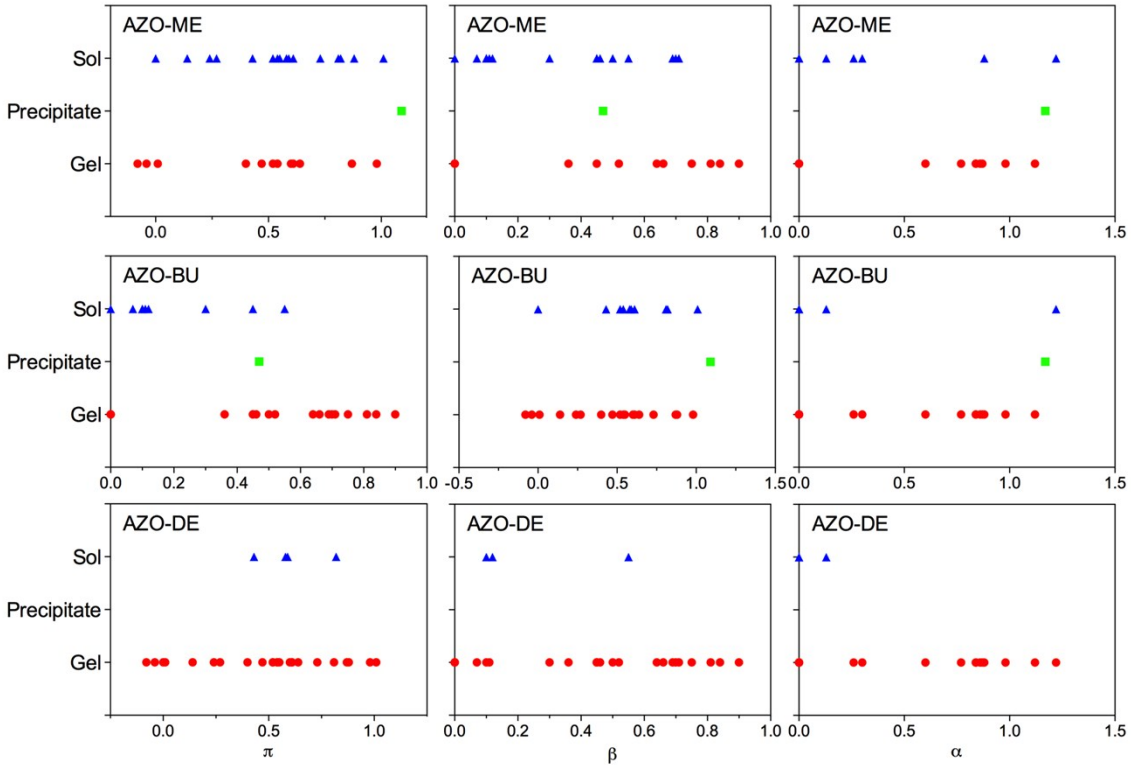

Figure S17: The capacity of the AZO gelators to form gels, precipitates or solutions as a function of Kamlet Taft Parameters, π, β, and α, of the solvents.

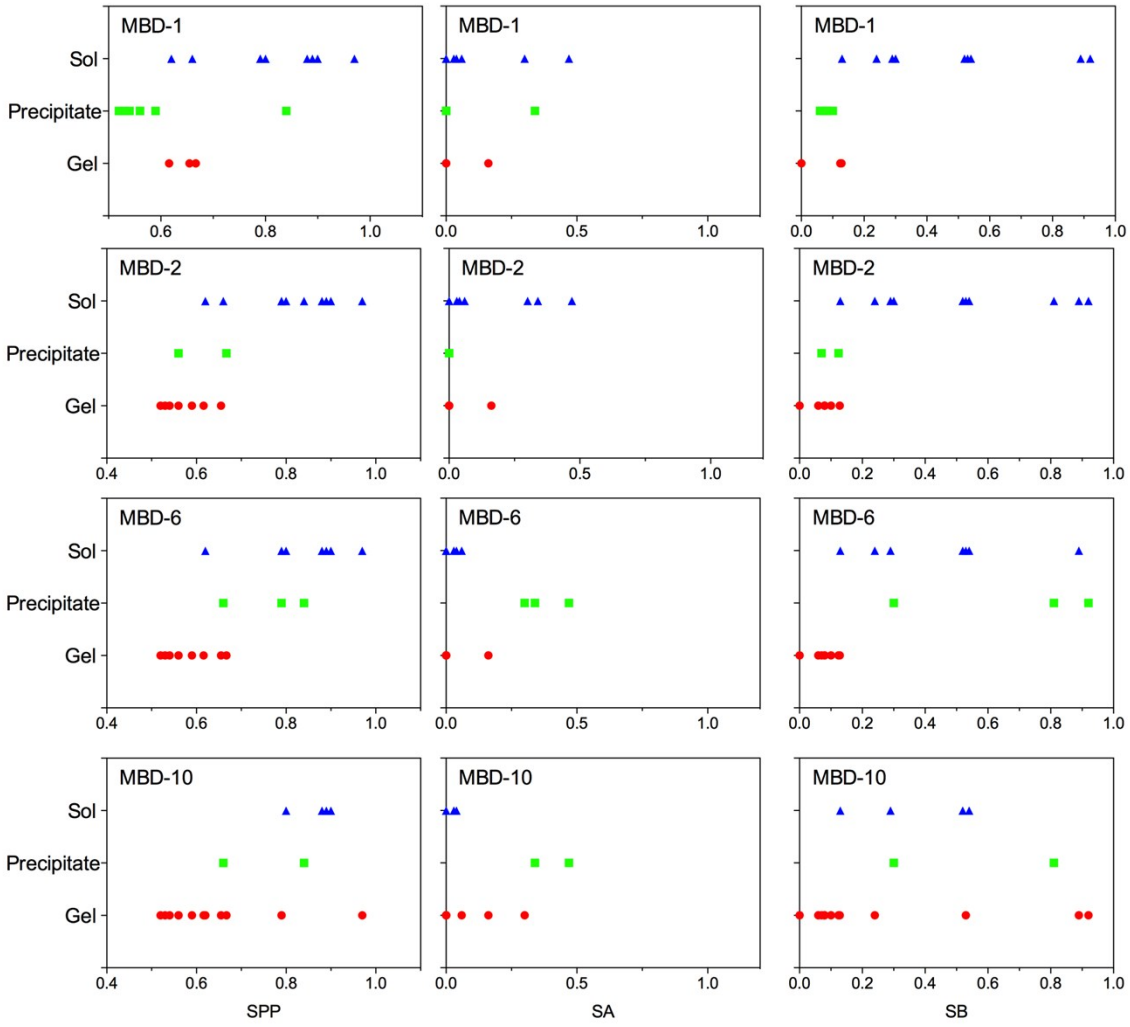

Figure S18: The capacity of the MBD gelators to form gels, precipitates or solutions as a function of Catalan's SPP, SA, and SB solvent parameters.

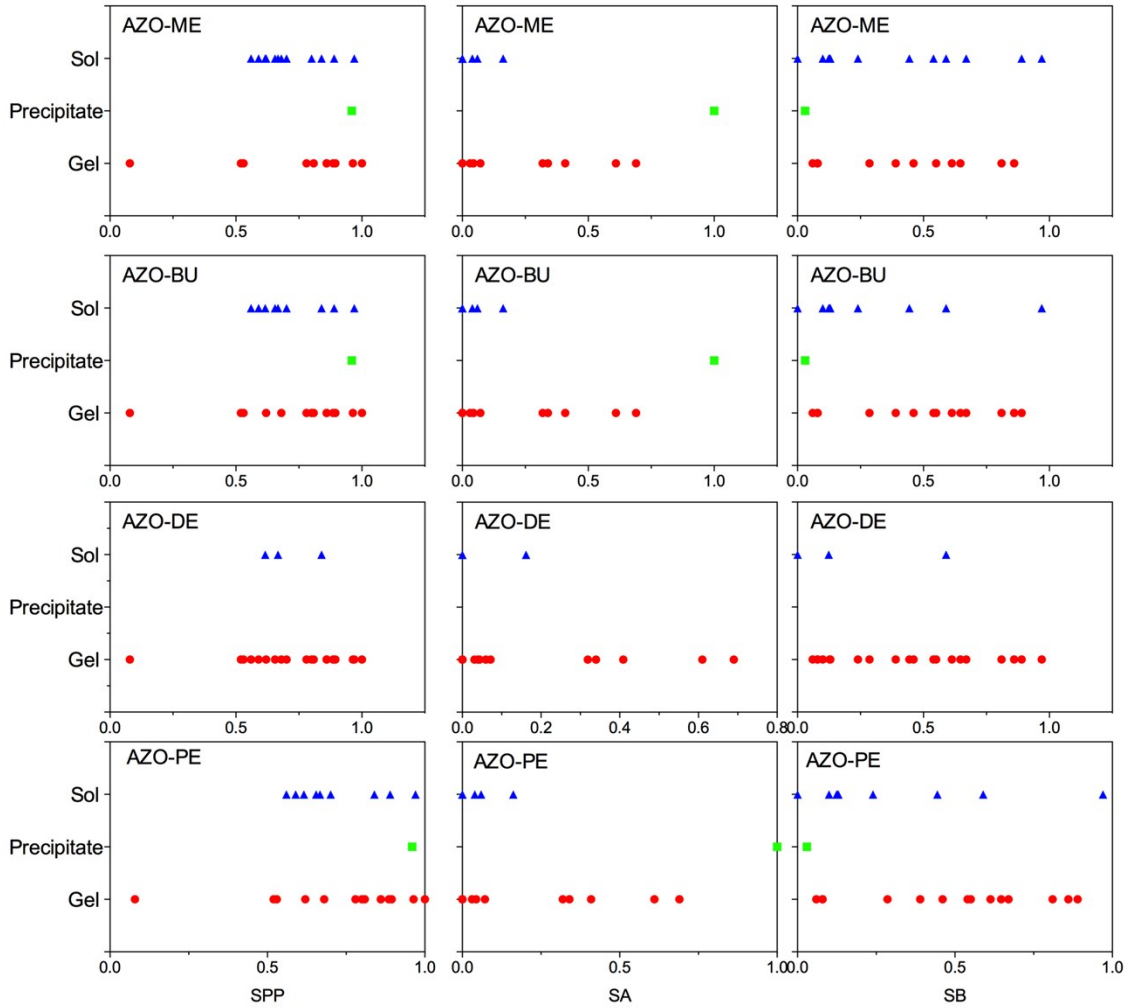

Figure S19: The capacity of the AZO gelators to form gels, precipitates or solutions as a function of Catalan's SPP, SA, and SB solvent parameters.

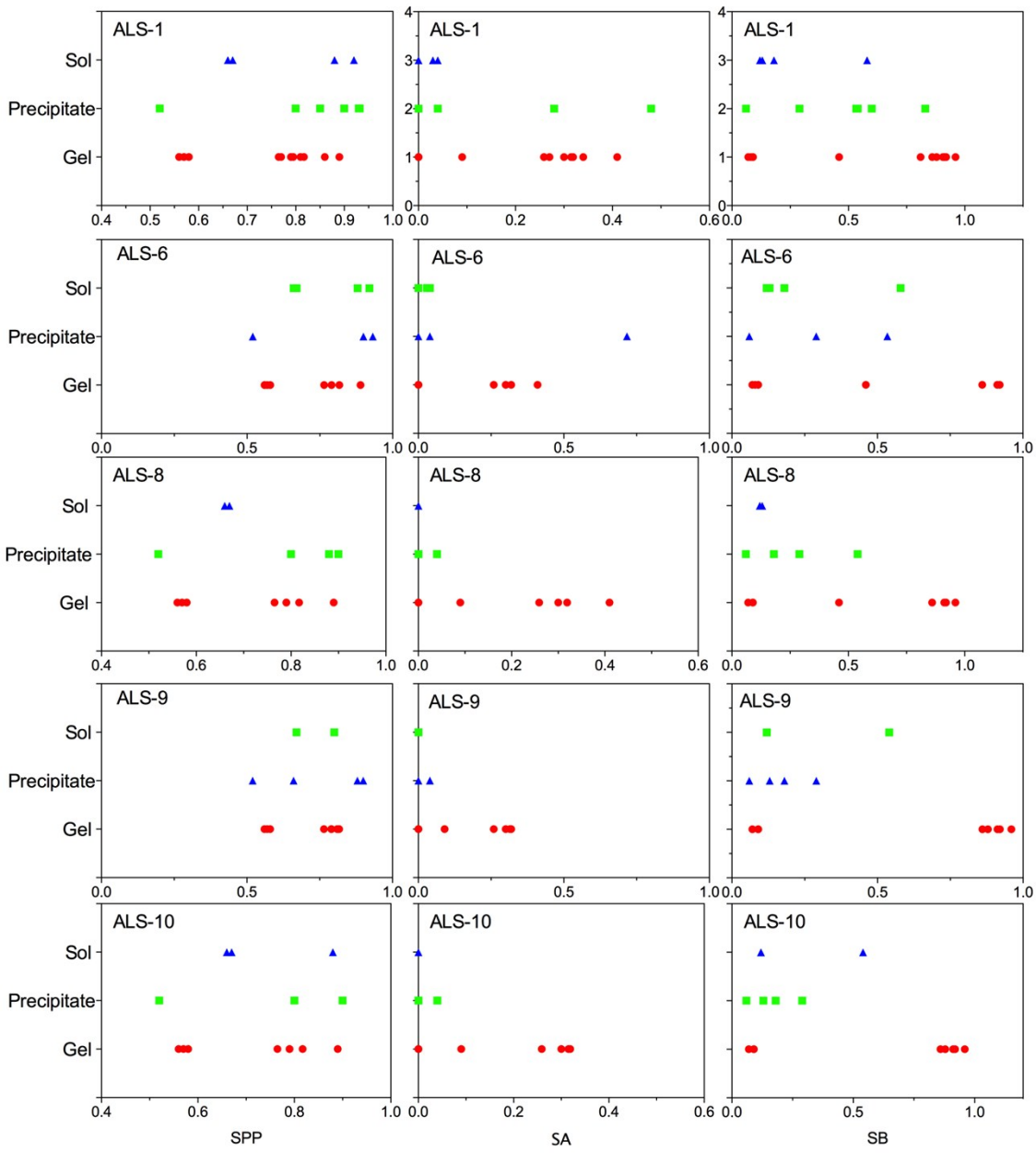

Figure S20: The capacity of the ALS gelators to form gels, precipitates or solutions as a function of Catalan's SPP, SA, and SB solvent parameters.

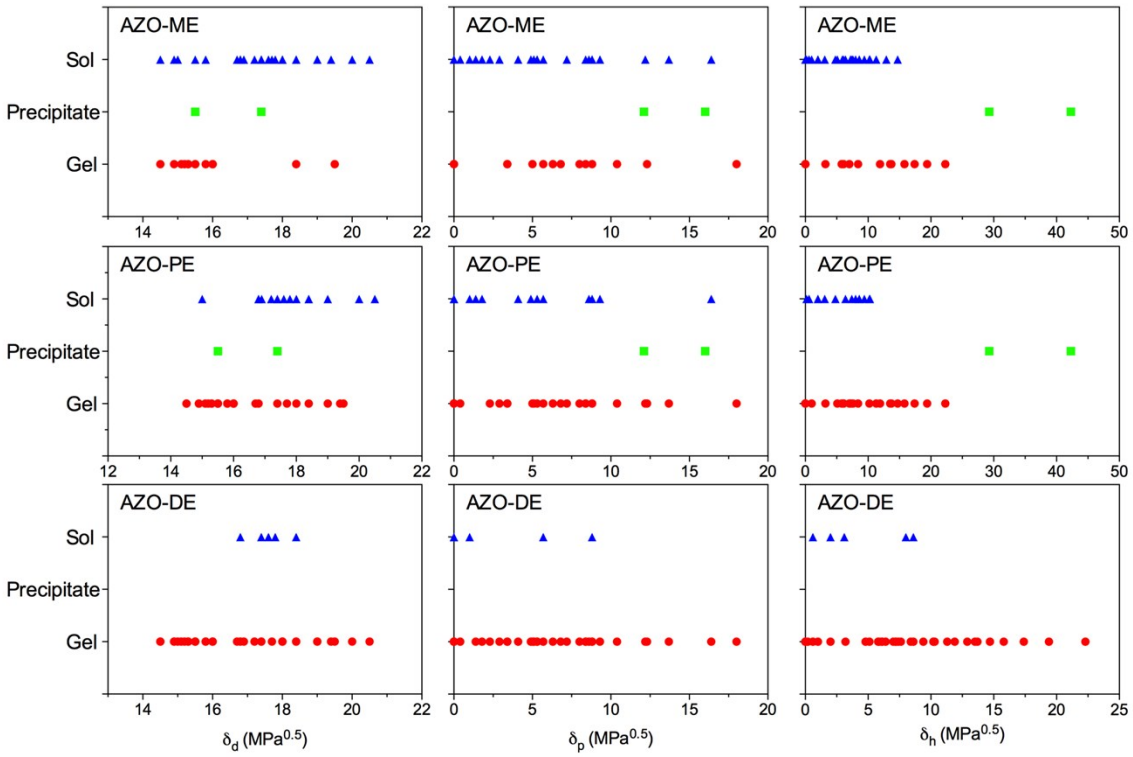

Figure S21: The capacity of the AZO derivatives to form gels, precipitates or solutions as a function of the dispersive Hansen solubility parameter (δ_d), polar Hansen solubility parameter (δ_p) and hydrogen- bonding Hansen solubility parameter (δ_h) of the solvents.

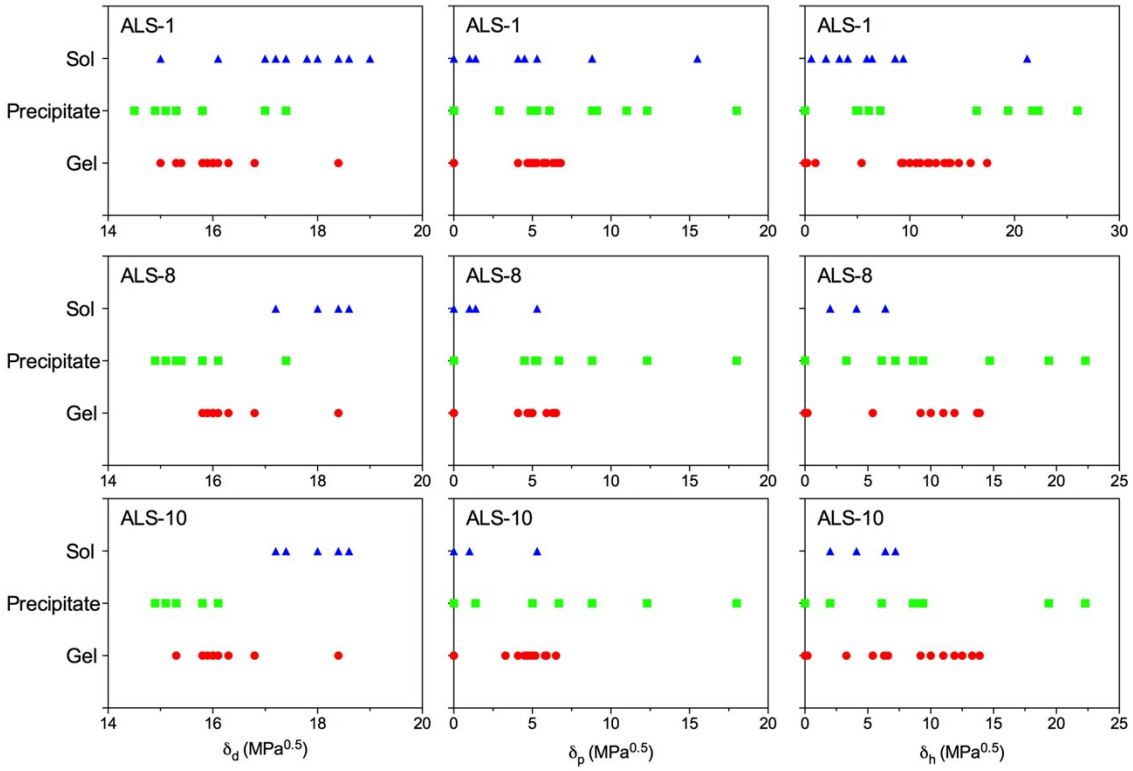

Figure S22: The capacity of the ALS derivatives to form gels, precipitates or solutions as a function of the dispersive Hansen solubility parameter (δ_d), polar Hansen solubility parameter (δ_p) and hydrogen- bonding Hansen solubility parameter (δ_h) of the solvents.

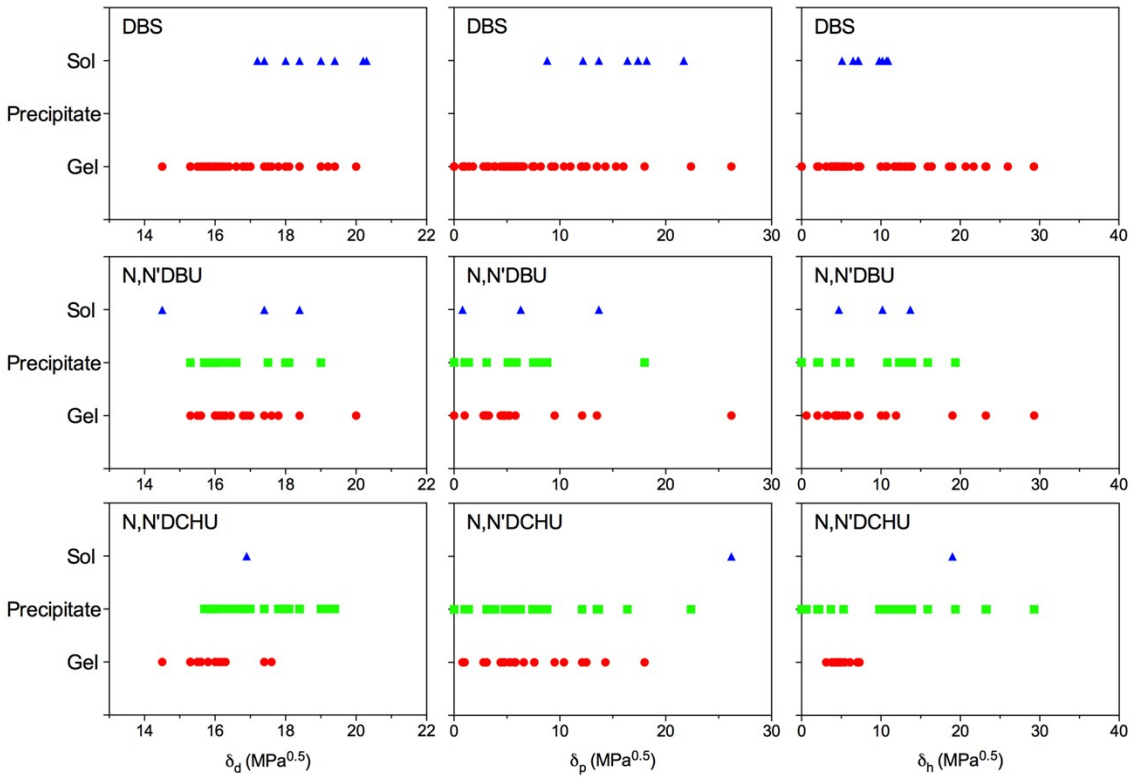

Figure S23: The capacity of the DBS, N,N'-DBU, N,N'-DCH to form gels, precipitates or solutions as a function of the dispersive Hansen solubility parameter (δ_d), polar Hansen solubility parameter (δ_p) and hydrogen- bonding Hansen solubility parameter (δ_h) of the solvents.

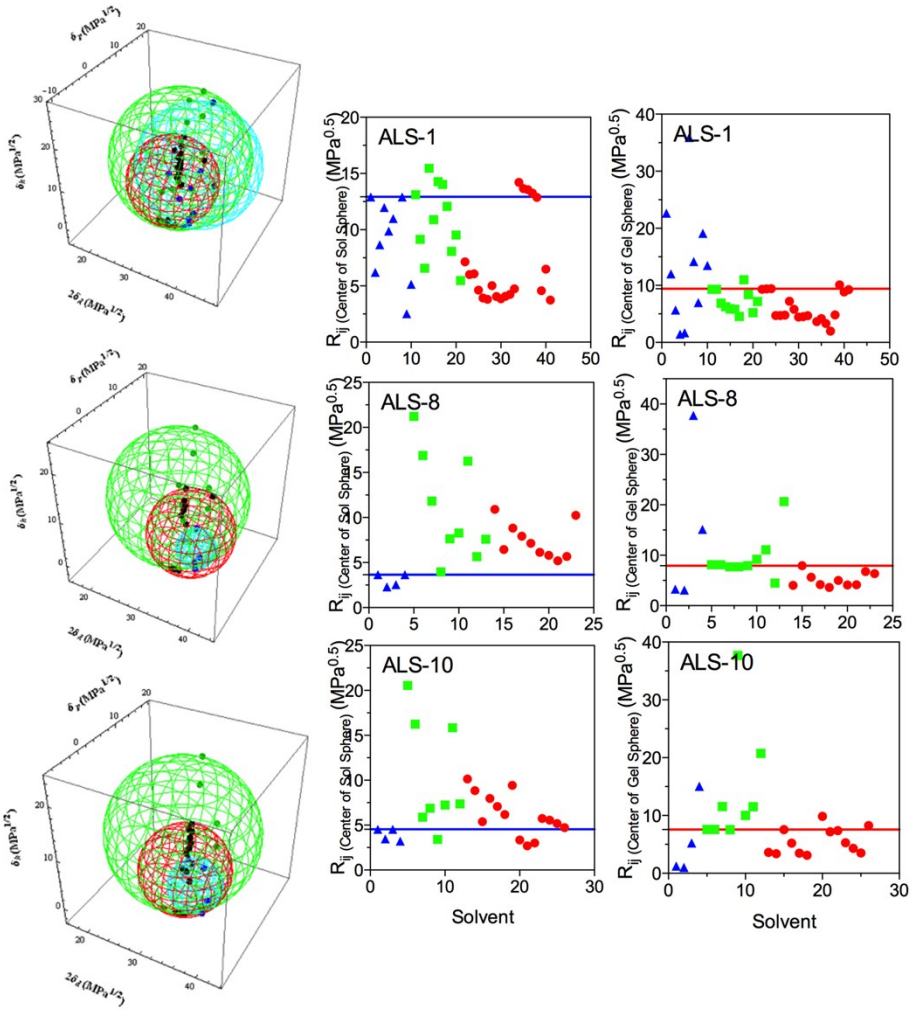

Figure S24: 3D Hanson space and distances in Hansen space to the centers of the sol and gelation spheres for ALS gelators. The blue horizontal line represents the radius of the solubility sphere, and the red line represents the radius of gel sphere. The x-axes of the gelators are comprised of arbitrary values to aid in the visualization of differences in R_{ij}.

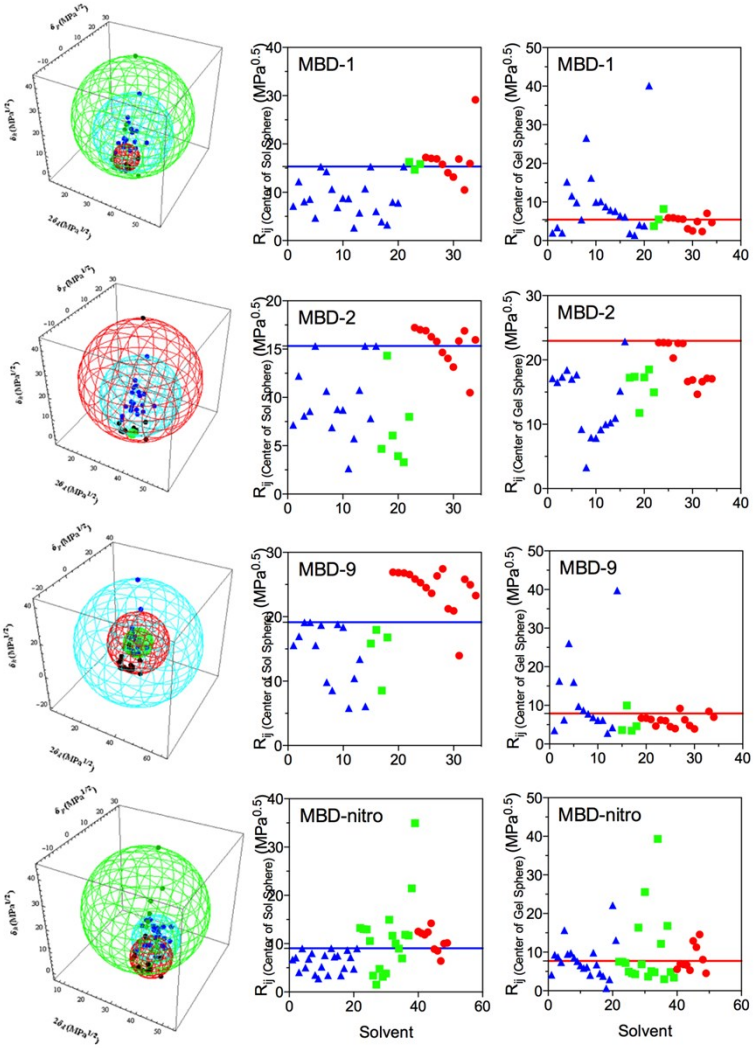

Figure S25: 3D Hanson space and distances in Hansen space to the center of the sol and gelation spheres for MBD gelators. The blue horizontal line represents the radius of the solubility sphere, and the red line represents the radius of the gel sphere. The x-axes are comprised of arbitrary values to aid in the visualization of differences in R_{ij}.

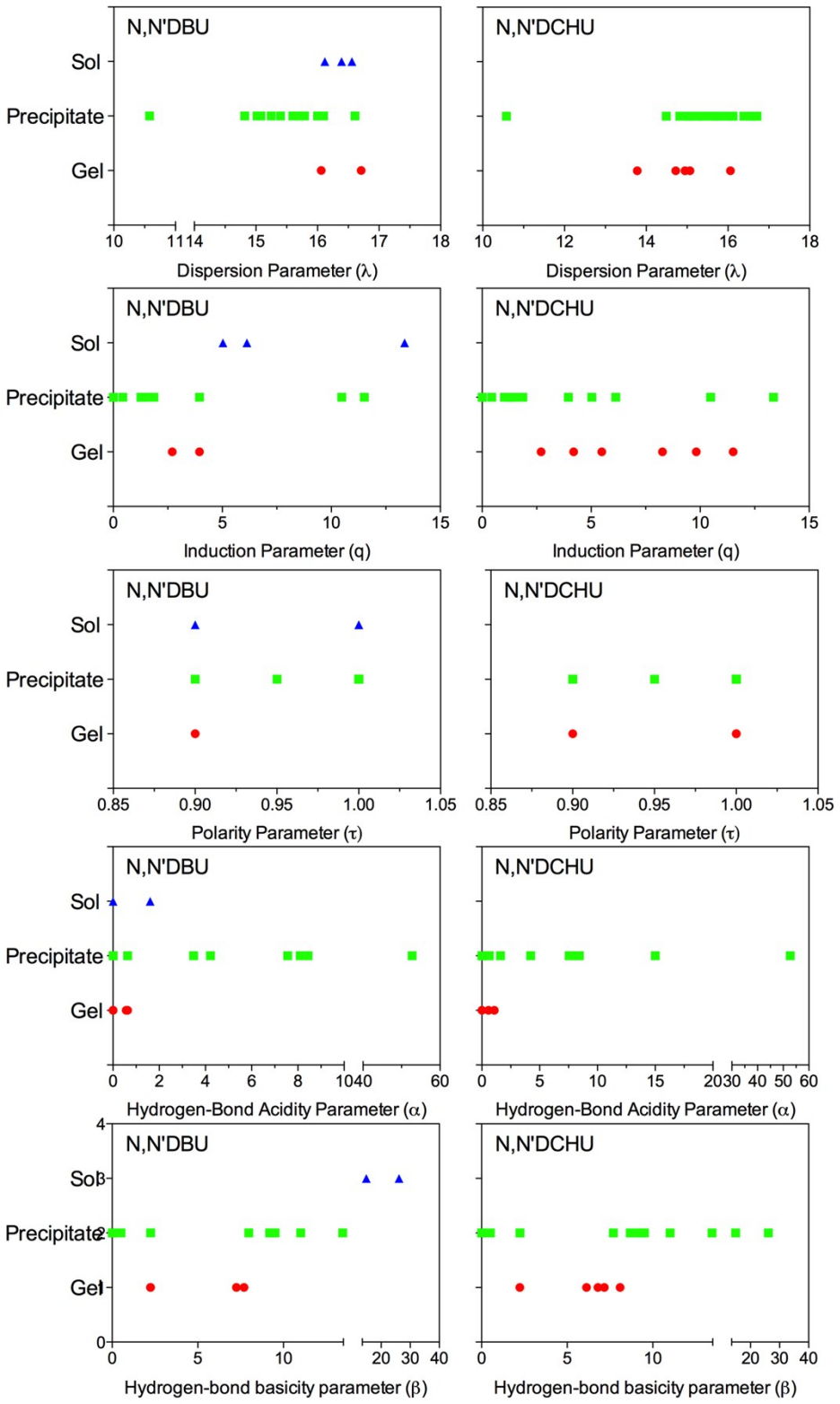

Figure S26: The capacity of the urea gelators to form gels, precipitates or solutions as a function of the MOSCED (**MO**dified **S**eparation of **C**ohesive **E**nergy **D**ensity) parameters (λ, τ, q, α and β) of the solvents.

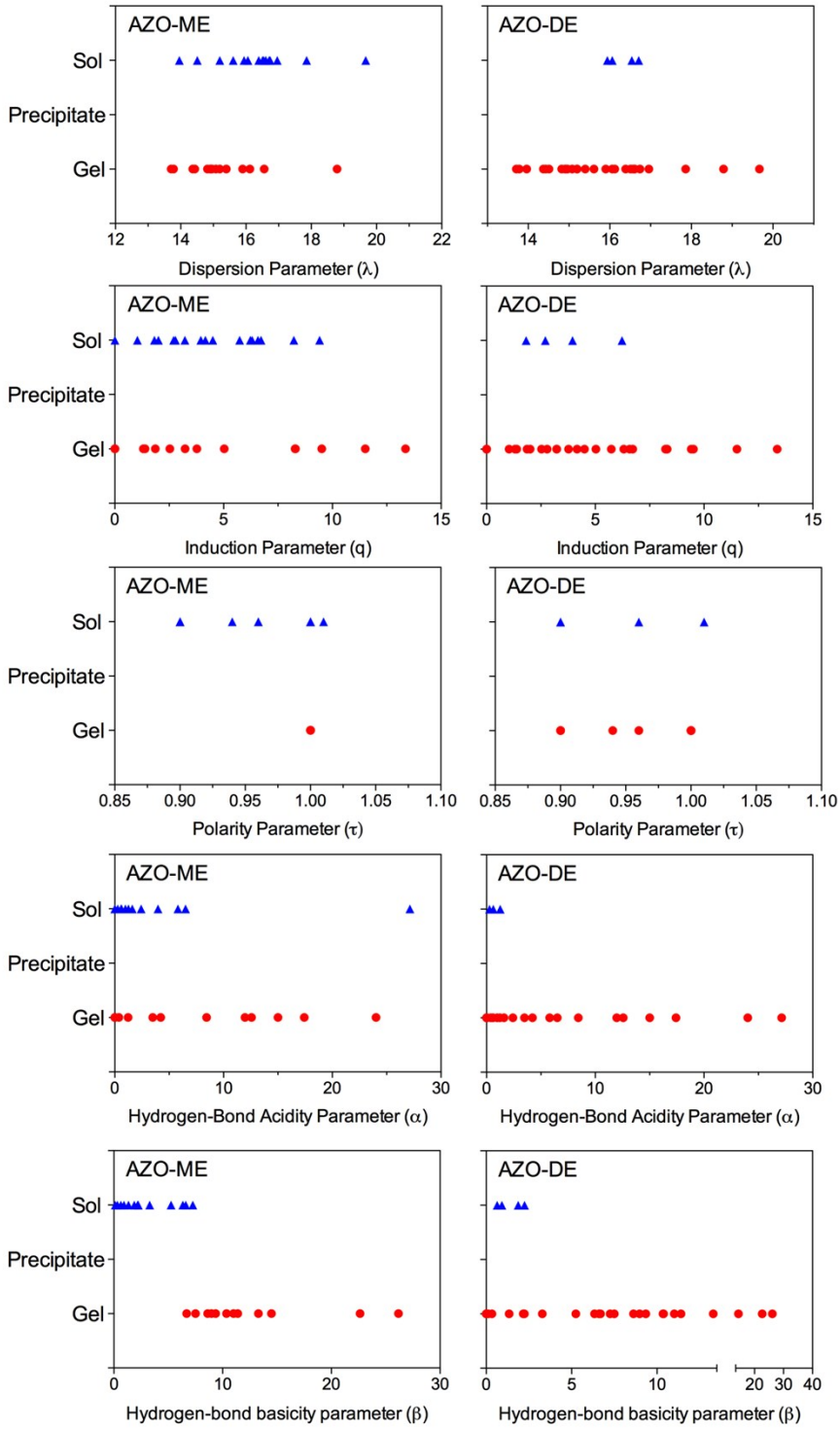

Figure S27: The capacity of the AZO gelators to form gels, precipitates or solutions as a function of the MOSCED (**MO**dified **S**eparation of **C**ohesive **E**nergy **D**ensity) parameters (λ, τ, q, α and β) of the solvents.

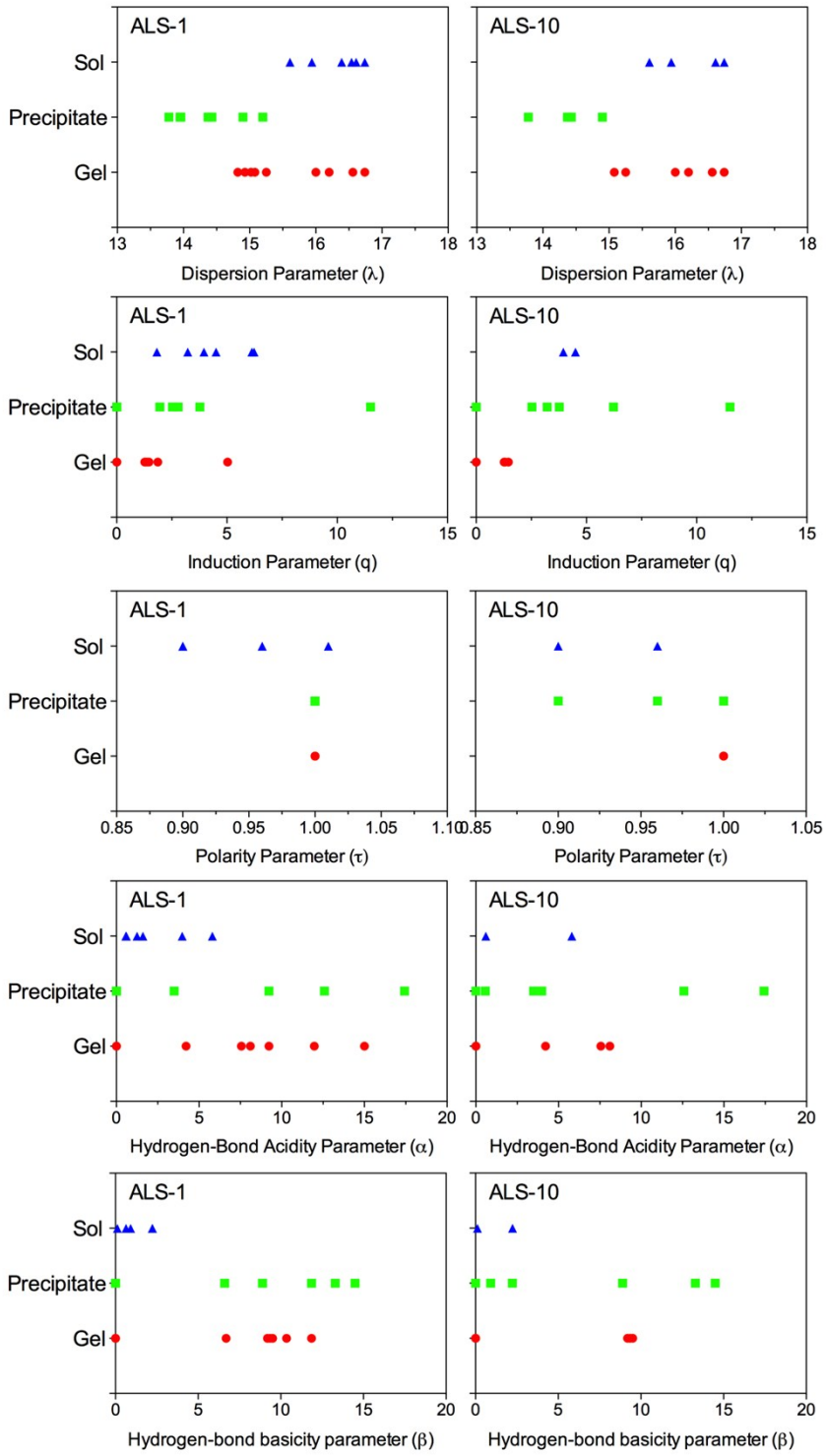

Figure S28: The capacity of the ALS gelators to form gels, precipitates or solutions as a function of the MOSCED (**MO**dified **S**eparation of **C**ohesive **E**nergy **D**ensity) parameters (λ, τ, q, α and β) of the solvents.

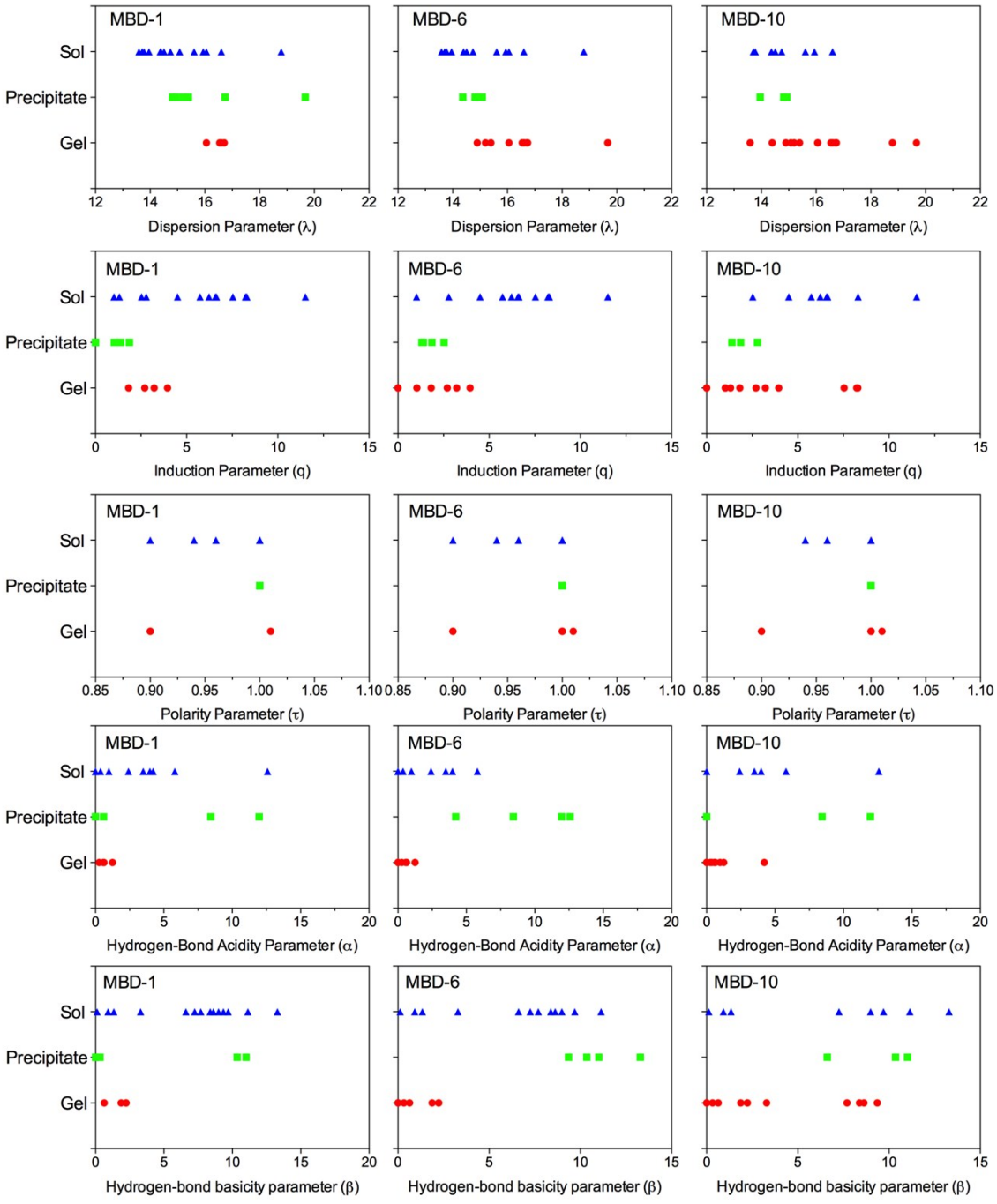

Figure S29: The capacity of the MBD gelators to form gels, precipitates or solutions as a function of the MOSCED (**MO**dified **S**eparation of **C**ohesive **E**nergy **D**ensity) parameters (λ, τ, q, α and β) of the solvents.